Scavenging of ^{231}Pa and ^{230}Th in the South Atlantic: Implications for the use of the $^{231}Pa/^{230}Th$ ratio as a paleoproductivity proxy

Entfernung der natürlichen Radionuklide Protactinium-231 und Thorium-230 aus der Wassersäule des Südatlantiks – Auswirkungen für die Verwendung des $^{231}Pa/^{230}Th$-Verhältnisses als Anzeiger für Paläoproduktivität

---

Hans-Jürgen Walter

Ber. Polarforsch. 282 (1998)
ISSN 0176 - 5027

4.11.98

Lieber Herr Fütterer,
endlich kann ich Ihnen ein Exemplar meiner gedruckten Dissertation überreichen. Es ist sehr schön in Ihnen jemand gefunden zu haben, der die kumulative Dissertation befürwortet. Ihr

Hans-Jürgen

Hans-Jürgen Walter

Alfred-Wegener-Institut für Polar- und Meeresforschung
Am Handelshafen 12, 27570 Bremerhaven

Die vorliegende Arbeit ist die inhaltlich unveränderte Fassung einer Dissertation, die 1998 am Fachbereich Geowissenschaften der Universität Bremen angefertigt wurde.

Contents

Summary

This study investigates the scavenging of the two natural radionuclides ^{230}Th (half-life: 75.400 yr) and ^{231}Pa (half-life: 32.500 yr) in the Atlantic Sector of the Southern Ocean. The research was conducted to find out whether in this region the unsupported $^{231}Pa/^{230}Th$ activity ratio ($_{xs}^{231}Pa/_{xs}^{230}Th$, corrected for detrital, U-supported activities of ^{231}Pa and ^{230}Th) is a reliable tracer for the mass flux of particulate matter, which forms the basis for its use to assess relative changes in bioproductivity of the ocean in the past.

The relationship between $_{xs}^{231}Pa/_{xs}^{230}Th$ ratio and mass flux holds north of the Polar Front, where low primary productivity coincides with low unsupported $^{231}Pa/^{230}Th$ ratios in surface sediments, with values below the production ratio of both radionuclides (0.093) in the water column. However, high $_{xs}^{231}Pa/_{xs}^{230}Th$ ratios far above 0.093, conventionally interpreted as a high-productivity signal, in surface sediments south of the Polar Front, especially throughout the Weddell Sea, are in contradiction with the low particle fluxes in this region. This observation implies that south of the Polar Front the $_{xs}^{231}Pa/_{xs}^{230}Th$ ratio is affected by secondary factors, in addition to the mass flux of particles.

Two possible explanations for the high $_{xs}^{231}Pa/_{xs}^{230}Th$ signal found in sediments south of the Polar Front are discussed: near-complete scavenging of radionuclide-enriched surface waters during short-time plankton blooms in austral summer (chapter 4), and a southward increase of a particulate phase with a high scavenging efficiency for ^{231}Pa (chapter 3).

The significance of the first possibility was investigated by analysis of sinking particles collected in sediment traps, deployed at various locations within the Antarctic Circumpolar Current, and in the Northern and Central Weddell Sea. Extremely high $_{xs}^{231}Pa/_{xs}^{230}Th$ ratios in all shallow moorings (mostly between 0.3 and 0.4), reflecting strongly enhanced scavenging of ^{231}Pa relative to ^{230}Th, are generated during short-time high-productivity events (diatom blooms) in austral summer, when most of the annual radionuclide flux occurs. The high $_{xs}^{231}Pa/_{xs}^{230}Th$ signal is weakened during downward transport of the bloom particles in the water column by a continuous exchange with suspended particles, which have a lower $_{xs}^{231}Pa/_{xs}^{230}Th$ ratio. Despite the strong N-S enrichment of the dissolved concentrations of ^{230}Th and ^{231}Pa in surface waters due to deep upwelling, a N-S increase in the export fluxes of both radionuclides from the upper water column, and thus a southward increase in the contribution of this layer to the buried flux in the sediment, is not seen. Even south of the Polar Front scavenging from deep waters is still found to be the major source of ^{230}Th and ^{231}Pa to the sediment. These findings make nearly quantitative stripping from a radionuclide-enriched upper water column an unlikely explanation for the high $_{xs}^{231}Pa/_{xs}^{230}Th$ ratios found in Southern Ocean's surface sediments south of the Polar Front and throughout the Weddell Sea.

Measurements of both dissolved and particulate fractions of ^{231}Pa and ^{230}Th in the deep water column, however, show a strong N-S decrease in the $^{230}Th/^{231}Pa$ fractionation factor, from typical open ocean values around 10 north of the Polar

Front to values between 1 and 2 south of 60°S. This observation clearly indicates that the high $_{xs}^{231}Pa/_{xs}^{230}Th$ signal in the sediments are produced by a N-S increase in the scavenging efficiency of ^{231}Pa relative to ^{230}Th, most probably due to a change in the chemical composition of particulate matter, and thus strongly supports the second possibility. It is speculated that biogenic opal, suggested not to significantly fractionate between ^{231}Pa and ^{230}Th, may explain the enhanced scavenging of ^{231}Pa south of the Polar Front. Further support for this assumption comes from the extremely high $_{xs}^{231}Pa/_{xs}^{230}Th$ ratios measured in the shallow traps south of the Polar Front, where fluxes are dominated by biogenic opal (up to 70%).

The results of this study clearly document that in the Southern Ocean, the $_{xs}^{231}Pa/_{xs}^{230}Th$ ratio cannot be applied as a reliable paleoproductivity proxy, as variations of the $_{xs}^{231}Pa/_{xs}^{230}Th$ ratio through time, usually interpreted to reflect changes in the total mass flux of particles, could also be explained by changes in the content of biogenic opal on sinking particles. The high affinity of ^{231}Pa to opal, however, could possibly be used to trace fluxes of biogenic opal to the sediment that have been totally dissolved (e.g. throughout the Weddell Sea).

In the Central Weddell Sea both short-term and long-term scavenging rates of ^{230}Th and ^{231}Pa are strongly reduced, which is a reflexion of both the low particle fluxes and the rapid ventilation of water masses. The low average depositional fluxes for ^{230}Th (33-43% of its production) in the sediment cores, integrated over the last 180ka, put into question the procedure to reconstruct paleofluxes of sedimentary components (C_{org}, biogenic opal, biogenic barium etc.) by excess ^{230}Th normalization. This model is based on the assumption that the flux of ^{230}Th to the seafloor is constant and equal to its production rate from ^{234}U in the overlying water column. Differences between measured and expected accumulation rates of ^{230}Th in oceanic sediments are interpreted to reflect the influence of sediment focussing (>100% of its production) and sediment winnowing (<100% of its production). According to this model the low ^{230}Th inventories in the sediment cores would be regarded as evidence for strong sediment winnowing, so that ^{230}Th-normalized vertical rain rates of sedimentary components would be overestimated by a factor 2-3. On the other hand, in the ACC, where depositional fluxes of ^{230}Th are expected to surpass production in the water column (>100%) the application of the ^{230}Th constant flux model would result in an underestimation of the true vertical rain rate of any sedimentary component.

In regions like the Weddell Sea, where low contents of biogenic carbonate prevent the establishment of a $\delta^{18}O$ stratigraphy, the exponential decay of the $_{xs}^{231}Pa/_{xs}^{230}Th$ ratio with time (half-life: 57.100 yr) provides an independent tool to determine average sediment accumulation rates.

Kurzfassung

Seitdem bekannt ist, daß die marine Produktivität in den Polarregionen ein wichtiger Steuerungsmechanismus für die Verteilung von CO_2 zwischen dem tiefen Ozean und der Atmosphäre ist und damit eine entscheidende Rolle für die globale Klimaentwicklung hat, wächst das Interesse an geeigneten Indikatoren, mit deren Hilfe sich Paläoproduktivitäten der Ozeane in der jüngsten Vergangenheit rekonstruieren lassen. Sie sollen zur Aufklärung der niedrigen CO_2-Gehalte in der glazialen Atmosphäre beitragen.

Einer dieser Paläoproduktivitäts-Indikatoren ist das $^{231}Pa/^{230}Th$-Aktivitätsverhältnis, das im Rahmen dieser Studie auf seine Verläßlichkeit im Südlichen Ozean hin untersucht wurde. Protactinium-231 (Halbwertszeit 32.500 Jahre) und Thorium-230 (Halbwertszeit 75.400 Jahre) sind natürliche Radionuklide, die kontinuierlich in der Wassersäule aus dem Zerfall ihrer Mutternuklide ^{235}U und ^{238}U mit einem konstanten Aktivitätsverhältnis von 0.093 gebildet werden. Der Fluß von ^{230}Th zum Meeresboden ist fast überall im Ozean konstant und entspricht genau seiner Produktionsrate in der Wassersäule. Demgegenüber wird ^{231}Pa bevorzugt in Gebieten mit hohem Partikelfluß abgelagert, wo der Fluß zum Meeresboden die Produktionsrate von ^{231}Pa in der Wassersäule übersteigt. Die Ursache für das unterschiedliche ozeanische Verhalten der beiden Radionuklide liegt in der geringeren Partikelreaktivität von ^{231}Pa, und der dadurch bedingten längeren ozeanischen Verweilzeit von 50-200 Jahren (im Vergleich zu 10-40 Jahren für ^{230}Th). Aus diesem Grund kann ^{231}Pa viel weiter horizontal im Ozean verteilt werden als ^{230}Th, bevor es im Sediment abgelagert wird. Die Fraktionierung der beiden Radionuklide in der Wassersäule ist gut dokumentiert in den $_{xs}^{231}Pa/_{xs}^{230}Th$-Aktivitätsverhältnissen ("xs" steht für die jeweilige korrigierte Aktivität, nach Abzug der detritischen Anteile von ^{230}Th und ^{231}Pa) von ozeanischen Sedimenten. In Gebieten mit niedrigem Partikelfluß, wo nur ein Teil des in der Wassersäule gebildeten ^{231}Pa in den darunterliegenden Sedimenten abgelagert wird (z.B. im offenen Ozean), sind die sedimentären $_{xs}^{231}Pa/_{xs}^{230}Th$-Verhältnisse niedriger als 0.093, während sie in Gebieten mit hohem Partikelfluß (z.B. in Auftriebsgebieten an den Ozeanrändern) größer als 0.093 sind. Diese besonders im Pazifischen Ozean gut ausgeprägte Beziehung zwischen dem $_{xs}^{231}Pa/_{xs}^{230}Th$ Verhältnis und dem Massenfluß von Partikeln bildet die Grundlage für die Anwendung des $_{xs}^{231}Pa/_{xs}^{230}Th$-Verhältnisses in datierten Sedimentkernen als Indikator zur Abschätzung von relativen Schwankungen in der ozeanischen Produktivität in den letzten 150.000 Jahren. Der entscheidende Vorteil des $_{xs}^{231}Pa/_{xs}^{230}Th$-Verhältnisses gegenüber den meisten anderen Paläoproduktivitäts-Anzeigern (wie z.B. organischem Kohlenstoff, biogenem Opal, biogenem Barium) ist, daß es selbst bei einer starken frühdiagenetischen Remineralisation der organischen Substanz am Meeresboden immer noch verläßliche Informationen über den Partikelfluß gibt.

Diese Studie befaßt sich eingehend mit dem "Scavenging" (Entfernung aus der Wassersäule) von ^{230}Th und ^{231}Pa im atlantischen Sektor des Südlichen Ozeans. Ziel der Arbeit ist es herauszufinden, ob das $_{xs}^{231}Pa/_{xs}^{230}Th$-Signal im Sediment auch in dieser Region in erster Linie eine Funktion des Massenflusses von partikulärem Material ist und somit für die Anwendung als Paläoproduktions-

Anzeiger geeignet ist. Dazu wurden umfangreiche Untersuchungen in der Wassersäule (gelöste und fein partikuläre Phase), an Sinkstoffallenmaterial, im Oberflächensediment sowie in Sedimentkernen durchgeführt.

Nördlich der heutigen Position der Polarfront, die im Südatlantik bei etwa 50° südlicher Breite liegt, ist das $_{xs}^{231}Pa/_{xs}^{230}Th$-Verhältnis ein guter Indikator für den Massenfluß von Partikeln. Sehr niedrige $_{xs}^{231}Pa/_{xs}^{230}Th$-Verhältnisse in den Oberflächensedimenten (kleiner als 0.093) stimmen mit der niedrigen Bioproduktivität in dieser Region überein. Südlich der Polarfront und insbesondere im Weddellmeer sind die $_{xs}^{231}Pa/_{xs}^{230}Th$-Verhältnisse in den Oberflächensedimenten hingegen sehr hoch (0.13 bis 0.17). Derart hohe $_{xs}^{231}Pa/_{xs}^{230}Th$-Verhältnisse, die man sonst nur von Hochproduktionsgebieten an den Ozeanrändern kennt (z.B. aus dem Panama und Guatemala Becken), stehen im Widerspruch zur niedrigen Produktivität in dieser Region. Diese Beobachtung ist ein klares Anzeichen dafür, daß das $_{xs}^{231}Pa/_{xs}^{230}Th$-Signal südlich der Polarfront durch sekundäre Faktoren zusätzlich zum Massenfluß von Partikeln bestimmt wird.

Zwei mögliche Erklärungen für die hohen $_{xs}^{231}Pa/_{xs}^{230}Th$-Verhältnisse in Sedimenten südlich der Polarfront wurden im Rahmen dieser Arbeit diskutiert. Erstens: eine nahezu vollständige Entfernung von ^{230}Th und ^{231}Pa aus mit Radionukliden angereichertem Oberflächenwasser, ausgelöst durch kurzzeitige produktive Phasen im antarktischen Sommer (Kapitel 4). Zweitens: ein nach Süden hin zunehmender Anteil einer partikulären Phase, die eine hohe Affinität gegenüber ^{231}Pa besitzt (Kapitel 3).

Zur Abschätzung der Bedeutung der ersten Möglichkeit auf das sedimentäre $_{xs}^{231}Pa/_{xs}^{230}Th$-Signal wurden Analysen an Sinkstoffallenmaterial durchgeführt, das in verschiedenen Regionen des Antarktischen Zirkumpolarstroms (ACC) sowie im nördlichen und zentralen Weddellmeer gesammelt wurde. Die $_{xs}^{231}Pa/_{xs}^{230}Th$-Verhältnisse in allen oberflächennahen Sinkstoffallen (flacher als 700m) sind extrem hoch (in der Regel zwischen 0.3 und 0.4), was auf ein stark erhöhtes Scavenging von ^{231}Pa relativ zu ^{230}Th hindeutet. Dieses ungewöhnlich hohe Signal wird während kurzzeitiger Hochproduktionsphasen im antarktischen Sommer (Planktonblüten) in der euphotischen Zone gebildet. In dieser Zeit finden zwischen 75 und 95% des jährlichen Partikel- und Radionuklidflusses statt. Bei ihrem Transport durch die Wassersäule wird das hohe $_{xs}^{231}Pa/_{xs}^{230}Th$-Signal der in der euphotischen Zone gebildeten Partikel, durch einen kontinuierlichen Austausch mit suspendierten Partikeln der tieferen Wassersäule, die eine mit der Wassertiefe zunehmend niedrigere $_{xs}^{231}Pa/_{xs}^{230}Th$-Signatur aufweisen, immer mehr abgeschwächt. Trotz der als Folge des tiefen Auftriebs nach Süden hin stark zunehmenden Radionuklid-Konzentrationen im Oberflächenwasser gibt es keine Anzeichen für eine Zunahme im Exportfluß von ^{230}Th und ^{231}Pa von der oberen Wassersäule mit der geograhischen Breite. Diese Feststellung schließt eine Erklärung der hohen $_{xs}^{231}Pa/_{xs}^{230}Th$-Verhältnisse in den Oberflächensedimenten südlich der Polarfront durch ein fast quantitatives Scavenging der beiden Radionuklide im Oberflächenwasser während der kurzen produktiven Zeit im antarktischen Sommer aus. Vielmehr zeigt sich, daß auch in dieser von extremer Saisonalität geprägten Region das $_{xs}^{231}Pa/_{xs}^{230}Th$-Signal im Sediment in erster Linie durch Scavenging im Tiefenwasser bestimmt wird.

Messungen der gelösten und partikulären Anteile von ^{231}Pa und ^{230}Th in der tiefen Wassersäule des Südatlantiks zeigen einen Gradient im $^{230}Th/^{231}Pa$-Fraktionierungsfaktor (F) mit der geographischen Breite. Dieser ist folgendermaßen definiert:

$$F = \frac{(^{230}Th/^{231}Pa)_{part}}{(^{230}Th/^{231}Pa)_{diss}}$$

F-Faktoren im Bereich von 10, typisch für den offenen Ozean, die auf eine erhöhte Präferenz für die Adsorption von ^{230}Th relativ zu ^{231}Pa an Partikel hinweisen, treten nur nördlich der Polarfront auf. Nach Süden hin nimmt der F-Faktor stark ab und erreicht relativ konstante Werte zwischen 1 und 2 südlich von 60°S. Die starke Nord-Süd Abnahme des F-Faktors deutet darauf hin, daß die hohen $_{xs}^{231}Pa/_{xs}^{230}Th$-Verhältnisse in Oberflächensedimenten südlich der Polarfront auf eine Zunahme der Scavenging Effizienz von ^{231}Pa relativ zu ^{230}Th, wahrscheinlich durch eine Änderung in der chemischen Zusammensetzung von partikulärem Material, zurückzuführen sind. Die starke Nord-Süd Zunahme des Gehalts an biogenem Opal auf partikulärem Material, der praktisch keine Fraktionierung bei der Adsorption von ^{230}Th und ^{231}Pa zeigt (F-Faktor = 1.1), könnte der Grund für das erhöhte Scavenging von ^{231}Pa südlich der Polarfront sein. Dafür sprechen auch die extrem hohen $_{xs}^{231}Pa/_{xs}^{230}Th$-Verhältnisse in Sinkstofffallenmaterial südlich der Polarfront mit einem Opalgehalt von bis zu 70% des gesamten Sedimentationsflusses.

Die Ergebnisse dieser Studie machen deutlich, daß das $_{xs}^{231}Pa/_{xs}^{230}Th$-Verhältnis im Südlichen Ozean kein verläßlicher Anzeiger für den Massenfluß von partikulärem Material ist, was wahrscheinlich auf die hohen Opalgehalte der Sinkstoffe zurückzuführen ist. Die hohe Affinität von ^{231}Pa gegenüber biogenem Opal hat wichtige Konsequenzen für die Interpretation von $_{xs}^{231}Pa/_{xs}^{230}Th$-Verhältnissen in datierten Sedimentkernen. Zeitliche Variationen im $_{xs}^{231}Pa/_{xs}^{230}Th$-Verhältnis, die normalerweise als Anzeichen für Änderungen im Massenfluß von partikulärem Material interpretiert werden, könnten nämlich auch auf zeitliche Änderungen in der chemischen Zusammensetzung von partikulärem Material (Schwankungen im Opal-Gehalt) zurückzuführen sein. Die Anwendung des $_{xs}^{231}Pa/_{xs}^{230}Th$-Verhältnisses zur Abschätzung von relativen Schwankungen in der Paläoproduktivität im Südlichen Ozean verlangt daher die genaue Kenntnis über glaziale-interglaziele Änderungen im Opal-Gehalt von partikulärem Material. Verläßliche paläozeanographische Rekonstruktionen sind ohnehin nur in Kombination mit weiteren unabhängigen Paläoproduktivitäts-Anzeigern (wie z.B. biogenem Barium, authigenem Uran) möglich. Die hohe Affinität von ^{231}Pa gegenüber biogenem Opal könnte möglicherweise dazu benutzt werden, vergangene Opalflüsse, die im Sediment nicht erhalten sind, wie dies z.B. im Weddellmeer der Fall ist, zu erkennen.

Sowohl die Sedimentfallenergebnisse, also auch der im Sediment gespeicherte Langzeit-Bericht deuten auf ein im Weddellmeer stark reduziertes Scavenging von ^{230}Th (nur ca. 40% der Produktion) und ^{231}Pa (ca. 50% der Produktion) hin. Dies ist eine Folge der geringen Partikelflüsse, sowie der kurzen Residenzzeit der

Wassermassen im Weddellbecken, welche in etwa der ozeanischen Residenzzeit von ^{230}Th entspricht. Dies hat zur Folge, daß mehr als die Hälfte des im Weddellmeer gebildeten ^{230}Th und etwa die Hälfte des dort gebildeten ^{231}Pa durch horizontale Advektion in andere Regionen des Südlichen Ozeans transportiert werden, wo sie schließlich in den Sedimenten abgelagert werden. Das Weddellmeer stellt somit eine Quelle für ^{230}Th und ^{231}Pa dar.

Die niedrigen ^{230}Th Inventare (nur 33 bis 43% der Produktion) in Sedimenten des Weddellmeeres während der letzten 180.000 Jahre schränken die Anwendung des ^{230}Th Konstanten-Fluß-Modells zur Abschätzung von vertikalen Partikelflüssen von biogenen Komponenten, wie z.B organischem Kohlenstoff, biogenem Opal, biogenem Barium, in dieser Region stark ein. Insbesondere im Südlichen Ozean, wo durch starke Bodenströmungen bedingter lateraler Sedimenttransport (Erosion, Fokussierung) häufig keine verläßlichen Aussagen mehr über den vertikalen Fluß biogener Komponenten erlaubt, findet dieses Modell in der Paläozeanographie weite Anwendung. Es basiert darauf, daß der Sedimentationsfluß von ^{230}Th überall im Ozean konstant ist und genau seiner Produktionsrate aus ^{234}U in der darüberliegenden Wassersäule entspricht, und damit 100% beträgt. Die Aktivität von ^{230}Th im Oberflächensediment ist somit umgekehrt proportional zur Massenfluß. Die zerfallskorrigierte Aktivität von ^{230}Th kann dann als Referenz zur Abschätzung von vertikalen Flußraten jeder beliebigen sedimentären Komponente benutzt werden. Nach diesem Modell würden die niedrigen ^{230}Th Inventare in den Sedimentkernen als Indiz für das Auftreten von starker Sediment-Erosion an diesen Lokalitäten interpretiert (57 bis 67% ihrer ursprünglichen Inventare wären nachträglich erodiert worden). Ohne eine entsprechende Korrektur für das reduzierte Scavenging von ^{230}Th würden die vertikalen Flußraten biogener Komponenten im Weddellmeer nach diesem Modell also um einen Faktor 2 bis 3 überschätzt. Die aus dem Weddellmeer exportierten Anteile von ^{230}Th und ^{231}Pa werden in Gebieten mit höherem Partikelfluß, wahrscheinlich innerhalb des ACC, der eine Senke für ^{231}Pa und ^{230}Th ist, abgelagert. Entsprechend ist auch in dieser Region die Anwendung des ^{230}Th Konstanten-Fluß-Modells eingeschränkt, weil das zusätzliche Scavenging von ^{230}Th zur lokalen Produktion als Anzeichen für Sediment-Fokussierung betrachtet würde. Folglich würden die vertikalen Flüsse sedimentärer Komponenten unterschätzt.

Im Weddellmeer, wo aufgrund der niedrigen Gehalte von biogenem Karbonat im Sediment eine Altersbestimmung mittels δ^{18}O-Stratigraphie nicht möglich ist, wird immer noch nach geeigneten Methoden zur Altersklassifizierung der dortigen Sedimente gesucht. Gute Ergebnisse verspricht man sich von einer neuen radiostratigraphische Methode, die auf der Interpretation von Maxima und Minima in den Konzentrationen von ^{230}Th in den Kernen basiert. In diesem Modell wird angenommen, daß das charakteristische Maximum in der Aktivität von ^{230}Th, das in fast allen Kernen des Weddellmeeres zu sehen ist, das Interglazial-Stadium 5e reflektiert. Einen Beweis für diese Vermutung gibt es bislang jedoch noch nicht. Der exponentielle Zerfall des $_{xs}^{231}$Pa/$_{xs}^{230}$Th-Verhältnisses mit der Kerntiefe bietet hier eine unabhängige Methode zur Bestimmung von durchschnittlichen Sedimentationsraten und damit zur Überprüfung dieser These. Die Ergebnisse der Sedimentkerne des zentralen Weddellmeeres lassen vermuten, daß das charakteristische $_{xs}$ ^{230}Th -Maximum tatsächlich Interglazial 5e reflektiert und somit eine zusätzliche Hilfe bei der Alterseinstufung von Sedimenten sein kann.

1 Introduction

1.1 The reconstruction of past productivity: Tracers proposed for the Southern Ocean

Oceanic productivity is considered to be an important factor regulating the partitioning of CO_2 between the deep ocean and the atmosphere (e.g. Broecker and Peng, 1982). In the euphotic zone, CO_2 is taken up by phytoplankton and converted into organic matter. The fraction of the organic carbon that escapes heterotrophic regeneration and remineralization is exported from the euphotic zone into the deep sea. This so-called 'biological carbon pump' provides a continuous flux of particulate organic material from the surface to the deep ocean (e.g. Eppley and Peterson, 1979; Broecker and Peng, 1982; Martin et al. 1987), and lowers the partial pressure of CO_2 in surface waters (e.g. Berger et al., 1989; Wolf-Gladrow, 1994). Since there is a continuous exchange between the atmospheric and oceanic CO_2 reservoirs (e.g. Wolf-Gladrow, 1994), areas of high export productivity, such as the equator and coastal upwelling regions, act as effective sinks for CO_2.

In large areas of the oceans, primary productivity is limited by the availability of nutrients (phosphate and nitrate) in the mixed layer (Broecker and Peng, 1982; Berger et al., 1989). This does not hold for the Southern Ocean where nutrient concentrations in surface waters are high (e.g. Levitus et al., 1993), and thus cannot limit biological productivity. This gave rise to the hypothesis that the Southern Ocean has a high potential to take up CO_2 from the atmosphere if primary production increases (Knox and McElroy, 1984; Sarmiento and Toggweiler, 1984; Siegenthaler and Wenk, 1984). Martin (1990) postulated that iron, which at present limits biological productivity in the Southern Ocean, was supplied in glacial periods from the desert areas of Patagonia by aeolian dust. The removal of the iron limitation could have enabled phytoplankton to consume nearly all of the nutrients upwelled into the surface waters (Martin, 1990). Model calculations (e.g. Sarmiento and Toggweiler, 1984) have shown that the increase in bioproductivity, expected from complete consumption of nutrients, indeed would be sufficient to explain the low atmospheric CO_2 concentrations that have existed during glacial periods (e.g. Berner et al., 1980; Barnola et al., 1987; 1991). An unambiguous means of assessing past changes in ocean productivity, however, has been lacking.

In order to verify the validity of this 'polar nutrient hypothesis', attempts have been made to reconstruct nutrient contents of glacial Southern Ocean surface waters from the $\delta^{13}C$ and Cd/Ca record in foraminiferal calcite. However, both tracers have failed to provide evidence for the greatly increased bioproductivity expected from iron fertilization. Rather, the lower $\delta^{13}C$ record of planktonic foraminifera implies higher glacial nutrient concentrations in surface waters (e.g. Charles and Fairbanks, 1990), whereas Cd/Ca ratios suggest relatively constant phosphate concentrations (Boyle, 1988; 1992; Keigwin and Boyle, 1989). Various explanations for the disagreement of the two tracer records have been given (summarized in Boyle, 1994), but none of them has yet been proved to be satisfactory. In recent years, the $\delta^{15}N$ signal in organic matter has been proposed as a new tracer for surface nutrient utilization (Francois et al., 1992; 1993, Calvert et al., 1992; Altabet and Francois, 1994). First paleoceanographic applications provided evidence that the Southern Ocean was more depleted in nutrients during the Last Glacial Maximum (Francois

et al., 1993; Francois et al., submitted). However, it has not yet been clarified to what extent the preferential preservation of some groups of organic compounds during early diagenetic processes (e.g. Jumars et al., 1989) may alter the primary $\delta^{15}N$ isotopic signal from the euphotic zone (Altabet and Francois, 1994). This uncertainty limits a more general application of the $\delta^{15}N$ signal as a proxy for nutrient utilization in the past.

Past changes in surface ocean productivity may, in principal, also be assessed from the burial rates of organic carbon (C_{org}) and carbonate (e.g. Berger et al., 1987). However, both compounds are particularly susceptible to remineralization in the water column and during early diagenesis in the sediment (e.g. Berger, 1973; Emerson and Hedges, 1988). In view of this, there is no consensus whether or not the variations in C_{org} and carbonate content preserved in the sediments reflect real changes in productivity or changes in preservation efficiency. In the Southern Ocean, export of organic carbon and nutrients to the deep sea is largely driven by diatoms (e.g. Wefer and Fischer, 1991) resulting in the deposition of biogenic opal in the sediments (DeMaster, 1981; Schlüter et al., submitted). Investigators have therefore used opal accumulation rates to reconstruct productivity of the overlying water column (Charles et al., 1991; Mortlock et al., 1991). These authors found that the zone of high opal productivity moved northward during glacial periods, whereas the total amount of opal accumulation integrated over the entire Southern Ocean was unaffected or even decreased (Mortlock et al., 1991). There are, however, two uncertainties in their interpretation of the opal records. First, the authors did not consider the effect of lateral sediment redistribution, which can dramatically affect accumulation rates in this region (Francois et al., 1993; Kumar, 1994), and thus obscure the 'true' changes in accumulation rates caused by changes in vertical rain rate. Second, biogenic opal is also subject to dissolution at the sediment water interface (e.g. Van-Bennekom et al., 1988; Schlueter et al., submitted). Especially in areas of very low accumulation rates, such as the Weddell Sea, biogenic opal can dissolve almost completely at the sediment surface (Schlueter et al., submitted).

A more recent evaluation by Kumar et al. (1995), using a ^{230}Th-normalization approach (Francois et al., 1993, 1995) to correct for lateral sediment transport points to a twofold increased opal burial rate in cores north of the Polar Front during glacial periods. These new findings thus support the hypothesis of an enhanced export productivity in the Southern Ocean during glacial periods. In order to further constrain their hypothesis an independent approach, based on the record of authigenic uranium, was made (Kumar et al., 1995). In oxic porewater, U is present as a soluble carbonte complex, whereas under reducing conditions (e.g. caused by a high flux of metabolizable organic matter) U is reduced and precipitates, creating a pore water gradient, which transports U from the overlying seawater into the sediments (Klinkhammer and Palmer, 1991). Indeed, Kumar and his collegues found very large peaks of authigenic U in glacial sections of cores in the subantarctic zone, which were taken as evidence for a strong increase in the flux of organic carbon in the glacial Southern Ocean, even larger than suggested from the increase in opal flux (Kumar et al., 1995). However, accumulation rates of authigenic U in sediments are not only controlled by the export flux of metabolizable organic matter, but also by the concentration of O_2 in bottom waters. Since there is evidence for a glacial reduction of O_2 concentrations in bottom waters in two cores from the Indian sector of the Southern Ocean (Francois et al., submitted), these authors suggested that this may also hold for the Atlantic sector. This led Francois et

al. (submitted) to argue, that the large authigenic U peaks found in the glacial section of Atlantic cores by Kumar et al. (1995) could also be explained by a decrease in bottom water oxygen concentration, without the need of an enhanced export flux of organic carbon.

In recent years the search for proxies for export productivity that are less sensitive to diagenetic overprints has been intensified. Biogenic Barium is suggested to be such a tracer (e.g. Dymond et al., 1992; Nürnberg, 1995). The reliability of Ba as a productivity proxy rests on the strong association of barite particles with export productivity (e.g. Dehairs et al., 1980; Dymond et al., 1992; Francois et al., 1995). Under oxic conditions barite is very stable (Dymond et al., 1992) and thus potentially better preserved than other traditional proxies. Caution must be taken, however, when interpreting biogenic Ba fluxes in rapidly accumulating reducing sediments, where barite may dissolve (Nürnberg, 1995, Francois et al., submitted). Accumulation rates of biogenic Ba in the sediment have been used to assess past changes in productivity of the Southern Ocean (Shimmield et al., 1994, Frank, 1995, Frank et al., 1995, Nürnberg, 1995, Bonn, 1995). An uncertainty in most of these paleoceanographic approaches (Shimmield et al., 1994, Nürnberg, 1995, Bonn, 1995), however, is the inability to distinguish between changes in accumulation resulting from productivity-controlled vertical rain rates and those resulting from variations in lateral sediment redistribution. Only recently, 230Th-normalization has been applied to Ba data (Frank, 1995, Frank et al., 1995, Francois et al. submitted). Based on the vertical rain rates of biogenic Ba these authors concluded that the increase in glacial productivity north of the Polar Front must have been much smaller than previously assumed (e.g. Kumar et al., 1995), and therefore does not support the idea of a glacial iron fertilization to account for the drawdown for atmospheric CO_2 (e.g. Martin, 1990, Kumar et al., 1995).

1.2 The $^{231}Pa/^{230}Th$ ratio, a useful tracer for paleoproductivity in the Southern Ocean?

The paleoceanographic informations gathered thus far from the Southern Ocean by the various tracer approaches clearly demonstrate that there is no general consensus about the polar nutrient hypothesis. It must be emphasized, however, that each of these tracers incorporates a set of assumptions, some of which are largely unproven, so that general interpretations are subject to considerable uncertainty. This led to the development of new independent methods of evaluating past changes in ocean productivity, one of which is the $^{231}Pa/^{230}Th$ activity ratio (Kumar et al., 1993; Francois et al., 1994; Yu, 1994), which is the subject of this study. The principles on which this paleoceanographic tool is based are discussed in detail in chapter 2. A high $^{231}Pa/^{230}Th$ ratio stands for a high particle flux and a low ratio for a low particle flux. The major advantage of using this radionuclide ratio, is that, unlike other proxies e.g. C_{org}, carbonate, biogenic opal, biogenic Ba, authigenic U, it is not affected by dissolution on the seafloor and thus will retain information on vertical rain rates even when significant post-depositional dissolution occurs. Moreover, it is insensitive to effects of sediment redistribution (e.g. Kumar et al., 1993; Francois et al., 1993).

Recent multitracer approaches in the Atlantic sector of the Southern Ocean have shown that north of the Polar Front the glacial $^{231}Pa/^{230}Th$ record is consistent with

that of biogenic opal (Kumar et al., 1995; Francois et al., submitted) and authigenic U (Kumar et al., 1995), which underlines its potential as a tracer to reconstruct paleoproductivity. The $^{231}Pa/^{230}Th$ record thus adds to the argument of a glacial increase in export productivity in the Southern Ocean north of the Polar Front (Kumar et al., 1995). In one core south the Polar Front (54°S), however, high glacial $^{231}Pa/^{230}Th$ ratios, conventionally interpreted to reflect high productivity, did not support the expected glacial decrease in export productivity deduced from the decreasing accumulation rates of biogenic opal and authigenic U (Kumar et al., 1993; 1995). Moreover, unusually high $^{231}Pa/^{230}Th$ ratios south of the Polar Front, in conflict with the known low productivity, have also been reported in some modern Southern Ocean sediments (Lao et al., 1992a; Yu et al., 1996). These observations, together with those of Rutgers van der Loeff and Berger (1993) of a southward increase with latitude in the scavenging preference of ^{231}Pa relative to ^{230}Th, led previous authors (Lao et al., 1992a; Rutgers van der Loeff and Berger, 1993; Kumar et al., 1995) to suggest that south of the Polar Front the $^{231}Pa/^{230}Th$ is influenced by secondary factors. Unequivocal evidence for their speculation, however, is still lacking.

1.3 Objectives of this study

The primary objective of this study is therefore to find out whether at high latitudes in the South Atlantic, the $^{231}Pa/^{230}Th$ ratio is still a reliable tracer for the mass flux of particles. Only if this can be ascertained, the $^{231}Pa/^{230}Th$ signal buried in the sediment can be reliably used to assess relative changes in export production in the past. Towards this objective the factors that control scavenging of ^{231}Pa and ^{230}Th in this region were investigated.

It is known from other oceanic regions that in addition to the mass flux the $^{231}Pa/^{230}Th$ ratio can be influenced by several other factors (for a review see chapter 2). One of those is the chemical composition of particles (Anderson et al., 1983b; Shimmield et al., 1988; Taguchi et al., 1989; Anderson et al., 1992; Lao et al., 1992; Rutgers van der Loeff and Berger, 1993). E.g. it is suggested that ^{231}Pa exhibits a stronger affinity for scavenging by biogenic opal and MnO_2 than by other particulate phases (e.g. Anderson et al., 1992). If true, then this preference could possibly result in high $^{231}Pa/^{230}Th$ ratios, independent from the particle flux, in sediments south of the Polar Front where sedimenting fluxes are dominated by biogenic opal (e.g. Wefer and Fischer, 1991).

Moreover, scavenging of ^{231}Pa and ^{230}Th might be influenced by two particularities of the Southern Ocean: first its high seasonality in primary production (El-Sayed and Taguchi, 1981; Smith and Nelson, 1986), and second the high concentrations of ^{231}Pa and ^{230}Th in surface waters resulting from deep upwelling (Rutgers van der Loeff and Berger, 1993). The $^{231}Pa/^{230}Th$ signal buried in the sediment could, at least in part, result from nearly quantitative stripping of ^{231}Pa and ^{230}Th in surface waters during short-time high productivity events (plankton blooms).

It is to be clarified to what extent these secondary factors affect the relationship between $^{231}Pa/^{230}Th$ ratio and total mass flux in the Southern Ocean. To answer this question the following strategy was employed:

- $^{231}Pa/^{230}Th$ ratios were analyzed in surface sediments throughout the South Atlantic, in areas of variable mass fluxes and compositions of particulate matter, to find out where the ratio is primarily determined by the particle flux, and where the influence of secondary factors becomes predominant.

- The influence of the chemical composition of particulate matter on the relative scavenging efficiency of ^{231}Pa and ^{230}Th was investigated by determining $^{230}Th/^{231}Pa$ fractionation factors (defined in chapter 2), as well as by analysis of $^{231}Pa/^{230}Th$ ratios in sinking particles with known chemical composition.

- The significance of scavenging from the upper water column during high-flux periods was estimated by calculating export fluxes of ^{231}Pa and ^{230}Th from this layer.

- For the Weddell Sea the role of an additional factor namely the export of dissolved ^{231}Pa and ^{230}Th by horizontal advection was investigated by calculating short- and long-term burial fluxes of both radionuclides.

In summary, the goal of this study is to better understand the $^{231}Pa/^{230}Th$ signal in Southern Ocean sediments. Only if the various factors controlling the scavenging of ^{231}Pa and ^{230}Th in this region are well known, a reliable application of this paleoceanographic tool is possible. This study may thus help to solve some of the problems and inconsistencies involved in the reconstruction of past changes in export production of the Southern Ocean by the various tracer approaches.

1.4 Outline of this study

This study includes three chapters (2 to 4) representing previously published or submitted articles. In Chapter 2 (Reliability of the $^{231}Pa/^{230}Th$ activity ratio as a tracer for bioproductivity of the ocean: Walter H.J., Rutgers van der Loeff M.M. and Francois R. *Proxies in Paleoceanography - Examples from the South Atlantic. Fischer G. and Wefer G. (eds.), in press)* a state of the art review of the strength of the $^{231}Pa/^{230}Th$ ratio as a tracer for bioproductivity is given. It describes in detail the oceanographic behavior of ^{231}Pa and ^{230}Th, and discusses the conditions required for establishing a clear relationship between the $^{231}Pa/^{230}Th$ ratio in the sediment and the mass flux of particles. It provides a model explaining the large-scale distributions of $^{231}Pa/^{230}Th$ ratios in deep-sea sediments in a closed and a ventilated ocean basin. Based on compiled data from the modern Pacific, the Atlantic and the Southern Ocean, an evaluation is given of the reliability of the $^{231}Pa/^{230}Th$ ratio as a paleoproductivity proxy in these ocean basins. It should be noted that the discussion of the Southern Ocean includes the highlights of chapter 3, since these new data challenge the existing interpretation of $^{231}Pa/^{230}Th$ ratios in this region. Chapter 3 (Enhanced scavenging of 231Pa relative to 230Th in the South Atlantic south of the Polar Front: Implications for the use of the $^{231}Pa/^{230}Th$ ratio as a paleoproductivity proxy: Walter H.J., Rutgers van der Loeff M.M. and Hoeltzen H. *Earth Planet. Sci. Lett. 149 (1997) 85-100)* then addresses the fractionation between ^{231}Pa and ^{230}Th in the Southern Ocean in more detail. It is examined in how far a change in the chemical composition of particles influences

the fractionation between the two radionuclides. Chapter 4 (Surface and deep-water scavenging of ^{231}Pa and ^{230}Th under high seasonality in mass flux: Implications for lateral distribution in the Atlantic sector of the Southern Ocean: Walter H.J., Rutgers van der Loeff M.M., Hoeltzen H., Bathmann U. and Fischer G. *submitted to Deep Sea Research)* discusses the influence of nearly quantitative stripping of ^{231}Pa and ^{230}Th in surface waters during short high-flux periods on the $^{231}Pa/^{230}Th$ signal in the sediment. It is further discussed to what extent the Weddell Sea is a net source for ^{231}Pa and ^{230}Th to other regions of the Southern Ocean.

2 Reliability of the $^{231}Pa/^{230}Th$ activity ratio as a tracer for bio-productivity of the ocean

H.J. Walter[1], M.M. Rutgers van der Loeff[1] and R. Francois[2]

[1] Alfred Wegener Institute for Polar and Marine Research, Bremerhaven, Germany
[2] Department of Marine Chemistry, Woods Hole Oceanographic Institution, Woods Hole, Massachusetts, USA

2.1 Abstract

In large areas of the world's oceans, there is a relationship between the mass flux of particulate matter and the unsupported $^{231}Pa/^{230}Th$ ($_{xs}^{231}Pa/_{xs}^{230}Th$) activity ratio of recent sediments. This observation forms the basis for using the $_{xs}^{231}Pa/_{xs}^{230}Th$ ratio as a proxy for past changes in export productivity. However, a simple relationship between $_{xs}^{231}Pa/_{xs}^{230}Th$ ratio and particle flux requires that the water residence time in an ocean basin is far in excess of the scavenging residence time of ^{231}Pa, and that the composition of sinking particles maintains a strong preference for the adsorption of ^{230}Th over ^{231}Pa with a constant $^{230}Th/^{231}Pa$ fractionation factor (F). The best correlation between $_{xs}^{231}Pa/_{xs}^{230}Th$ ratio and mass flux is found in the Pacific ocean. In the Atlantic, the contrast in the $_{xs}^{231}Pa/_{xs}^{230}Th$ ratios between open ocean (low flux regions) and ocean margins (high flux regions) is much less pronounced due to the shorter residence time of deep water, resulting in less effective boundary scavenging of ^{231}Pa. In the Southern Ocean, south of the Polar Front, there is no more a simple relationship between $_{xs}^{231}Pa/_{xs}^{230}Th$ and particle flux. This is a result of a southward decrease in F, probably reflecting the increased opal content of sinking particles. Opal does not fractionate ^{231}Pa and ^{230}Th significantly. This lack of fractionation results in high $_{xs}^{231}Pa/_{xs}^{230}Th$ ratios in opal-dominated regions, even in areas of very low particle fluxes such as the Weddell Sea. The $_{xs}^{231}Pa/_{xs}^{230}Th$ ratio can therefore only be used as a paleoproductivity proxy if, in the time interval of interest, changes in the basin ventilation rate and differential scavenging of both radionuclides due to changes in the chemical composition of particulate matter can be excluded.

2.2 Introduction

The $^{231}Pa/^{230}Th$ activity ratio in sediments has been proposed and used (Lao et al., 1992a; 1992b; Kumar et al., 1993; Francois et al., 1993; Kumar, 1994; Yu, 1994; Boyle, 1996; Kumar et al., 1995; Yang et al., 1995) as a tracer to assess changes in bioproductivity of the ocean during the last 150.000 years. The major advantage of the $^{231}Pa/^{230}Th$ ratio compared to other productivity tracers (e.g. C_{org}, biogenic opal, biogenic Ba) is its insensitivity to remineralization of the biogenic detritus both in the water column and in surface sediments (Anderson et al., 1983a; 1983b; Lao et al., 1992a; 1992b; 1993; Kumar et al., 1993).

$^{231}Pa/^{230}Th$ ratios are also affected by secondary processes, which complicate their interpretation in terms of export production. Its reliability as a paleoproductivity

proxy can be tested by comparing unsupported $^{231}Pa/^{230}Th$ ratios ($_{xs}^{231}Pa/_{xs}^{230}Th$, corrected for detrital, U-supported activities of ^{231}Pa and ^{230}Th) in modern oceanic sediments with primary production in surface waters. Using this approach, we outline the conditions required for producing a linear relationship between the particle flux (as an index for export production) and the $_{xs}^{231}Pa/_{xs}^{230}Th$ ratio in the sediment. We also establish the circumstances under which the influence of other factors, such as the advective transport of ^{231}Pa between ocean basins and changes in the chemical composition of settling particles, become predominant and limit the use of the $_{xs}^{231}Pa/_{xs}^{230}Th$ ratio as an indicator of paleoproductivity.

2.2.1 Theory

Both ^{231}Pa (half-life: 32.500 years and ^{230}Th (half-life: 75.400 years) are natural radionuclides, which are continuously produced in seawater by in situ decay of their dissolved progenitors ^{235}U and ^{234}U (their only significant source in the ocean). Since the residence time of uranium in the ocean (several hundred thousand years; Cochran, 1982; Chen et al., 1986) is long compared to the mixing time of the oceans (approx. thousand years, Broecker and Peng, 1982), the distribution of U throughout the oceans is very homogenous. As a result, both ^{231}Pa and ^{230}Th are produced in seawater at a constant rate with an initial $^{231}Pa/\ ^{230}Th$ activity ratio of 0.093. In contrast to U, ^{231}Pa and ^{230}Th are particle reactive and are scavenged to the sea floor on time scales of about 50-200 years and 5-40 years, respectively (Nozaki et al., 1981; Anderson et al., 1983a; 1983b; Nozaki and Nakanishi, 1985; Nozaki and Yamada, 1987; Huh and Beasley, 1987; Rutgers van der Loeff and Berger, 1993; Guo et al., 1995). Because these time scales are short compared to their half-lives, radioactive decay in the water column can be neglected. Consequently, if ^{230}Th and ^{231}Pa are scavenged from the water column without fractionation, we should expect an ocean-wide $_{xs}^{231}Pa/_{xs}^{230}Th$ ratio in newly formed sediment equal to the production ratio of 0.093.

Variable $_{xs}^{231}Pa/_{xs}^{230}Th$ ratios in surface sediments throughout the oceans indicate that both radionuclides follow different pathways of removal from seawater. Because of its short residence time in the water column, horizontal transport of ^{230}Th before scavenging is minimal over most of the ocean. As a result, the flux of ^{230}Th to the seafloor is nearly identical to its rate of production in the water column (Anderson et al., 1983a; 1983b; Bacon et al., 1985; Taguchi et al., 1989; Yu, 1994). In contrast, the longer oceanic residence time for dissolved ^{231}Pa allows a large scale diffusive transport of this nuclide over basin-wide distances prior to scavenging, resulting in its preferential removal in high particle flux regions (Anderson et al., 1983a; 1983b; Yang et al., 1986; Bacon, 1988; Lao et al., 1992b; 1993; Yu et al., 1996). Since ^{231}Pa is often found at ocean margins (DeMaster, 1979; Anderson et al. 1983a; 1983b; Shimmield et al., 1986), this preferential removal is known as "boundary scavenging".

2.2.2 Boundary scavenging

In principle, three requirements have to be met for effective boundary scavenging of a particle reactive element. First, there must be intensified scavenging at the ocean

margins or other areas of the oceans to produce horizontal gradients in the dissolved radionuclide concentration. These gradients will then maintain a net diffusive transport from low particle flux regions (with low scavenging rates) to high particle flux regions (with high scavenging rates). Second, the scavenging residence time of the radionuclide must be longer than the timescale required for diffusive lateral mixing within the ocean basin, so that significant quantities of the dissolved radionuclide generated in low flux regions can be transported to high flux regions prior to being removed from the water column. Third, the mean residence time of water in the ocean basin must be long compared to the scavenging residence time of the radionuclide and the time required for lateral mixing within the basin.

In order to demonstrate how these three factors affect the large-scale distributions of ^{231}Pa and ^{230}Th throughout the ocean, a simplified version of the scavenging model developed for the Pacific ocean by Bacon (1988) is used (model A, in Fig.2-1). In contrast to the original model, in our illustration the influence of the chemical composition of particulate matter on the scavenging of ^{231}Pa and ^{230}Th is not considered.

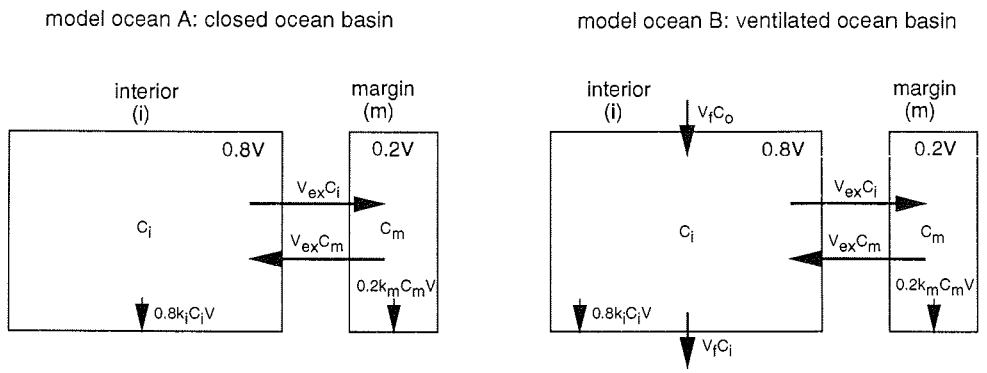

Fig.2-1: Box model illustration of a closed (model A) and a ventilated (model B) idealized ocean basin. Model parameters are given in Table 2-1. Horizontal arrows show lateral fluid exchange between boxes i and m at a rate v_{ex}, whereas depositional fluxes are indicated by the small vertical arrows at the bottom of each box. In model B, the two large vertical arrows illustrate flushing of the interior box at a rate v_f. See text for further details.

The ocean (volume V) is divided into two boxes, an interior box represented with suffix i, with 80% of the total volume of the ocean (0.8V), and a margin box with suffix m containing 20% (0.2V) of the total volume of the ocean (Fig.2-1). Each box has average radionuclide concentrations C_i and C_m, respectively. There is horizontal fluid exchange between boxes i and m at a rate v_{ex}. The scavenging rates in each box are given by rate coefficients k. The material balances for ^{230}Th in boxes i and m at steady state are respectively,

$$0.8P_{Th}V = 0.8k_i{}^{Th}C_i{}^{Th}V + v_{ex}(C_i{}^{Th}-C_m{}^{Th}), \quad (1)$$

$$0.2P_{Th}V = 0.2k_m{}^{Th}C_m{}^{Th}V - v_{ex}(C_i{}^{Th}-C_m{}^{Th}), \quad (2)$$

For ^{231}Pa the equations are equivalent. The model parameters are shown in Table 2-1 and in Fig.2-2 (a-c). As both ^{231}Pa and ^{230}Th are produced from their conservative progenitors ^{235}U and ^{234}U, their respective production rates are uniform throughout the ocean (Fig.2-2 a).

Table 2-1: Model parameters

production rates P ($dpm \cdot m^{-3} \cdot a^{-1}$)	P^{Th}	0.0252*
	P^{Pa}	0.00233*
scavenging residence times τ_s (a)		
ocean interior	$\tau_{s_i}{}^{Th}$	30
	$\tau_{s_i}{}^{Pa}$	300
ocean margin	$\tau_{s_m}{}^{Th}$	6
	$\tau_{s_m}{}^{Pa}$	60
horizontal mixing rate v_{ex} (a^{-1})	v_{ex}/V	0.00333
flushing rate v_f (a^{-1})	v_f/V	0.004

* calculated from the activities of ^{234}U and ^{235}U in seawater

In both boxes a strong preference for the adsorption of ^{230}Th over ^{231}Pa with kTh = 10kPa is assumed (Anderson et al., 1983a). The particle flux is chosen to be five times higher at the ocean margin than in its interior (Berger et al., 1989) (Fig.2-2 b), and it is assumed that the scavenging rate coefficients k in both boxes are proportional to the particle flux, so that $k_m = 5k_i$. As $\tau_s = 1/k$, the scavenging residence times for ^{231}Pa ($\tau_s{}^{Pa}$) and ^{230}Th ($\tau_s{}^{Th}$) are five times higher in box i as in m (Fig.2-2 c), in agreement with literature data (Anderson et al., 1983a; Bacon, 1988; Huh and Beasley, 1987; Nozaki and Yamada, 1987). A value of 300 years is taken for V/v_{ex}, which is in between the values used by Bacon (1988) and Anderson et al. (1990) of 710 and 95 years, respectively.

The dissolved concentrations of ^{231}Pa and ^{230}Th (Fig.2-2 d) can now be calculated by solving equations (1) and (2). As $\tau_{s_i}{}^{Th}$ (30 years) is small compared to V/v_{ex} (300 years), only a minor fraction of the ^{230}Th produced in the ocean interior can be transported laterally to the margin before being scavenged. Consequently, the flux of ^{230}Th (F_{Th}) approximately equals its rate of production (P_{Th}), and even in the high particle flux regions at the margin F_{Th} only slightly exceeds P_{Th} (Fig.2-2 e). In contrast, $\tau_{s_i}{}^{Pa}$ (300 years) is equal to V/v_{ex}, so that a smaller fraction of the ^{231}Pa produced in the ocean interior is scavenged from the water column. The remainder is transported laterally to the ocean margin, where it is scavenged more efficiently by the higher vertical fluxes, resulting in F_{Pa} strongly exceeding P_{Pa}. This simple model illustrates how the differential partitioning of ^{230}Th and ^{231}Pa between a vertical and a lateral flux leads to a basin-wide fractionation of the two radionuclides (Fig.2-2 f). In the ocean interior, where particle fluxes are low, $^{231}Pa/^{230}Th$ ratios on sinking particles do not reach the production ratio of 0.093, whereas values far exceed 0.093 at the margin, where particle fluxes are much higher.

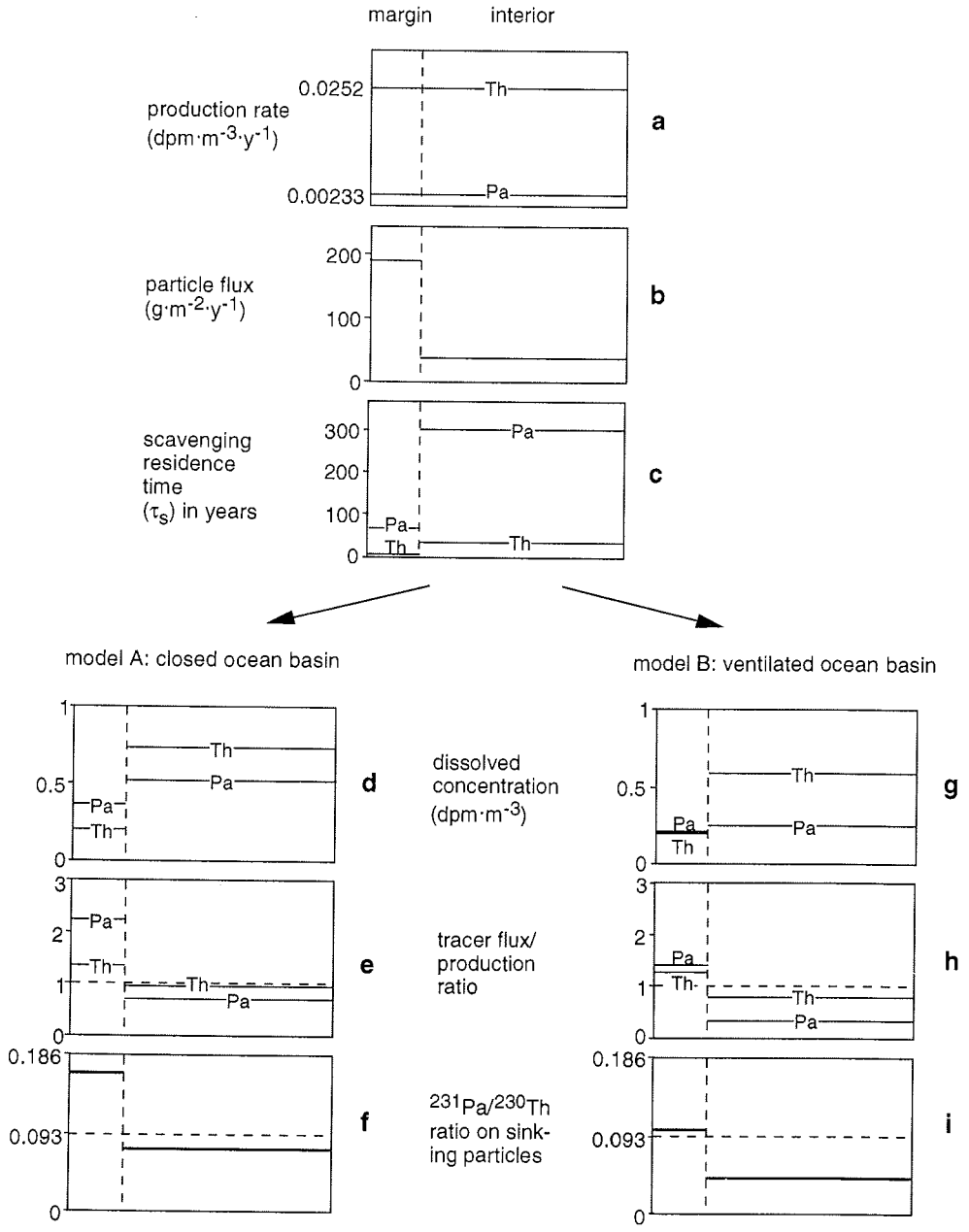

Fig.2-2 (a-i): Model results of two hypothetical scenarios (closed and ventilated basin) in an idealized ocean to demonstrate the basin-wide fractionation of ^{231}Pa and ^{230}Th and the resulting consequences for the sedimentary $^{231}Pa/^{230}Th$ record. See text for explanation.

Accordingly, we should expect a relationship between the $^{231}Pa/^{230}Th$ ratio on sinking particles and the mass flux of particulate matter to the seafloor. Yu (1994) found a positive correlation between $_{xs}^{231}Pa/_{xs}^{230}Th$, measured in sediment traps deployed for a year or longer in the deep sea, and the mass flux of particulate matter (Fig.2-3). Low $_{xs}^{231}Pa/_{xs}^{230}Th$ ratios below the production ratio were only observed in areas with low particle fluxes (less than $70 g/m^2 \cdot a$) such as open ocean gyres. At higher mass fluxes, $_{xs}^{231}Pa/_{xs}^{230}Th$ ratios exceed the production ratio by up to 2.5 times, thereby supporting the hypothesis of a strong lateral transport of dissolved ^{231}Pa from low to high particle flux regions. The sediment trap data show some scatter (R = 0.86), however, reflecting the influence of deep water residence time in ocean basins and particle composition (see below).

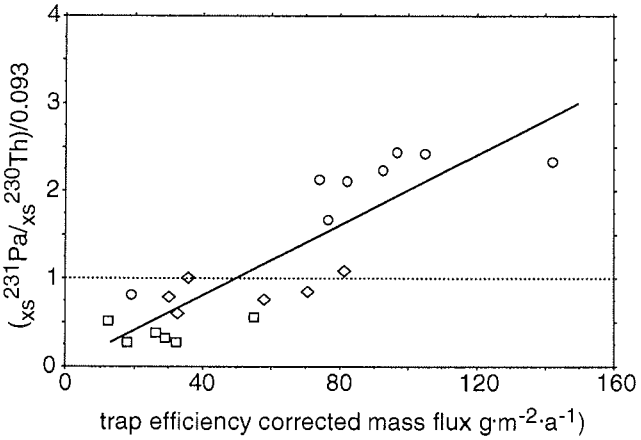

Fig.2-3 Relationship between normalized $_{xs}^{231}Pa/_{xs}^{230}Th$ ratio and the mass flux of particles measured in sediment traps (trap efficiency corrected according to Bacon et al., 1985), deployed in the Pacific (circles), the Atlantic (squares), and in the Southern Indian Ocean (diamonds). Reproduced with permission from Yu (1994).

Similarily, the $_{xs}^{231}Pa/_{xs}^{230}Th$ ratios of newly formed sediments should reflect the mass flux of particles from the overlying water column, and thus should be a measure for the bioproductivity of the surface ocean, provided that the conditions for boundary scavenging are met.

2.3 Results and Discussion

2.3.1 Pacific Ocean

A plot of all available $_{xs}^{231}Pa/_{xs}^{230}Th$ data measured in Holocene Pacific sediments (compiled in Table 2-2) together with data on primary production in $gC \cdot m^{-2} \cdot y^{-1}$ (after Berger et al., 1987), clearly demonstrates the validity of this relationship for the Pacific (Fig.2-4 a). High $_{xs}^{231}Pa/_{xs}^{230}Th$ ratios above the production ratio occur in the high productivity regions both at the margins and at the equator (Fig.2-4 b)

where primary production exceeds 100gC·m^{-2}·y^{-1}. In contrast, low $_{xs}^{231}$Pa/$_{xs}^{230}$Th ratios are found in the central gyre where primary production is less than 50gC·m^{-2}·y^{-1}. Exceptions to this general rule are the high $_{xs}^{231}$Pa/$_{xs}^{230}$Th ratios found in the vicinity of the East Pacific Rise (indicated by crosses), reflecting enhanced scavenging of ^{231}Pa by Fe- and Mn- oxides produced at hydrothermal vents (Shimmield and Price, 1988, see below). High ratios are also found in the SE-Pacific, south of 55°S, where primary production is less than 100gC·m^{-2}·y^{-1} (see chapter 2.3.3, Southern Ocean). Apart from these local exceptions, the $_{xs}^{231}$Pa/$_{xs}^{230}$Th record in surface sediments throughout the Pacific agrees well with the trends expected from model 1A.

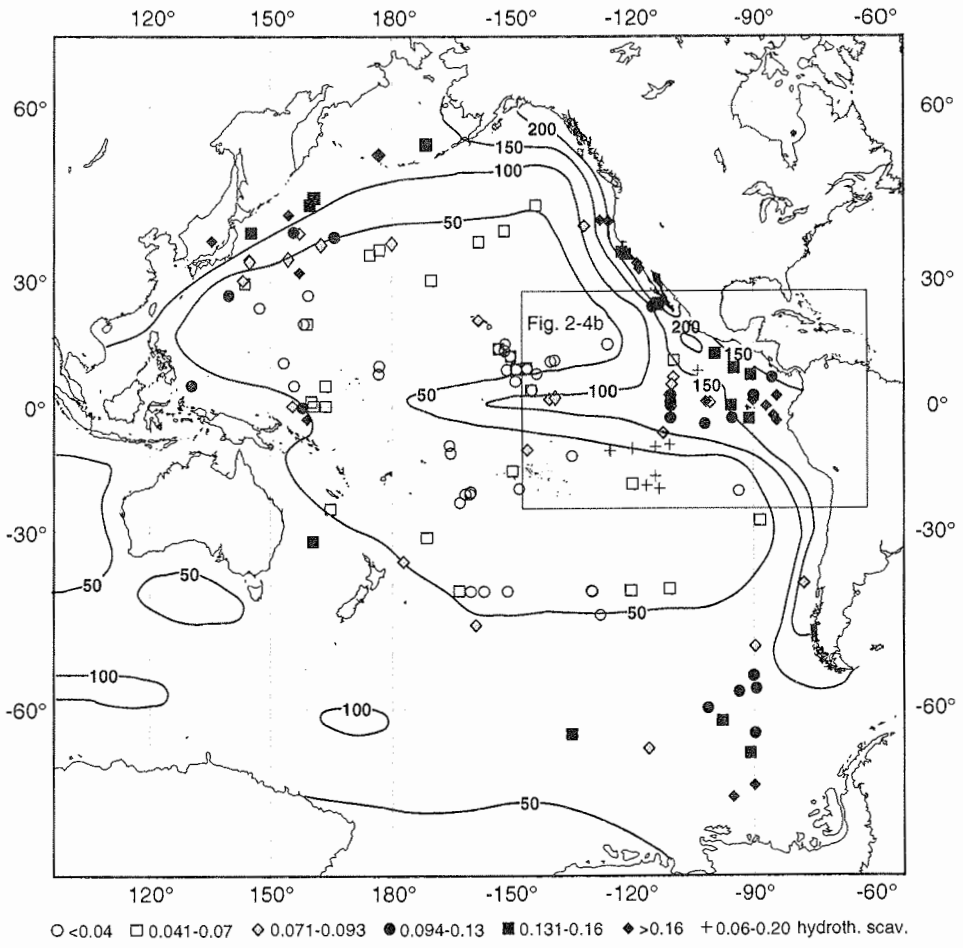

Fig.2-4a: Distribution of $_{xs}^{231}$Pa/$_{xs}^{230}$Th ratios in Holocene sediments throughout the Pacific Ocean with isolines of estimated primary productivity in gC·m^{-2}·y^{-1} (after Berger et al., 1987).

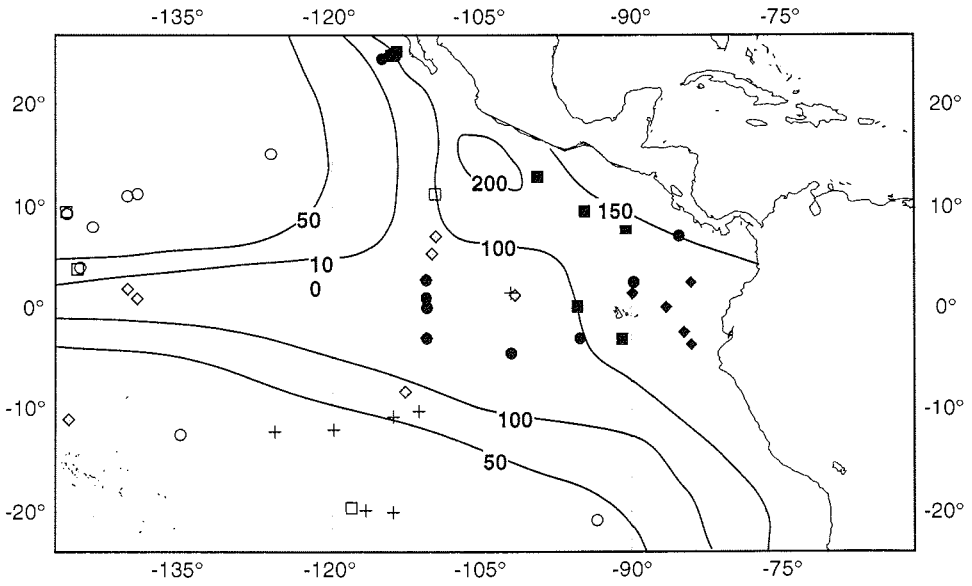

Fig.2-4b: Distribution of $_{xs}^{231}Pa/_{xs}^{230}Th$ ratios in Holocene sediments of the equatorial Pacific with isolines of estimated primary productivity in $gC \cdot m^{-2} \cdot y^{-1}$ (after Berger et al., 1987).

Based on Fig.2-3, $_{xs}^{231}Pa_0/_{xs}^{230}Th_0$ ratios (suffix 0 indicating corrected for decay and for ingrowth from authigenic ^{235}U and ^{234}U since the time of deposition) of dated sediment cores have been used to assess variability through time of particle fluxes as an indicator for paleoproductivity (Lao et al., 1992b; Kumar et al., 1993; 1995; Francois et al., 1993; Kumar, 1994; Yu, 1994; Yang et al., 1995). Lao et al. (1992b) have applied this model in the Pacific ocean over the last 25.000 years. They found higher $_{xs}^{231}Pa_0/_{xs}^{230}Th_0$ ratios in open ocean sediments during the last glacial period, which were partly compensated by lower $_{xs}^{231}Pa_0/_{xs}^{230}Th_0$ ratios at the margins. These findings were interpreted as reflecting reduced boundary scavenging of ^{231}Pa during the last glacial period, caused by a generally higher particle flux, thus enabling more ^{231}Pa to be scavenged in the open ocean waters.

2.3.2 Atlantic Ocean

A comprehensive study of $_{xs}^{231}Pa/_{xs}^{230}Th$ ratios in Holocene sediments by Yu et al. (1996) has revealed that, in contrast to the Pacific, boundary scavenging is suppressed in the Atlantic (Table 2-3, Fig.2-5 a). Even in the upwelling region off Western Africa where the primary production reaches values of more than 200g $C \cdot m^{-2} \cdot y^{-1}$, the $_{xs}^{231}Pa/_{xs}^{230}Th$ ratios of surface sediments only barely reach their production ratio in the water column (Fig.2-5 b). These findings agree well with an earlier study in the same area by Legeleux (1994) who found evidence for boundary scavenging of ^{231}Pa only at one location on the continental slope (2000m water depth), with a $_{xs}^{231}Pa/_{xs}^{230}Th$ ratio in the sediment of 0.16 and a flux/production ratio for ^{231}Pa of 1.4. Yu et al. (1996) have explained the lack of

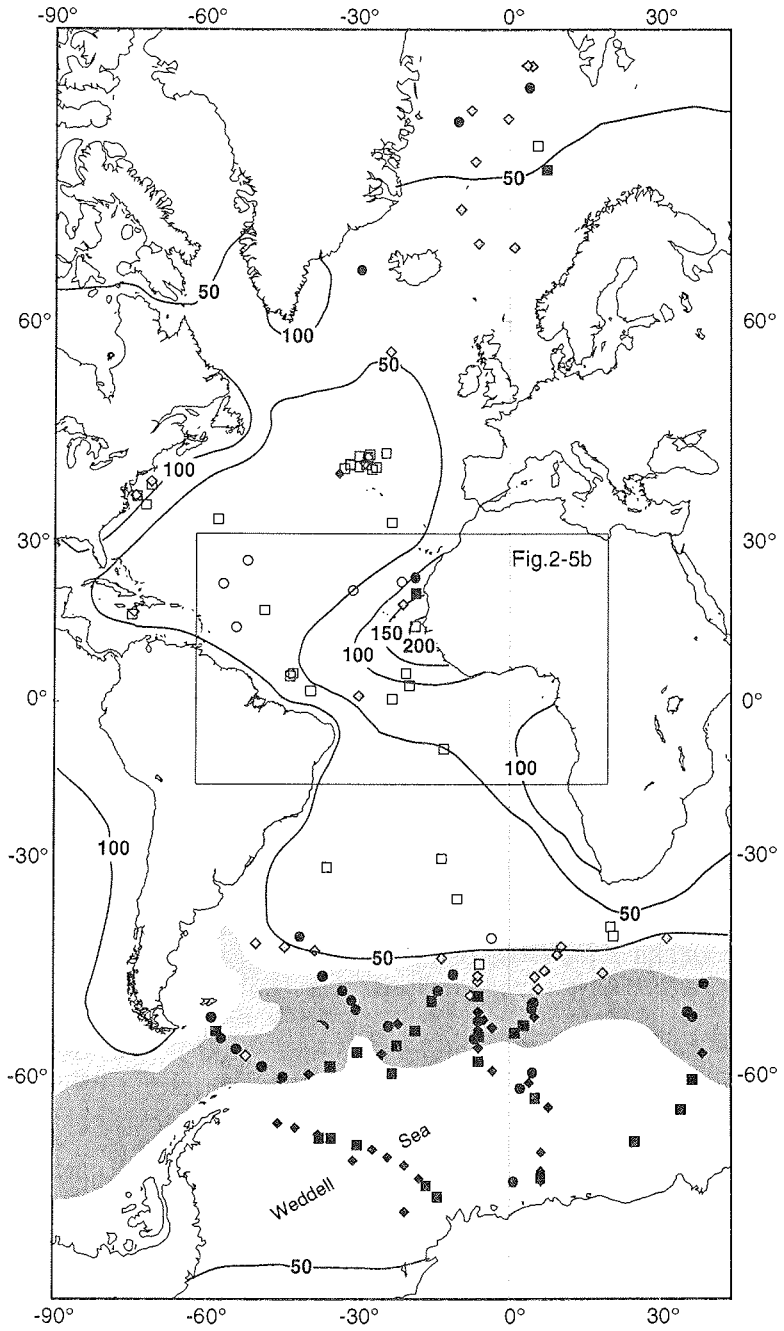

Fig.2-5a: Distribution of $_{xs}^{231}Pa/_{xs}^{230}Th$ in Holocene sediments throughout the Atlantic Ocean with isolines of estimated primary productivity in $gC \cdot m^{-2} \cdot y^{-1}$ (after Berger et al., 1987). (Symbols as in Fig.2-4a). Light shaded: area between Subantarctic Front and Polar Front (Polar Frontal Zone), and dark shaded: area between Polar Front and ACC-Weddell Gyre (Antarctic Zone) (after Orsi et al., 1995).

expression of intense boundary scavenging in the Atlantic by the short mean residence time of NADW (ca. 200 years; Broecker, 1979; Stuiver et al., 1984), which is similar to both the scavenging residence time of ^{231}Pa and the time required for basin-wide lateral mixing. As a result, diffusive transport and advection are equally important in removing ^{231}Pa from the Atlantic water column. From the mean $_{xs}^{231}Pa/_{xs}^{230}Th$ ratio in surface sediments north of 50°S, they estimate that about half of the ^{231}Pa produced in the Atlantic north of 50°S is deposited in the underlying sediments and the remainder is advected to the south in the North Atlantic Deep Water (NADW). Consequently, in addition to its local production, Yu et al. (1996) suggest that the South Atlantic south of 50°S receives a fraction of dissolved ^{231}Pa imported from the north that is scavenged from the water column after entering the Antarctic Circumpolar Current (ACC) south of 50°S (Yu et al., 1996; see also chapter 2.3.3, Southern Ocean).

The effect of advection on boundary scavenging can be illustrated by modifying model A in the way that the interior ocean (i) is ventilated at a rate v_f of $0.005 \cdot a^{-1}$ ($1/v_f = 200$ years, the estimated residence time of deep waters in the Atlantic) with water that does not contain any ^{231}Pa and ^{230}Th (C_o^{Pa} and $C_o^{Th} = 0$), e.g. newly formed NADW (model B in Fig.2-1). All other model parameters are taken to be equal to model A. The new material balance for ^{230}Th (again, equivalent eqs. hold for ^{231}Pa) in boxes i and m at steady state is,

$$0.8P_{Th}V = 0.8k_i^{Th}C_i^{Th}V + v_{ex}(C_i^{Th}-C_m^{Th}) + v_f(C_i^{Th} - C_o^{Th}), \quad (3)$$

$$0.2P_{Th}V = 0.2k_m^{Th}C_m^{Th}V - v_{ex}(C_i^{Th}-C_m^{Th}) \quad (4)$$

The results of model B are shown in Fig.2-2 (g-i). Compared to the closed ocean basin (Fig.2-2 d), the dissolved concentrations of ^{231}Pa (Fig.2-2 g) in boxes i and m are much lower. This is a consequence of the basin ventilation, resulting in a water residence time in box i of 200 years which is similar to both the scavenging residence time of ^{231}Pa and the time required for horizontal mixing (see table 2-1). As a result, about half of the ^{231}Pa produced in the ocean interior is not transported laterally to the margin but is exported. Consequently, fluxes of ^{231}Pa to the sediment in the ocean interior (Fig.2-2 h) are much lower than in the closed ocean basin (Fig.2-2 e), and even at the margin F_{Pa} only slightly exceeds P_{Pa}. Export of ^{230}Th is much less pronounced as $\tau_{s_i}^{Th} << V/v_f$, thus enabling most of the ^{230}Th to be scavenged within the basin. Despite the strong effect of advection, a gradient of $^{231}Pa/^{230}Th$ ratios on sinking particles between box i and m is still seen (Fig.2-2 i), although the overall values are lower compared to the closed ocean basin (Fig.2-2 f). These model results are in agreement with the $_{xs}^{231}Pa/_{xs}^{230}Th$ ratios measured in Holocene sediments throughout the Atlantic north of 50°S (Fig.2-5 a).

Based on these results, the interpretation of changes in the $_{xs}^{231}Pa/_{xs}^{230}Th$ ratio through time caused by changes in paleoproductivity can be made in the Atlantic ocean, provided that there is no substantial change in the basin ventilation rate. A total shutdown of the global conveyer belt circulation, or changes in the production rate of deep water in the Atlantic in the past, would strongly influence the export rate of ^{231}Pa. Hence, variations through time of the $_{xs}^{231}Pa_0/_{xs}^{230}Th_0$ signal, rather than being due to changes in the bioproductivity of the ocean, could reflect changes in

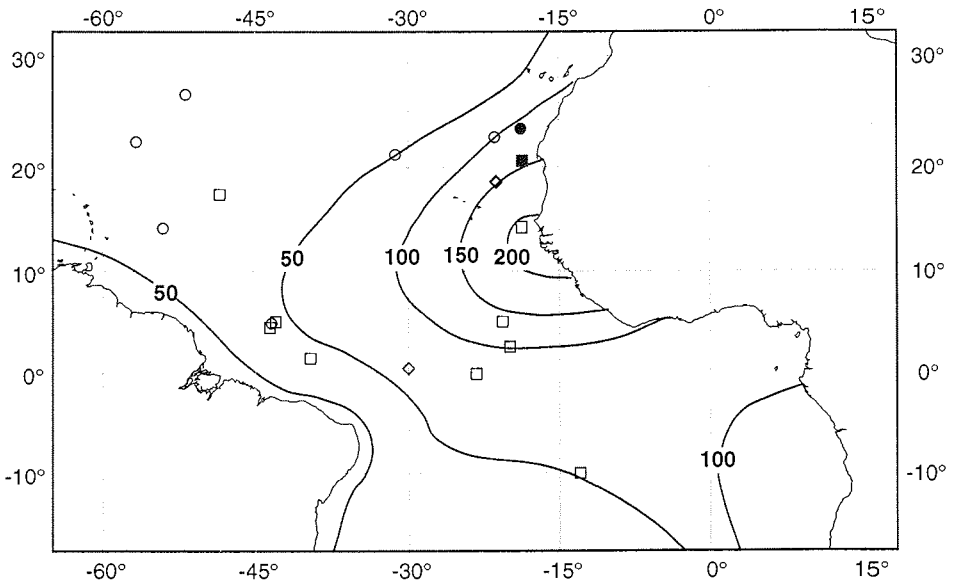

Fig.2-5b: Distribution of $_{xs}^{231}Pa/_{xs}^{230}Th$ ratios in Holocene sediments of the equatorial Atlantic Ocean with isolines of estimated primary productivity in $gC \cdot m^{-2} \cdot y^{-1}$ (after Berger et al., 1987). Symbols as in Fig.2-4a.

the magnitude of the conveyer belt circulation. For the last glacial, there are indications of a similar export rate of deep water from the Atlantic to the Southern Ocean, based on the similarity of the $_{xs}^{231}Pa/_{xs}^{230}Th$ distribution patterns in modern Atlantic and Last Glacial Maximum (LGM) Atlantic sediments (Yu et al. 1996). This observation implies that, neglecting the effects of the chemical composition of particles which becomes very important south of 50°S (see chapter 2.3.3, Southern Ocean), the $_{xs}^{231}Pa_0/_{xs}^{230}Th_0$ ratio should provide reasonable results about changes in bioproductivity in the LGM (Kumar et al., 1995; Francois et al., submitted).

2.3.3 Southern Ocean

A further complication of the relationship between $_{xs}^{231}Pa/_{xs}^{230}Th$ ratio and particle flux is apparent in results from the Southern Ocean. The first investigation of ^{231}Pa and ^{230}Th in this region was carried out by DeMaster (1979). In rapidly accumulating (up to 100cm/ka) siliceous sediments within the Antarctic Circumpolar Current (ACC) between 48°S and 55°S, DeMaster found evidence for preferential deposition of ^{231}Pa relative to ^{230}Th, with inventories of ^{230}Th and ^{231}Pa exceeding the production rate in the water column by up to 6 and 14 times, respectively. Moreover, he showed that the $^{231}Pa/^{230}Th$ deposition ratio was up to five times higher than the production ratio of 0.093. DeMaster explained his findings by a boundary scavenging effect and hypothesized that, due to the high particle flux within the ACC, scavenging of ^{231}Pa and ^{230}Th is so effective that both

radionuclides are quantitatively stripped from the water column. This would imply that the high $_{xs}^{231}Pa/_{xs}^{230}Th$ ratios in sediments underlying the ACC reflect both the local production of the two radionuclides in the water column and the remaining fractions of dissolved ^{231}Pa and (less important) of ^{230}Th imported from the Atlantic Ocean by advection (Yu et al., 1996).

Several recent findings indicate that a simple boundary scavenging model cannot be directly applied in the Southern Ocean. First, total mass fluxes measured in sediment traps located at 50°S (PF) and 55°S (BO1/2) within the ACC are 38.3g·m^{-2}·y^{-1} (Wefer and Fischer, 1991) and 53g·m^{-2}·y^{-1} (Fischer and Wefer, unpublished), respectively. Although not corrected for trapping efficiency, these are much lower fluxes than measured in upwelling regions such as the Panama Basin or the California margin (>100g·m^{-2}·y^{-1}; Honjo, 1982; Yu, 1994). These low fluxes are also in agreement with primary production being much lower (in general less than 100gC·m^{-2}·y^{-1}), than in upwelling regions (sometimes exceeding 200gC·m^{-2}·y^{-1}, Fig.2-4 a,b; Fig.2-5 a,b). According to Fig.2-3, such mass flux would be insufficient to enhance ^{231}Pa scavenging above its rate of production in the water column. Second, according to the reversible scavenging model of Bacon and Anderson (1982), the concentrations of ^{231}Pa and ^{230}Th in the water column should adjust to the flux of particulate matter. Consequently, the high particle fluxes postulated by DeMaster (1979) should lead to a depletion of their dissolved activities relative to regions with low particle fluxes. Actually, there are no indications of a depletion of ^{231}Pa and ^{230}Th in the water column within the ACC relative to the less productive regions to the north and south (Rutgers van der Loeff and Berger, 1993; Walter et al., 1997). Third, a recent study of surface sediments in the Atlantic sector of the Southern Ocean (Fig.2-5) has revealed that the region of high $_{xs}^{231}Pa/_{xs}^{230}Th$ ratios is not restricted to the area of the ACC, but persists throughout the Weddell Sea (Walter et al., 1997). This is in contrast to the low particle fluxes of this region compared to the ACC, inferred from sediment trap data (< 50g·m^{-2}·y^{-1}; Fischer et al. 1988; Wefer and Fischer 1991) and fluxes of biogenic opal through the sediment-water interface deduced from pore water measurements of silicate (Schlüter et al., submitted). The latter observation unequivocally illustrates the decoupling between $_{xs}^{231}Pa/_{xs}^{230}Th$ ratio and the mass flux of particulate matter in this region. As boundary scavenging cannot explain the observations above, another factor than the mass flux must be responsible for the high $_{xs}^{231}Pa/_{xs}^{230}Th$ ratios in the sediments within and south of the ACC.

As discussed above, the application of the $_{xs}^{231}Pa/_{xs}^{230}Th$ ratio as a paleoproductivity proxy requires a constant $^{230}Th/^{231}Pa$ fractionation factor (F) with a strong preference for the adsorption of ^{230}Th over ^{231}Pa on particles. The F-factor is defined as

$$F = \frac{(^{230}Th/^{231}Pa)_{part}}{(^{230}Th/^{231}Pa)_{diss}} \qquad (5)$$

The few data on F-factors available from the literature (Anderson et al., 1983a; 1983b; Nozaki and Nakanishi, 1985; Scholten et al., 1995) show that this assumption holds for large areas of the world's oceans. However, in the Atlantic sector of the Southern Ocean it has been shown to be no longer valid (Rutgers van

der Loeff and Berger, 1993; Walter et al., 1997). Typical open ocean values of F around 10 (Anderson et al., 1983a; 1983b), indicating a strong preference for the adsorption of ^{230}Th relative to ^{231}Pa on particles, were only observed north of 48°S (Fig.2-6). To the south, F decreases strongly and implies a change in the scavenging preference of ^{230}Th over ^{231}Pa, either due to a southward decrease in the scavenging efficiency of ^{230}Th, an increase in the scavenging efficiency of ^{231}Pa, or both.

The N-S decrease in F (Rutgers van der Loeff and Berger, 1993; Walter et al., 1997) is well correlated with a respective increase in the content of biogenic opal on sedimenting particles (Fischer et al., 1988; Wefer and Fischer, 1991). An experimental study on the adsorption of ^{230}Th and ^{231}Pa on different solid phases by Anderson et al. (1992) has shown that amorphous silica does not fractionate ^{231}Pa and ^{230}Th (F = 1.1; Fig.2-7), possibly because of its high affinity for ^{231}Pa (DeMaster, 1979; Taguchi et al., 1989; Anderson et al., 1992; Lao et al., 1992b; Kumar et al., 1995). The increased predominance of opal may explain the latitudinal decrease in F. Support for this suggestion comes from the analysis of $_{xs}^{231}Pa/^{230}Th$ ratios in settling particles (collected by sediment traps), where estimated F values are negatively correlated with the content of opal of these particles (Tab.2-4).

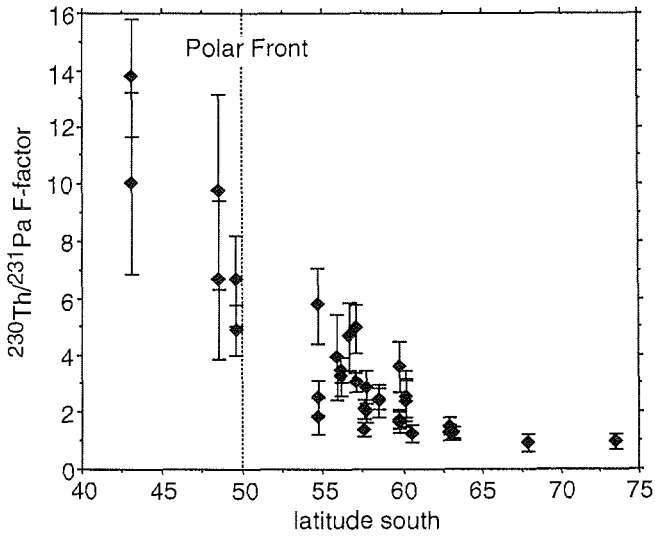

Fig.2-6: Plot of the $^{230}Th/^{231}Pa$ fractionation factor F against latitude in the Atlantic sector of the Southern Ocean (from Walter et al., 1997).

Based on these observations it is concluded that biogenic opal might explain the enhanced scavenging of ^{231}Pa relative to ^{230}Th south of the Polar Front, at least in the Atlantic sector of the Southern Ocean (Walter et al., 1997). This would imply that in regions where the sedimenting flux is dominated by biogenic opal, the $_{xs}^{231}Pa/_{xs}^{230}Th$ ratio is no more a reliable indicator for the mass flux of particles.

Table 2-4: Opal contents and $_{xs}^{231}Pa/_{xs}^{230}Th$ ratios of sinking particles, and estimated F-factor (from Walter et al., 1997)

trap	latitude	longitude	depth (m)	mass flux $g \cdot m^{-2} \cdot a^{-1}$	opal (%)	$_{xs}^{231}Pa/_{xs}^{230}Th$	*($^{231}Pa/^{230}Th$) dissolved	F-factor
PF 1-4	50° 09.0' S	05° 46.4' E	700	38.3	40	0.322 ± 0.066	0.599 ± 0.064	1.86 ± 0.43
BO 1+2	54° 20.2' S	03° 20.2' W	450	53.1	62	0.344 ± 0.034	0.465 ± 0.036	1.35 ± 0.17
WS 3	64° 54.1' S	02° 33.8' W	360	33.7	70	0.278 ± 0.016	0.280 ± 0.058	1.01 ± 0.23

Data on mass flux and opal content of PF 1-4 and WS-3 are from Wefer and Fischer (1991), and of BO 1+2 from Wefer and Fischer (unpublished).
Errors are 1σ propagated from counting statistics and blank.
*interpolated from latitudinal gradient of dissolved $^{231}Pa/^{230}Th$ ratios

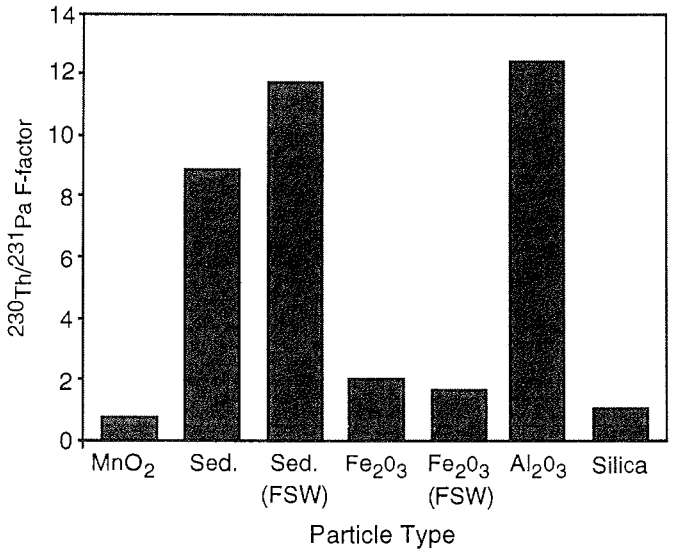

Fig.2-7: $^{230}Th/^{231}Pa$ fractionation factors for different particle types, determined in artificial seawater, as well as for Fe_2O_3 and natural sediments in filtered seawater (FSW). Reproduced with permission from Anderson et al. (1992).

In the Southern Ocean, where high flux rates of biogenic opal to the sediment also have occurred in the past, as is well documented by the circumantarctic opal belt (DeMaster, 1981), it is suggested that the use of the $_{xs}^{231}Pa/_{xs}^{230}Th$ ratio as a paleoproductivity proxy is strongly limited (Walter et al., 1997). Variations of the $_{xs}^{231}Pa_0/_{xs}^{230}Th_0$ ratio through time, usually interpreted as reflecting changes in the total mass flux of particles, could also result from changes in the content of biogenic opal on sinking particles.

2.3.4 Weddell Sea

Over most of the oceans the depositional flux of ^{230}Th approximately equals its local rate of production with little net lateral transport (Anderson et al., 1983a; 1983b; Bacon et al., 1985; Suman and Bacon, 1989; Francois et al., 1990; Yu, 1994). Even in the Atlantic Ocean north of 50°S, despite the strong effect of advection, 85-90% of the ^{230}Th produced is still scavenged within the Atlantic and only 10-15% are advected to the south (Yu et al., 1996). If the flux/production ratio for ^{230}Th remains still close to 1 in the Southern Ocean (or slightly above 1 due to advection of dissolved ^{230}Th from the Atlantic), the mass balance for ^{231}Pa can be calculated (Yu et al., 1996). By taking a mean $_{xs}^{231}Pa/_{xs}^{230}Th$ rain ratio of 0.165 for the region south of 50°S, they estimated that the depositional flux of ^{231}Pa throughout the entire Southern Ocean balances in situ production plus ^{231}Pa import from the Atlantic Ocean, suggesting this region to be an important sink for ^{231}Pa.

The assumption of a constant flux/production ratio of ^{230}Th around 1 does not appear to be valid throughout the entire Southern Ocean. Based on measurements of the dissolved and particulate concentrations of ^{230}Th in the water column of the South Atlantic, Rutgers van der Loeff and Berger (1993) hypothesized that in the Central Weddell Sea south of the Antarctic Weddell boundary (AWB), scavenging rate of ^{230}Th might be strongly reduced relative to the regions to the north (ACC). They based their suggestion on both the extremely low particle fluxes (Fischer et al., 1988; Schlueter et al., submitted) and the short residence time of water in the Weddell Sea (35 years; Rutgers van der Loeff and Berger, 1993) comparable to the scavenging residence time of ^{230}Th. Further support for low scavenging rates in the Central Weddell Sea comes from the sedimentary record, with extremely low ^{210}Pb inventories of only 15% of its production rate (Rutgers van der Loeff and Berger, 1991). These findings are confirmed by a still ongoing investigation of the inventories of ^{231}Pa and ^{230}Th, in three sediment cores from the Western Central Weddell Sea (Walter et al., in prep.). The selected area is characterized by slow bottom currents, so that effects of lateral sediment redistribution are only small, which is a reflection of sluggish circulation of the center of the Weddell Gyre compared to the outer parts such as the northern Weddell (Pudsey et al., 1988). Therefore, it is not to be expected that the core locations are influenced by sediment winnowing (Pudsey et al., 1988). Results from the core PS1508 (67°00.1'S/32°23.5'W) have shown that over the last 150ka only 37% and 52% of the production of ^{230}Th and ^{231}Pa, respectively, are found in the sediment. These observations imply a N-S change in the scavenging efficiency not only for ^{231}Pa, but also for ^{230}Th. If this observation holds for the entire Weddell Sea, this would suggest that most of the ^{230}Th and ^{231}Pa produced in this basin must be advected to other regions of the Southern Ocean prior to scavenging, such as the ACC where particle fluxes are higher. Hence, the Weddell Sea would not be a sink for ^{231}Pa, and the high average $_{xs}^{231}Pa/_{xs}^{230}Th$ ratios of 0.15 found in surface sediments (Fig.2-5 a) reflect an increase in the scavenging efficiency of ^{231}Pa relative to ^{230}Th, probably related to the high opal contents of sedimenting particles.

Further evidence for an advective export of ^{230}Th of up to 50% of the production comes from other ocean basins with short residence times of deep waters (<100 years), such as the North Atlantic and the Arctic Seas (Moran et al., 1995; Moran et

al., 1997; Vogler et al., submitted). The export of ^{230}Th has to be taken into account when using its flux to the sediment as a reference to predict depositional fluxes of ^{231}Pa (e.g. Anderson et al., 1994; Yu, 1996) in such regions.

2.3.5 Enhanced scavenging of ^{231}Pa by Mn- and Fe-oxides

In our simple box model illustration, we have shown that the large-scale distributions of ^{231}Pa and ^{230}Th in oceanic surface sediments can be explained by assuming a homogenous particle composition with a strong preference for the adsorption of ^{230}Th relative to ^{231}Pa. This assumption is reasonable, provided that scavenging of both radionuclides is primarily determined by the mass flux of particles. There are exceptions, however, as shown for the Southern Ocean. There is experimental evidence that as for opal, fractionation between ^{231}Pa and ^{230}Th is also limited on manganese oxides and hematite, with $^{230}Th/^{231}Pa$ fractionation factors of 0.8 and 2.1, respectively (Fig.2-7). Hydrothermal plumes emanating in the vicinity of mid-ocean ridges are an important localized source for Mn- and Fe-oxides. They are effective scavengers for ^{231}Pa and, to a lesser extent, for ^{230}Th relative to the surrounding area (German et al., 1991; Frank et al., 1994). This so-called hydrothermal scavenging leads to high $_{xs}^{231}Pa/_{xs}^{230}Th$ ratios in ridge sediments, as found in the vicinity of the East Pacific Rise, (Shimmield and Price, 1988, see also Fig.2-4 a,b). Further evidence for enhanced scavenging of ^{231}Pa relative to ^{230}Th is reported from the Panama and Guatemala basins and has been attributed to the presence of MnO_2 coated particles, originating from recycling of reduced Mn from suboxic sediments (Anderson et al., 1983b). The use of the $_{xs}^{231}Pa/_{xs}^{230}Th$ ratio as a paleoproductivity index is thus further limited near mid-ocean ridges and possibly in regions with diagenetic remobilization of Mn and near mid-ocean ridges.

2.4 Evaluation of the quality as a paleoproductivity proxy

As we have shown in the discussion above, the $_{xs}^{231}Pa/_{xs}^{230}Th$ ratio of oceanic surface sediments is determined by three different parameters: the mass flux of particles, their chemical composition and the hydrography. Consequently, it can only be applied as a reliable tracer for bioproductivity in the past, if the influence of the chemical composition and the hydrography is small. This condition appears to be met in the Pacific Ocean, where the $_{xs}^{231}Pa/_{xs}^{230}Th$ ratio is well correlated with particle flux and primary production. This region is an appropriate study area to apply the $_{xs}^{231}Pa_0/_{xs}^{230}Th_0$ ratio as an index for oceanic productivity in the past. Even under such circumstances, however, the $_{xs}^{231}Pa/_{xs}^{230}Th$ ratio can only provide relative intensities of export flux between low and high productivity regions.

Throughout the modern Atlantic Ocean, there is still a relationship between $_{xs}^{231}Pa/_{xs}^{230}Th$ ratio and mass flux of particles, but the overall values are lower due to the low residence time of deep water in this ocean basin. Nevertheless, during time periods with similar hydrographic conditions, the $_{xs}^{231}Pa_0/_{xs}^{230}Th_0$ ratio should reflect relative changes in paleoproductivity. Conversely, mean basin-wide $_{xs}^{231}Pa_0/_{xs}^{230}Th_0$ ratios can be used as a paleocirculation tracer (Yu et al., 1996).

Periods of reduced global thermohaline circulation would be characterized by higher mean $_{xs}^{231}Pa_0/_{xs}^{230}Th_0$ ratios in Atlantic sediments and higher contrasts in the $_{xs}^{231}Pa_0/_{xs}^{230}Th_0$ ratios between open ocean and ocean margin (as documented in today's Pacific).

In the Southern Ocean there is no more a simple relationship between $_{xs}^{231}Pa/_{xs}^{230}Th$ ratio and mass flux of particulate matter. This is a result of the strong latitudinal decrease in the scavenging preference of ^{230}Th over ^{231}Pa, probably related to the high contents of biogenic opal of sinking particles. As a consequence, in this region the $_{xs}^{231}Pa/_{xs}^{230}Th$ ratio cannot be applied as a reliable paleoproductivity proxy, as variations of the $_{xs}^{231}Pa_0/_{xs}^{230}Th_0$ ratio through time, usually interpreted to reflect changes in the total mass flux of particles, could also be explained by changes in the content of biogenic opal on sinking particles. The high affinity of ^{231}Pa to opal, however, could possibly be used to trace fluxes of biogenic opal to the sediment that have been totally dissolved (e.g. throughout the Weddell Sea, Walter et al., 1997). Nearly unpreferential scavenging of ^{230}Th and ^{231}Pa by manganese- and iron- oxides further limits the use of the $_{xs}^{231}Pa/_{xs}^{230}Th$ ratio near mid ocean ridges and in areas of diagenetic remobilization of manganese.

In conclusion, the $_{xs}^{231}Pa/_{xs}^{230}Th$ ratio can serve as a proxy for relative changes in paleoproductivity if, in the time interval of interest, changes in the basin ventilation rate and differential scavenging of both radionuclides due to changes in the chemical composition of particulate matter are not significant. The interpretation of the $_{xs}^{231}Pa/_{xs}^{230}Th$ ratio thus requires synoptic information on its basin-wide distribution and on past changes in composition of sedimenting particles. Reliable reconstructions of changes in paleoproductivity, however, can only be made in combination with other independent proxies, (like biogenic barium, authigenic uranium).

Recent improvements in mass spectrometric techniques (e.g. Chen et al., 1992; Cheng et al., 1996) now allow the study of the distributions of ^{230}Th and ^{231}Pa in the ocean in more detail. Small sample sizes of only 1-2 liters of seawater (compared to cubic meters with the traditionally alpha spectrometry), sufficient for the high precision determination of ^{230}Th (Moran et al., 1995; Moran et al., 1997; Vogler et al., submitted) and ^{231}Pa (Francois, pers. comm.; Vogler pers. comm.; Edmonds et al., unpubl. data), promise the detailed investigation of scavenging of both radionuclides even in the surface ocean, where their concentrations are extremely low. This new analytical technique could thus provide the required answers to some of the remaining open questions regarding the oceanographic behaviour of ^{230}Th and ^{231}Pa.

Table 2-2: Compiled data of $_{xs}{}^{231}Pa/_{xs}{}^{230}Th$ ratios of Holocene Pacific sediments.

sample	latitude	longitude	depth (cm)	$_{xs}{}^{231}Pa/_{xs}{}^{230}Th$	reference
RC14-121	54°51' N	170°41' W	25-27	0.154 ± 0.016	Lao et al. (1992a)
RC14-105	39°41' N	157°33' E	10-12	0.090 ± 0.005	Lao et al. (1992a)
V20-122	46°34' N	161°41' E	8-10	0.145 ± 0.007	Lao et al. (1992a)
V21-146	37°41' N	163°02' E	10-11	0.093 ± 0.005	Lao et al. (1992a)
V32-126	35°19' N	174°54' E	7-8	0.064 ± 0.003	Lao et al. (1992a)
V32-128	36°27' N	177°09' E	8-10	0.062 ± 0.005	Lao et al. (1992a)
W8709A-1	41°33' N	131°57' W	1-3	0.081 ± 0.003	Lao et al. (1992a)
W8709A-8	42°16' N	127°41' W	9-10	0.180 ± 0.011	Lao et al. (1992a)
W8709A-13	42°07' N	125°45' W	4-5	0.217 ± 0.036	Lao et al. (1992a)
V21-59	20°55' N	158°06' W	5-6	0.081 ± 0.004	Lao et al. (1992a)
V28-238	01°01' N	160°29' E	0-8	0.067 ± 0.003	Lao et al. (1992a)
RC11-210	01°49' N	140°03' W	5-7	0.073 ± 0.003	Lao et al. (1992a)
V19-28	02°22' S	84°39' W	17-19	0.200 ± 0.009	Lao et al. (1992a)
V19-29	03°35' S	83°56' W	17-19	0.183 ± 0.010	Lao et al. (1992a)
RC15-61	40°37' S	77°12' W	6-9	0.075 ± 0.004	Lao et al. (1992a)
MANOP R	38°00' N	158°00' W	0-5	0.043 ± 0.002	Lao et al. (1992a)
V20-88	40°11' N	151°39' W	top	0.044 ± 0.002	Lao et al. (1992a)
V20-85	44°54' N	143°37' W	0-1	0.044 ± 0.002	Lao et al. (1992a)
PS BC166	36°06' N	122°36' W	0-1	0.163 ± 0.019	Lao et al. (1992a)
PS BC133	36°12' N	122°16' W	0-1	0.966 ± 0.058	Lao et al. (1992a)
PS BC150	36°11' N	122°22' W	0-1	0.190 ± 0.047	Lao et al. (1992a)
PS BC151	35°38' N	121°37' W	0-1	0.157 ± 0.015	Lao et al. (1992a)
SCB QP2	32°35' N	118°10' W	0-10	0.198 ± 0.011	Lao et al. (1992a)
MANOP S	11°03' N	140°05' W	1.5-2.1	0.025 ± 0.001	Lao et al. (1992a)
MANOP C	01°02' N	138°56' W	1.5-2.1	0.064 ± 0.002	Lao et al. (1992a)
V18-299	16°07' S	149°40' W	0-5	0.044 ± 0.002	Lao et al. (1992a)
RC8-81	47°57' S	159°03' W	3-4	0.074 ± 0.003	Lao et al. (1992a)
E15-6	59°58' S	101°19' W	4-7	0.097 ± 0.006	Lao et al. (1992a)
E17-9	63°05' S	135°07' W	7-10	0.148 ± 0.005	Lao et al. (1992a)
KK1, core1	14°07' N	153°10' W	0-1	0.040 ± 0.001	Anderson et al. (1983)
KK1, core2	15°20' N	151°34' W	0-3	0.034 ± 0.001	Anderson et al. (1983)
KH-80-2-5	40°00.2' N	156°00.0' E	0-1	0.128 ± 0.014	Yang et al. (1986)
KH-80-2-6	39°02.5' N	166°00.3' E	2-3	0.113 ± 0.011	Yang et al. (1986)
KH-80-2-8	38°03.3' N	179°45.7' W	0-1	0.073 ± 0.005	Yang et al. (1986)
KH-80-2-9	30°00.0' N	170°00.8' W	0-2	0.045 ± 0.003	Yang et al. (1986)
KH-75-3-2-2	30°00.0' N	143°30.8' E	0-2.5	0.091 ± 0.007	Yang et al. (1986)
KH-75-3-14-2	34°23.8' N	145°01.8' E	0-3	0.076 ± 0.007	Yang et al. (1986)
KH-84-3-5	39°57.5' N	145°26.3' E	0-1.5	0.144 ± 0.021	Yang et al. (1986)
KH-84-3-16	38°17.2' N	135°29.5' E	0-1.5	0.413 ± 0.055	Yang et al. (1986)
KH-83-3-BC	43°18.0' N	154°42.4' E	0-1	0.290 ± 0.034	Yang et al. (1986)
KH-83-3-C	45°01.5' N	159°59.7' E	0-1	0.161 ± 0.012	Yang et al. (1986)
KH-83-3-D	34°52.0' N	154°46.2' E	0-1	0.090 ± 0.008	Yang et al. (1986)
KH-80-3-16	31°43.5' N	157°26.7' E	0-1.5	0.195 ± 0.032	Yang et al. (1986)
KH-79-1-5	05°10.9' N	130°27.9' E	0-1.5	0.095 ± 0.015	Yang et al. (1986)
KH-79-4-5	29°16.8' N	144°02.0' E	0-1.5	0.058 ± 0.008	Yang et al. (1986)
KH-79-4-6	23°47.5' N	147°37.4' E	0-1.5	0.022 ± 0.005	Yang et al. (1986)
KH-79-4-7	10°47.3' N	153°43.1' E	0-1	0.033 ± 0.005	Yang et al. (1986)
KH-79-4-8	05°00.6' N	156°08.6' E	0-1.5	0.026 ± 0.007	Yang et al. (1986)
KH-79-4-9	00°17.5' S	158°06.7' E	0-1	0.123 ± 0.020	Yang et al. (1986)
KH-79-4-10	03°19.0' S	159°18.4' E	0-1.5	0.175 ± 0.036	Yang et al. (1986)
KH-79-4-12	31°59.7' S	160°37.3' E	0-5	0.136 ± 0.028	Yang et al. (1986)
KH-79-4-14	24°57.2' S	165°08.7' E	0-2	0.062 ± 0.008	Yang et al. (1986)
KH-79-4-18	00°00.7' S	163°59.7' E	0-2	0.049 ± 0.004	Yang et al. (1986)
KH-79-4-19	05°03.4' N	165°55.3' E	0-2	0.042 ± 0.003	Yang et al. (1986)
KH-79-4-22	20°02.7' N	158°36.0' E	0-2	0.040 ± 0.003	Yang et al. (1986)
KH-78-3-4	53°30.0' N	177°15.5' E	0-2.5	0.219 ± 0.027	Yang et al. (1986)
KH-74-4-21	26°45.7' N	139°42.5' E	2-8	0.105 ± 0.015	Yang et al. (1986)
KH-71-5-12-3	11°01.4' S	146°01.5' W	3-6	0.091 ± 0.007	Yang et al. (1986)
KH-71-5-15-2	20°22.8' S	148°02.6' W	3-6	0.034 ± 0.002	Yang et al. (1986)
KH-71-5-24-2	46°19.3' S	127°46.4' W	0-2	0.034 ± 0.002	Yang et al. (1986)
KH-71-5-42-2	27°34.8' S	88°03.0' W	0-2	0.054 ± 0.011	Yang et al. (1986)
KH-71-5-44-2	20°50.1' S	93°21.2' W	6-8	0.025 ± 0.002	Yang et al. (1986)
KH-71-5-53-2	08°15.3' S	112°42.1' W	5-8	0.080 ± 0.006	Yang et al. (1986)
KH-78-1-1036	08°00.3' N	176°57.1' E	0-4	0.031 ± 0.002	Yang et al. (1986)
KH-78-1-1038	10°00.2' N	176°59.3' E	0-4	0.027 ± 0.002	Yang et al. (1986)
Valdivia 10127	13°41.7' N	151°59.0' W	2-4	0.031 ± 0.002	Mangini and Sonntag (1977)
Valdivia 10141	09°06.5' N	148°46.7' W	0-2	0.028 ± 0.004	Mangini and Sonntag (1977)
251KG	41°56.8' S	163°04.5' W	topmost layer	0.042 n.i.	Schmitz et al. (1986)
242KG	42°00.9' S	160°12.8' W	topmost layer	0.036 n.i.	Schmitz et al. (1986)
228KG	42°01.3' S	156°58.1' W	topmost layer	0.034 n.i.	Schmitz et al. (1986)
198KG	42°00.3' S	150°58.6' W	topmost layer	0.029 n.i.	Schmitz et al. (1986)
79KG	41°57.4' S	129°52.7' W	topmost layer	0.040 n.i.	Schmitz et al. (1986)
46KG	41°59.3' S	120°12.7' W	topmost layer	0.048 n.i.	Schmitz et al. (1986)
23KG	41°36.6' S	110°41.3' W	topmost layer	0.053 n.i.	Schmitz et al. (1986)
G972	36°15.5' S	176°53.9' W	topmost layer	0.071 n.i.	Schmitz et al. (1986)
G981	31°22.6' S	171°13.8' W	topmost layer	0.050 n.i.	Schmitz et al. (1986)
G993	23°32.1' S	162°54.1' W	topmost layer	0.036 n.i.	Schmitz et al. (1986)
214KG	21°36.0' S	161°32.0' W	topmost layer	0.032 n.i.	Schmitz et al. (1986)
210KG	21°36.0' S	160°30.0' W	topmost layer	0.023 n.i.	Schmitz et al. (1986)
KLH 093	01°13.9' N	102°03.8' W	7.5	0.161 ± 0.028	Frank et al. (1994)
KLH 068	01°13.9' N	101°36.7' W	2.5	0.071 ± 0.025	Frank et al. (1994)

Table 2-2: continued

sample	latitude	longitude	depth(cm)	$xs^{231}Pa/xs^{230}Th$	reference
PS 2661	51°24.5' S	89°20.7' W	0-0.5	0.079 ± 0.004	this study
PS 2667	55°39.1' S	89°48.9' W	0-0.5	0.096 ± 0.003	this study
PS 2675	57°52.9' S	93°30.1' W	0-0.5	0.101 ± 0.003	this study
PS 2678	61°30.0' S	97°41.1' W	0-0.5	0.133 ± 0.005	this study
PS 2684	69°25.0' S	95°01.4' W	0-0.5	0.172 ± 0.004	this study
PS 2686	68°19.3' S	89°37.6' W	0-0.5	0.175 ± 0.006	this study
PS 2692	65°08.3' S	90°41.0' W	0-0.5	0.139 ± 0.006	this study
PS 2697	62°59.8' S	89°59.8' W	0-0.5	0.119 ± 0.004	this study
PS 2714	57°26.8' S	89°16.3' W	0-0.5	0.098 ± 0.004	this study
154-10	10°17.1' S	111°19.7' W	0-1	0.160 ± 0.009	Shimmield and Price (1988)
154-8	10°48.5' S	113°52.1' W	0-1	0.110 ± 0.008	Shimmield and Price (1988)
154-6	12°04.2' S	119°46.7' W	2-3	0.077 ± 0.006	Shimmield and Price (1988)
154-5	12°19.1' S	125°36.2' W	1-2	0.070 ± 0.005	Shimmield and Price (1988)
154-4	12°37.3' S	134°51.0' W	6-7	0.037 ± 0.002	Shimmield and Price (1988)
154-18	20°01.9' S	113°51.4' W	0-2	0.199 ± 0.012	Shimmield and Price (1988)
154-19	19°50.3' S	116°37.8' W	0-1	0.076 ± 0.006	Shimmield and Price (1988)
154-20	19°39.8' S	117°58.0' W	0-1	0.057 ± 0.003	Shimmield and Price (1988)
145-8	24°57.0' N	113°30.0' W	0-1	0.120 ± 0.005	Shimmield et al. (1986)
145-7	24°42.0' N	114°06.0' W	0-1	0.088 ± 0.004	Shimmield et al. (1986)
163-7	24°57.0' N	113°30.0' W	0-2	0.145 ± 0.010	Shimmield et al. (1986)
163-14	24°42.0' N	113°42.0' W	0-1	0.141 n.i.	Shimmield et al. (1986)
163-10	24°36.0' N	114°03.0' W	0-2	0.131 ± 0.005	Shimmield et al. (1986)
163-9	24°15.0' N	115°00.0' W	0-1	0.097 ± 0.008	Shimmield et al. (1986)
V18-258	11°52.0' N	165°45.0' W	0-5	0.028 ± 0.002	Ku (1965)
P7	02°36.3' N	83°59.2' W	7	0.286 n.i.	Yang et al. (1995)
A47-16	09°02.3' N	151°11.4' W	0-1	0.028 ± 0.002	Cochran and Krishnaswami (1980)
B52-39	11°14.8' N	139°04.1' W	0-1	0.033 ± 0.002	Cochran and Krishnaswami (1980)
C57-58	15°09.5' N	125°54.4' W	0-1	0.034 ± 0.002	Cochran and Krishnaswami (1980)
BC31	33°45.0' N	118°48.0' W	0-1	0.500 n.i.	Huh etal. (1987)
10132	06°13.2' N	148°57.3' W	0-4	0.038 ± 0.004	Mueller and Mangini (1980)
10149	09°30.5' N	146°09.5' W	0-2	0.042 ± 0.005	Mueller and Mangini (1980)
10175	09°19.3' N	146°01.1' W	0-2	0.022 ± 0.002	Mueller and Mangini (1980)
10145	03°59.5' N	144°49.3' W	0-2	0.033 ± 0.014	Mueller and Mangini (1980)
10147	03°50.2' N	145°01.7' W	0-2	0.044 ± 0.006	Mueller and Mangini (1980)
10140	09°15.0' N	148°44.5' W	0-2	0.044 ± 0.009	Mueller and Mangini (1980)
10141	09°06.5' N	148°46.7' W	0-2	0.035 ± 0.005	Mueller and Mangini (1980)
1858 21 bl	12°19.2' N	150°03.0' W	0-3	0.043 ± 0.006	Mangini and Kuehnel (1987)
1858 151 bl	12°20.4' N	150°10.2' W	0-3	0.032 ± 0.003	Mangini and Kuehnel (1987)
1858 163 bl	09°16.2' N	146°01.8' W	0-3	0.027 ± 0.005	Mangini and Kuehnel (1987)
1858 195 bl	09°40.2' N	146°05.4' W	0-3	0.023 ± 0.008	Mangini and Kuehnel (1987)
1858 232 bl	09°21.0' N	146°03.0' W	0-3	0.034 ± 0.008	Mangini and Kuehnel (1987)
1858 254 bl	09°19.8' N	146°05.4' W	0-3	0.031 ± 0.004	Mangini and Kuehnel (1987)
1858 358 bl	08°00.6' N	143°33.0' W	0-3	0.034 ± 0.006	Mangini and Kuehnel (1987)
VNTR01-01PC	11°15.0' N	109°36.6' W	1-3	0.056 ± 0.002	this study
VNTR01-02PC	07°11.4' N	109°45.0' W	0-2	0.073 ± 0.003	this study
VNTR01-03GC	07°10.2' N	109°44.4' W	0-2	0.089 ± 0.002	this study
VNTR01-04GC	05°21.0' N	110°05.4' W	0-2	0.093 ± 0.004	this study
VNTR01-05GC	02°45.6' N	110°34.8' W	0-2	0.094 ± 0.004	this study
VNTR01-06GC	02°45.6' N	110°33.0' W	0-2	0.092 ± 0.004	this study
VNTR01-07GC	01°01.2' N	110°34.2' W	0-2	0.116 ± 0.003	this study
VNTR01-08PC	00°02.4' N	110°28.8' W	4-6	0.113 ± 0.004	this study
VNTR01-09GC	03°00.0' S	110°30.0' W	0-2	0.109 ± 0.004	this study
VNTR01-10GC	04°30.6' S	102°01.2' W	0-2	0.128 ± 0.006	this study
VNTR01-11GC	00°08.4' N	95°20.4' W	1-3	0.137 ± 0.006	this study
VNTR01-12GC	03°00.6' S	95°04.2' W	0-2	0.119 ± 0.003	this study
VNTR01-13GC	03°05.4' S	90°49.2' W	0-2	0.143 ± 0.004	this study
VNTR01-15GC	01°29.4' N	89°51.6' W	0-2	0.167 ± 0.007	this study
VNTR01-16PC	02°36.0' N	89°43.8' W	0-2	0.106 ± 0.004	this study
Y69-071P	00°05.4' N	86°28.8' W	1-3	0.193 ± 0.006	this study
Y71-3-02	07°10.2' N	85°09.0' W	0-2	0.121 ± 0.005	this study
VNTR01-19PC	07°54.6' N	90°26.4' W	0-2	0.136 ± 0.006	this study
VNTR01-21GC	09°35.4' N	94°36.0' W	0-2	0.150 ± 0.006	this study
VNTR01-22GC	13°00.6' N	99°22.2' W	0-2	0.154 ± 0.007	this study
oj erdc bx88	00°03.0' S	155°52.2' E	3.9	0.087 ± 0.004	this study
oj erdc bx125	00°03.0' S	161°00.0' E	4.3	0.053 ± 0.003	this study
V21-71	27°54' N	162°31' E	0-2	0.036 ± 0.002	Ku (1966)
V18-258	11°52' S	165°45' W	0-5	0.036 ± 0.002	Ku (1966)
E11-11	64°50' S	114°28' W	0-5	0.078 ± 0.003	Ku (1966)

n.i.: not indicated
errors are given as 1σ

Table 2-3: Compiled data of $_{xs}^{231}Pa/_{xs}^{230}Th$ ratios of Holocene Atlantic sediments.

sample	latitude	longitude	depth (cm)	$_{xs}^{231}Pa/_{xs}^{230}Th$	reference
RC-13-259	53°53' S	04°56' W	23	0.213 ± 0.009	Kumar (1994)
RC-13-271	51°59' S	04°31' E	31	0.110 ± 0.004	Kumar (1994)
RC-13-254	48°34' S	05°07' E	13	0.071 ± 0.003	Kumar (1994)
RC-15-93	46°06' S	13°13' W	33	0.082 ± 0.003	Kumar (1994)
RC-15-94	42°54' S	20°51' W	15	0.051 ± 0.003	Kumar (1994)
V22-108	43°11' S	03°15' W	13	0.038 ± 0.001	Kumar (1994)
All76-3	41°33' S	20°12' E	0-1	0.048 ± 0.003	DeMaster (1979)
RC 15-101	42°59' S	41°34' W	4-7	0.094 ± 0.009	DeMaster (1979)
VM 29-105	48°05' S	18°41' E	3-6	0.090 ± 0.003	DeMaster (1979)
All 76-16	53°00' S	35°38' E	0-1	0.123 ± 0.007	DeMaster (1979)
RC 17-58	53°31' S	36°38' E	7-9	0.111 ± 0.007	DeMaster (1979)
RC 13 259	53°33' S	04°56' E	5-8	0.294 ± 0.026	DeMaster (1979)
RC 11 76	54°23' S	22°08' W	10-13	0.193 ± 0.017	DeMaster (1979)
RC 13 255	54°35' S	02°54' E	4-7	0.143 ± 0.008	DeMaster (1979)
RC 13 271	59°39' S	04°31' E	14-16	0.127 ± 0.006	DeMaster (1979)
GPC 5	33°41' S	57°37' W	32	0.054 ± 0.003	Bacon and Rosholt (1982)
oce 152 bc8	39°46.5' N	70°57.9' W	0-0.5	0.071 ± 0.007	Anderson et al. (1991)
oce 152 bc5	39°08.0' N	70°56.0' W	0-0.5	0.063 ± 0.003	Anderson et al. (1991)
en 179-bc7	37°25.1' N	73°49.4' W	0-1	0.051 ± 0.006	Anderson et al. (1991)
en 179-bc4	37°31.7' N	74°02.3' W	1-2	0.071 ± 0.011	Anderson et al. (1991)
en 187-bc6	37°24.0' N	73°49.7' W	0-1	0.055 ± 0.007	Anderson et al. (1991)
chn 82-23	41°38' N	27°20' W	0-5	0.057 ± 0.003	Ku et al. (1972)
chn 82-24	41°43' N	32°51' W	0-5	0.047 ± 0.002	Ku et al. (1972)
chn 82-25	42°19' N	28°35' W	0-6	0.041 ± 0.003	Ku et al. (1972)
chn 82-26	42°10' N	31°38' W	0-10	0.057 ± 0.003	Ku et al. (1972)
chn 82-28	42°00' N	29°54' W	0-10	0.055 ± 0.004	Ku et al. (1972)
chn 82-30	41°51' N	26°28' W	0-10	0.065 ± 0.004	Ku et al. (1972)
chn 82-31	42°23' N	31°48' W	0-10	0.050 ± 0.003	Ku et al. (1972)
chn 82-32	43°45' N	27°47' W	0-10	0.058 ± 0.004	Ku et al. (1972)
chn 82-33	42°29' N	28°40' W	0-10	0.070 ± 0.007	Ku et al. (1972)
chn 82-41	43°22' N	28°14' W	0-10	0.093 ± 0.005	Ku et al. (1972)
chn 82-42	43°20' N	28°05' W	0-10	0.061 ± 0.004	Ku et al. (1972)
All 42-41	22°14' N	56°39' W	0-5	0.039 ± 0.004	Ku et al. (1972)
v 9-97	00°23' N	29°52' W	5-8	0.084 ± 0.004	Ku (1966)
v 10-95	26°31' N	51°47' W	0-6	0.023 ± 0.003	Ku (1966)
v 16-21	17°17' N	48°28' W	2-10	0.053 ± 0.003	Ku (1966)
v 12-122	17°00' N	74°24' W	10-15	0.077 ± 0.007	Ku (1966)
CH 75-2-8	14°01' N	54°01' W	2-4	0.031 ± 0.002	Anderson et al. (1983)
core 12310	23°30' N	18°43' W	2-4	0.102 ± 0.013	Mangini and Dieter-Haass (1983)
ktb 10	21°03.0' N	31°12.0' W	0-1	0.033 ± 0.004	Legeleux (1994)
ktb 14	18°28.0' N	21°03.0' W	0-1	0.070 ± 0.005	Legeleux (1994)
ktb 12	21°04.0' N	31°09.0' W	0-1	0.032 ± 0.004	Legeleux (1994)
ktb 11	18°30.0' N	21°05.0' W	0-1	0.070 ± 0.009	Legeleux (1994)
ktb 09	20°32.0' N	18°36.0' W	0-1	0.160 ± 0.037	Legeleux (1994)
OCE 152-BC1	39°48.7' N	70°56.6' W	0-2	0.082 ± 0.008	Anderson et al. (1994)
OCE 152-BC9	39°41.9' N	70°54.8' W	0-0.5	0.091 ± 0.007	Anderson et al. (1994)
EN 123 BC4	39°48.2' N	70°55.7' W	1-1.5	0.076 ± 0.008	Anderson et al. (1994)
EN 123 BC6	39°48.8' N	70°55.4' W	0-1	0.066 ± 0.006	Anderson et al. (1994)
EN 123 BC3	39°34.9' N	70°55.2' W	0-1	0.061 ± 0.005	Anderson et al. (1994)
EN 123 BC1	39°08.2' N	70°55.5' W	1-1.5	0.053 ± 0.003	Anderson et al. (1994)
EN 179 BC2	37°37.5' N	74°10.0' W	4-5	0.050 ± 0.011	Anderson et al. (1994)
EN 179 BC3	37°38.4' N	74°08.6' W	2-3	0.075 ± 0.016	Anderson et al. (1994)
EN 187 BC4	37°37.3' N	74°13.3' W	3-4	0.063 ± 0.023	Anderson et al. (1994)
EN 187 BC10	36°52.5' N	74°36.8' W	1-2	0.089 ± 0.029	Anderson et al. (1994)
EN 187 BC8	36°52.0' N	74°34.4' W	1-2	0.053 ± 0.015	Anderson et al. (1994)
EN 187 BC5	37°37.1' N	74°10.0' W	4-5	0.069 ± 0.014	Anderson et al. (1994)
EN 187 BC11	37°02.3' N	74°34.3' W	2-3	0.062 ± 0.023	Anderson et al. (1994)
EN 187 BC9	36°52.2' N	74°33.8' W	6-8	0.075 ± 0.014	Anderson et al. (1994)
17729	75°00.0' N	0°00.0' E	0-1	0.078 ± 0.006	Scholten et al. (1995)
21893	74°52.1' N	10°06.6' W	0-1	0.101 ± 0.009	Scholten et al. (1995)
21895	75°24.8' N	07°18.6' W	0-1	0.076 ± 0.008	Scholten et al. (1995)
23293	72°37.3' N	06°35.5' W	0-1	0.079 ± 0.011	Scholten et al. (1995)
17725	77°27.6' N	04°34.8' E	0-1	0.077 ± 0.005	Scholten et al. (1995)
17726	75°29.9' N	03°33.7' E	0-1	0.072 ± 0.006	Scholten et al. (1995)
17728	76°31.2' N	03°37.5' E	0-1	0.105 ± 0.009	Scholten et al. (1995)
17730	72°06.7' N	07°23.3' E	0-1	0.145 ± 0.010	Scholten et al. (1995)
M 36/2	32°59.8' N	21°59.5' W	0	0.042 ± 0.009	Scholten, unpublished
M 36/2	54°36.7' N	21°09.0' W	0	0.073 ± 0.013	Scholten, unpublished
HM-94-18/3	73°30.0' N	05°41.0' E	0	0.045 ± 0.003	Yu (1994)
HM-71-19	69°29.0' N	09°31.0' W	0	0.077 ± 0.006	Yu (1994)
HM-79-26	66°54.0' N	05°56.0' W	0	0.071 ± 0.004	Yu (1994)
VM 27-086	66°36.0' N	01°07.0' E	9	0.087 ± 0.005	Yu (1994)
VM 28-014	64°47.0' N	29°34.0' W	13	0.108 ± 0.004	Yu (1994)
VM 29-179	44°00.0' N	24°32.0' W	16	0.044 ± 0.002	Yu (1994)
CHN 82-020	43°30.0' N	29°52.0' W	4-6	0.052 ± 0.003	Yu (1994)
CHN 82-015	43°22.0' N	28°14.0' W	3-4	0.069 ± 0.006	Yu (1994)
CHN 82-011	42°23.0' N	31°48.0' W	3.5-5	0.053 ± 0.004	Yu (1994)
CHN 82-004	41°43.0' N	32°51.0' W	2-4	0.065 ± 0.005	Yu (1994)
VM 30-097	41°00.0' N	33°56.0' W	5-16	0.272 ± 0.010	Yu (1994)
VM 26-176	36°00.0' N	72°00.0' W	8-10	0.066 ± 0.004	Yu (1994)
VM 23-100	22°41.0' N	21°18.0' W	10	0.035 ± 0.001	Yu (1994)
VM 30-049	18°26.0' N	21°05.0' W	10-15	0.082 ± 0.003	Yu (1994)
KNR 64-05	16°31.0' N	74°48.0' W	6-7.5	0.054 ± 0.003	Yu (1994)
VM 22-197	14°10.0' N	18°35.0' W	25	0.051 ± 0.003	Yu (1994)
EN 66-29	02°28.0' N	19°46.0' W	2-12	0.047 ± 0.003	Yu (1994)
EN 66-38	04°55.0' N	20°30.0' W	2.5-9.5	0.051 ± 0.003	Yu (1994)
KNR 110-55	04°57.0' N	42°54.0' W	4-17	0.052 ± 0.004	Yu (1994)

Table 2-3: continued

sample	latiude	longitude	depth (cm)	$xs^{231}Pa/xs^{230}Th$	reference
KNR 110-91	04°46.0' N	43°18.0' W	0	0.029 ± 0.002	Yu (1994)
KNR 110-82	04°20.0' N	43°29.0' W	0-13	0.046 ± 0.003	Yu (1994)
VM 25-059	01°22.0' N	39°29.0' W	8	0.042 ± 0.002	Yu (1994)
VM 30-040	00°12.0' S	23°08.0' W	15	0.040 ± 0.001	Yu (1994)
VM 22-174	10°04.0' S	12°49.0' W	8	0.050 ± 0.001	Yu (1994)
VM 19-240	30°35.0' S	13°17.0' W	20	0.040 ± 0.002	Yu (1994)
All 107-065	32°02.0' S	36°11.0' W	3-4	0.048 ± 0.004	Yu (1994)
RC 12-294	37°16.0' S	10°06.0' W	10	0.045 ± 0.003	Yu (1994)
All 107-022	54°48.0' S	03°20.0' W	3-4	0.231 ± 0.014	Yu (1994)
PS 1751	44°29.3' S	10°28.3' E	0-2	0.074 ± 0.004	Walter et al. (1997)
PS 1752	45°37.2' S	09°36.5' E	0-5	0.070 ± 0.003	Walter et al. (1997)
PS 1755	47°47.3' S	07°06.1' E	1-2	0.078 ± 0.004	Walter et al. (1997)
PS 1759	50°09.2' S	05°45.3' E	0-5	0.089 ± 0.004	Walter et al. (1997)
PS 1765	51°49.9' S	04°51.8' E	0-5	0.123 ± 0.006	Walter et al. (1997)
PS 1768	52°35.5' S	04°27.6' E	1-2	0.114 ± 0.008	Walter et al. (1997)
PS 1772	55°27.5' S	01°10.0' E	1-2	0.152 ± 0.009	Walter et al. (1997)
PS 1775	50°57.1' S	07°30.1' W	0-5	0.088 ± 0.004	Walter et al. (1997)
PS 1777	48°13.9' S	11°02.2' W	0-1.5	0.100 ± 0.006	Walter et al. (1997)
PS 1779	50°23.7' S	14°04.5' W	0-5	0.093 ± 0.005	Walter et al. (1997)
PS 1780	51°41.0' S	15°16.4' W	0-5	0.151 ± 0.008	Walter et al. (1997)
PS 1782	55°11.4' S	18°36.6' W	0-5	0.155 ± 0.008	Walter et al. (1997)
PS 1954	64°24.4' S	45°48.2' W	0.5-2	0.142 ± 0.008	Walter et al. (1997)
PS 1955	64°49.2' S	42°30.2' W	0-0.5	0.160 ± 0.010	Walter et al. (1997)
PS 1957	65°40.3' S	37°44.6' W	0-0.5	0.145 ± 0.007	Walter et al. (1997)
PS 1959	65°24.7' S	37°54.8' W	0-0.5	0.148 ± 0.007	Walter et al. (1997)
PS 1961	65°43.2' S	35°26.9' W	0.5-2	0.136 ± 0.008	Walter et al. (1997)
PS 1964	66°16.6' S	30°17.8' W	0.5-2	0.144 ± 0.009	Walter et al. (1997)
PS 1966	66°37.6' S	27°07.5' W	0-0.5	0.174 ± 0.009	Walter et al. (1997)
PS 1968	67°28.7' S	31°06.6' W	0-0.5	0.161 ± 0.010	Walter et al. (1997)
PS 1974	67°13.3' S	24°08.8' W	0.5-2	0.162 ± 0.008	Walter et al. (1997)
PS 1976	67°50.5' S	20°50.7' W	0.5-2	0.184 ± 0.011	Walter et al. (1997)
PS 1978	68°50.4' S	17°53.6' W	0.5-2	0.161 ± 0.008	Walter et al. (1997)
PS 1979	69°22.0' S	16°29.8' W	0.5-2	0.146 ± 0.008	Walter et al. (1997)
PS 1981	70°07.9' S	14°15.2' W	0.5-2	0.143 ± 0.008	Walter et al. (1997)
PS 1991	76°24.8' S	30°21.2' W	0-5	0.080 ± 0.009	Walter et al. (1997)
PS 2011	71°05.7' S	20°46.8' W	0-1	0.161 ± 0.009	Walter et al. (1997)
PS 2039	69°01.4' S	06°13.7' E	0-5	0.151 ± 0.009	Walter et al. (1997)
PS 2040	68°50.5' S	06°14.1' E	0-1	0.134 ± 0.008	Walter et al. (1997)
PS 2049	69°05.2' S	00°53.4' E	0-5	0.105 ± 0.006	Walter et al. (1997)
PS 2052	66°48.3' S	06°15.8' E	0-1	0.178 ± 0.009	Walter et al. (1997)
PS 2055	68°17.4' S	06°14.9' E	0-1.2	0.170 ± 0.010	Walter et al. (1997)
PS 2072	60°33.9' S	03°57.6' E	0-1	0.166 ± 0.007	Walter et al. (1997)
PS 2254	43°58.3' S	50°06.4' W	0-1	0.092 ± 0.005	Walter et al. (1997)
PS 2256	44°31.0' S	44°27.1' W	0-1	0.085 ± 0.008	Walter et al. (1997)
PS 2257	45°00.7' S	38°32.5' W	0-1	0.090 ± 0.005	Walter et al. (1997)
PS 2262	48°30.1' S	37°00.3' W	0-1	0.098 ± 0.007	Walter et al. (1997)
PS 2269	50°22.3' S	33°14.7' W	0-1	0.116 ± 0.006	Walter et al. (1997)
PS 2271	51°31.9' S	31°22.3' W	0-1	0.112 ± 0.006	Walter et al. (1997)
PS 2273	52°39.4' S	30°33.1' W	0-1	0.119 ± 0.007	Walter et al. (1997)
PS 2276	54°38.1' S	23°57.3' W	0-1	0.120 ± 0.007	Walter et al. (1997)
PS 2280	56°49.7' S	22°19.5' W	0-1	0.130 ± 0.007	Walter et al. (1997)
PS 2283	59°44.1' S	23°16.5' W	0-1	0.149 ± 0.008	Walter et al. (1997)
PS 2288	57°45.4' S	25°20.2' W	0-1	0.162 ± 0.011	Walter et al. (1997)
PS 2299	57°30.6' S	30°14.1' W	0-1	0.149 ± 0.008	Walter et al. (1997)
PS 2307	59°03.5' S	35°34.6' W	0-1	0.142 ± 0.008	Walter et al. (1997)
PS 2312	59°49.6' S	39°42.3' W	0-1	0.188 ± 0.012	Walter et al. (1997)
PS 2320	60°06.0' S	44°50.8' W	0-1	0.125 ± 0.007	Walter et al. (1997)
PS 2331	59°02.4' S	48°59.6' W	0-1	0.105 ± 0.008	Walter et al. (1997)
PS 2334	57°55.1' S	52°00.0' W	0-1	0.090 ± 0.005	Walter et al. (1997)
PS 2336	57°09.1' S	53°59.3' W	0-1	0.123 ± 0.006	Walter et al. (1997)
PS 2339	56°01.9' S	56°56.6' W	0-1	0.112 ± 0.006	Walter et al. (1997)
PS 2342	55°15.5' S	57°59.1' W	0-1	0.132 ± 0.009	Walter et al. (1997)
PS 2353	53°36.4' S	58°58.6' W	0-1	0.094 ± 0.008	Walter et al. (1997)
PS 2361	55°00.1' S	06°02.8' W	0-5	0.238 ± 0.013	Walter et al. (1997)
PS 2362	53°00.1' S	05°59.9' W	0-5	0.172 ± 0.010	Walter et al. (1997)
PS 2363	48°00.1' S	06°00.1' W	0-5	0.069 ± 0.003	Walter et al. (1997)
PS 2364	56°04.3' S	06°50.6' W	0-5	0.130 ± 0.008	Walter et al. (1997)
PS 2365	55°00.5' S	06°00.3' W	0-5	0.256 ± 0.015	Walter et al. (1997)
PS 2366	50°59.9' S	06°00.0' W	0-5	0.147 ± 0.010	Walter et al. (1997)
PS 2367	49°00.0' S	06°00.1' W	0-5	0.084 ± 0.004	Walter et al. (1997)
PS 2368	46°52.3' S	05°43.0' W	0-0.5	0.055 ± 0.003	Walter et al. (1997)
PS 2369	55°51.1' S	05°59.6' W	0-5	0.159 ± 0.007	Walter et al. (1997)
PS 2370	58°29.2' S	05°59.9' W	0-5	0.140 ± 0.008	Walter et al. (1997)
PS 2371	57°03.3' S	06°00.5' W	0-5	0.176 ± 0.009	Walter et al. (1997)
PS 2372	53°59.8' S	06°00.2' W	0-5	0.094 ± 0.005	Walter et al. (1997)
PS 2376	48°30.1' S	06°00.2' W	0-5	0.085 ± 0.004	Walter et al. (1997)
PS 2562	43°11.2´ S	31°35.2´ E	0-5	0.073 ± 0.003	Walter et al. (1997)
PS 2575	59°26.8´ S	03°12.4´ W	0-0.5	0.179 ± 0.010	Walter et al. (1997)
PS 2577	61°13.2´ S	02°11.7´ E	0-0.5	0.095 ± 0.004	Walter et al. (1997)
PS 2578	62°07.4´ S	05°01.8´ E	0-5	0.131 ± 0.006	Walter et al. (1997)
PS 2579	62°57.8´ S	07°46.4´ E	0-5	0.163 ± 0.009	Walter et al. (1997)
PS 2589	66°00.1´ S	24°58.6´ E	0-5	0.147 ± 0.006	Walter et al. (1997)
PS 2600	63°11.0´ S	34°31.6´ E	0-5	0.154 ± 0.006	Walter et al. (1997)
PS 2602	60°22.5´ S	36°34.9´ E	0-5	0.154 ± 0.007	Walter et al. (1997)
PS 2604	57°35.9´ S	38°35.4´ E	0-5	0.161 ± 0.009	Walter et al. (1997)
PS 2611	49°30.3´ S	38°49.6´ E	0-5	0.110 ± 0.005	Walter et al. (1997)

errors are given as 1σ

3 Enhanced scavenging of ^{231}Pa relative to ^{230}Th in the South Atlantic south of the Polar Front: Implications for the use of the $^{231}Pa/^{230}Th$ ratio as a paleoproductivity proxy

H.J. Walter, M.M. Rutgers van der Loeff and H. Höltzen

Alfred Wegener Institute for Polar and Marine Research, Bremerhaven, Germany

3.1 Abstract

The fractionation of ^{230}Th and ^{231}Pa was investigated throughout the Atlantic sector of the Southern Ocean. Published scavenging models generally assume that the $^{231}Pa/^{230}Th$ ratio of surface sediments is primarily determined by the mass flux of particles. This relationship holds north of the Polar Front, where low primary productivity coincides with ratios of unsupported $^{231}Pa/^{230}Th$ $_{xs}(^{231}Pa/^{230}Th)$ in surface sediments below the production ratio of both radionuclides in the water column. However, we observed high $_{xs}^{231}Pa/_{xs}^{230}Th$ ratios, conventionally interpreted as a high-productivity signal, in surface sediments south of Polar Front, especially throughout the Weddell Sea, in contradiction with the low particle flux of this region. Measurements of both dissolved and particulate fractions of ^{231}Pa and ^{230}Th in the water column revealed a strong N-S decrease of the Th/Pa-fractionation factor from typical open ocean values around 10 north of the Polar Front to values between 1 and 2 south of 60°S. This observation clearly indicates that the high $_{xs}^{231}Pa/_{xs}^{230}Th$ ratios in surface sediments south of the Antarctic Circumpolar Current are produced by a N-S increase in the relative scavenging efficiency of ^{231}Pa relative to ^{230}Th, most probably due to a change in the chemical composition of particulate matter, and not by a high mass flux. It is speculated that biogenic opal, suggested not to significantly fractionate ^{231}Pa and ^{230}Th, may explain the enhanced scavenging of ^{231}Pa to the south. This assumption is further supported by extremely high $^{231}Pa/^{230}Th$ ratios up to 0.34 in material collected with sediment traps south of the Polar Front, where fluxes are primarily determined by biogenic opal. Based on these results we conclude that in regions where the sedimenting flux is dominated by biogenic opal, the $^{231}Pa/^{230}Th$ ratio is not a reliable indicator for the mass flux of particles, thus limiting its use as a paleoproductivity proxy in the Southern Ocean.

3.2 Introduction

Oceanic bioproductivity is considered to be an important factor controlling the partitioning of CO_2 between deep ocean and atmosphere, which is termed as the "biological pump" (Eppley and Peterson, 1979; Broecker and Peng, 1982; Martin, 1990). In the euphotic zone of the surface ocean, CO_2 is taken up by phytoplankton and converted into organic matter, which then may sink to the deep ocean. Attempts have been made to explain variations in the atmospheric concentration of CO_2 in the past by differences in the bioproductivity of the oceans (Martin, 1990; Sarmiento and Toggweiler, 1984; Keir, 1990). Recently it was argued that iron as limiting factor for today's Southern Ocean productivity, was supplied in glacial periods by wind-blown dust (Kumar et al., 1995). A resulting increase in bioproductivity could have

contributed to the lower concentrations of CO_2 in the glacial atmosphere. Ideally, the productivity signal of the surface ocean should be stored in the underlying sediments but high and variable remineralization rates of most of the biogenic detritus in the water column and in surface sediments leave behind changes in preservation efficiency rather than real changes in productivity (Berger et al., 1987; Van-Bennekom et al., 1988; Bareille et al., 1991; Nürnberg, 1995). Hence, to reconstruct past changes in oceanic productivity we have to look for tracers (proxies) in oceanic sediments which have preserved their bioproductivity signal from the euphotic zone, independently from the preservation of biogenic material.

In this paper we focus on the $^{231}Pa/^{230}Th$ ratio which has been proposed to be such a tracer (Kumar et al., 1995; Lao et al., 1992a; 1992b; 1993; Francois et al., 1993; Kumar et al., 1993; Kumar, 1994; Yu, 1994). ^{231}Pa (half-life = 32.500 years) and ^{230}Th (half-life = 75.200 years) are natural radionuclides which are continuously produced in the water column by alpha decay of their dissolved progenitors ^{235}U and ^{234}U. As a result of its long oceanic residence time, the distribution of U in the ocean is very homogenous (Chen et al., 1986). Consequently, ^{231}Pa and ^{230}Th are produced uniformly throughout the water column at a constant initial activity ratio of 0.093. In contrast to U, ^{231}Pa and ^{230}Th are particle-reactive and are scavenged to the sea floor within 50-200 years and 10-40 years, respectively (Anderson et al., 1983a; 1983b; Nozaki et al., 1985; Rutgers van der Loeff and Berger, 1993; Yu et al., 1996). This small difference in particle reactivity of Pa and Th is responsible for a fractionation of the two radionuclides in the water column. Due to its short oceanic residence time over most of the ocean the flux of ^{230}Th to the sediment is assumed to equal its local rate of production in the water column, whereas the longer oceanic residence time for ^{231}Pa allows this nuclide to be transported over basin-wide distances prior to being scavenged. In large areas of the world's oceans it has been shown that the mass flux of particles is the primary factor controlling the scavenging of ^{231}Pa, and thus determines the ratio at which ^{231}Pa and ^{230}Th are deposited in the sediment (Kumar et al., 1993). This is well documented by $^{231}Pa/^{230}Th$ ratios lower than their production ratio of 0.093 in areas of low particle flux (e.g. in the central gyres), where only a minor fraction of the ^{231}Pa is scavenged to the underlying sediments with the remainder being transported laterally to regions of higher particle fluxes where it is removed more efficiently (e.g. Anderson et al., 1983a; 1983b). Consequently, $^{231}Pa/^{230}Th$ ratios in surface sediments in upwelling regions at ocean margins strongly exceed the production ratio. The enhanced scavenging at ocean margins is termed as "boundary scavenging", (for recent reviews of this process see Lao et al. 1992a; Bacon, 1988; Anderson et al. 1994). Based on this apparently well-established relationship between $^{231}Pa/^{230}Th$ ratio and mass flux (Yu, 1994), the $^{231}Pa/^{230}Th$ ratio has been used to assess past changes in oceanic productivity of dated sediment cores (Kumar et al., 1993; 1995; Lao et al., 1992a; 1992b; Francois et al., 1993). In this model variations of the $^{231}Pa/^{230}Th$ ratio through time were simply explained by changes in ocean productivity.

The application of the $^{231}Pa/^{230}Th$ ratio as a paleoproductivity proxy requires a constant $^{230}Th/^{231}Pa$ fractionation factor (indicated with letter "F"), which is defined as

$$F = \frac{(^{230}Th/^{231}Pa)_{part}}{(^{230}Th/^{231}Pa)_{diss}} \quad (1)$$

However, this assumption does not seem to be valid throughout the oceans (Rutgers van der Loeff and Berger, 1993). These authors measured a southward decrease of the $^{230}Th/^{231}Pa$ fractionation factor on a N-S transect across the Antarctic Circumpolar Current (ACC) in the South Atlantic, which was explained by a N-S increase in the scavenging efficiency of ^{231}Pa relative to ^{230}Th, may be due to a change in the chemical composition of suspended particulate matter. Their findings together with results of other authors (Kumar et al., 1995; Anderson et al., 1983a; 1983b; 1990; 1994; Shimmield et al., 1988; Taguchi et al., 1989, Lao et al., 1992a; 1992b) imply that in certain oceanic areas the chemical composition of particles has to be considered as an additional factor controlling the ratio at which ^{231}Pa and ^{230}Th are scavenged from the water column.

Furthermore, a recent study (Yu et al., 1996) has revealed that the hydrography may also control the scavenging of ^{231}Pa. They found that boundary scavenging of ^{231}Pa is not well pronounced in the Atlantic Ocean (in contrast to the Pacific Ocean, Yang et al., 1986), where even in the upwelling region off Western Africa the $^{231}Pa/^{230}Th$ ratios in surface sediments do not exceed the production ratio. The lack of boundary scavenging of ^{231}Pa in the Atlantic Ocean was explained by the short mean residence time of deep water (80-100 years, Leynaert et al., 1993), a timescale similar to that of Pa scavenging and horizontal mixing, which does not allow high concentrations of dissolved ^{231}Pa to build up in the central Atlantic Ocean, required for a large scale diffusive transport of ^{231}Pa to the ocean margins. Yu and co-workers estimated, that only half of the ^{231}Pa produced in the Atlantic north of 50°S is deposited in the underlying sediments, with the remainder being advected to the south with North Atlantic Deep Water (NADW). They further suggested that this exported amount of dissolved ^{231}Pa is removed to the sediments after entering the ACC south of 50°S. The enhanced scavenging of ^{231}Pa in the Southern Ocean south of the Polar Front was speculated to result from the high particle flux within the productive ACC (Yu, 1994; DeMaster, 1979; Boyle, 1996). If this assumption holds we should expect a decrease in the $^{231}Pa/^{230}Th$ ratios south of the productive ACC, for which Yu et al. (1996) found some support in the only three data points available to them.

The objective of this study is to find out whether in the South Atlantic the $^{231}Pa/^{230}Th$ ratio is still a reliable tracer for the mass flux of particles. To test whether earlier observations (Rutgers van der Loeff and Berger, 1993) of a latitudinal gradient of F, which are based on data from a single N-S transect, occur on a basin-wide scale, the water column was sampled on several transects throughout the South Atlantic. In addition, a large number of surface sediments were analyzed for ^{231}Pa and ^{230}Th to find out whether the latitudinal gradient of F is also reflected in the sedimentary $^{231}Pa/^{230}Th$ record, which would have important consequences for the use of the $^{231}Pa/^{230}Th$ ratio as a paleoproductivity proxy. Furthermore, to investigate, to what extent the breakdown of F in the Southern Ocean results from a N-S change in the chemical composition of particulate matter, $^{231}Pa/^{230}Th$ ratios were also determined in sediment trap samples with known chemical composition of sinking particles.

3.3 Sampling and analytical methods

The water column was sampled by in situ pumping to collect the dissolved and particulate fractions of ^{231}Pa and ^{230}Th. Samples were taken at 16 stations on several N-S transects across the Antarctic Circumpolar Current throughout the Atlantic sector of the Southern Ocean during Polarstern expeditions ANT X/5 (August-September 1992), ANT X/6 (October-November 1992) and ANT XI/4 (March-May 1994), and at 4 stations in the Southern Weddell Sea during ANT IX/3 (Jan-March 1991) (Fig.3-1). Surface sediment samples were taken at each pumping station and from a large number of additional locations, including expedition ANT IX/2 (Fig.1). Details on station locations are given in the respective cruise reports (ANT IX/2 and ANT IX/3: Bathmann et al. (1992), ANT X/5: Gersonde (1993), ANT X/6: Bathmann et al. (1994), ANT XI/4: Kuhn, in prep.).

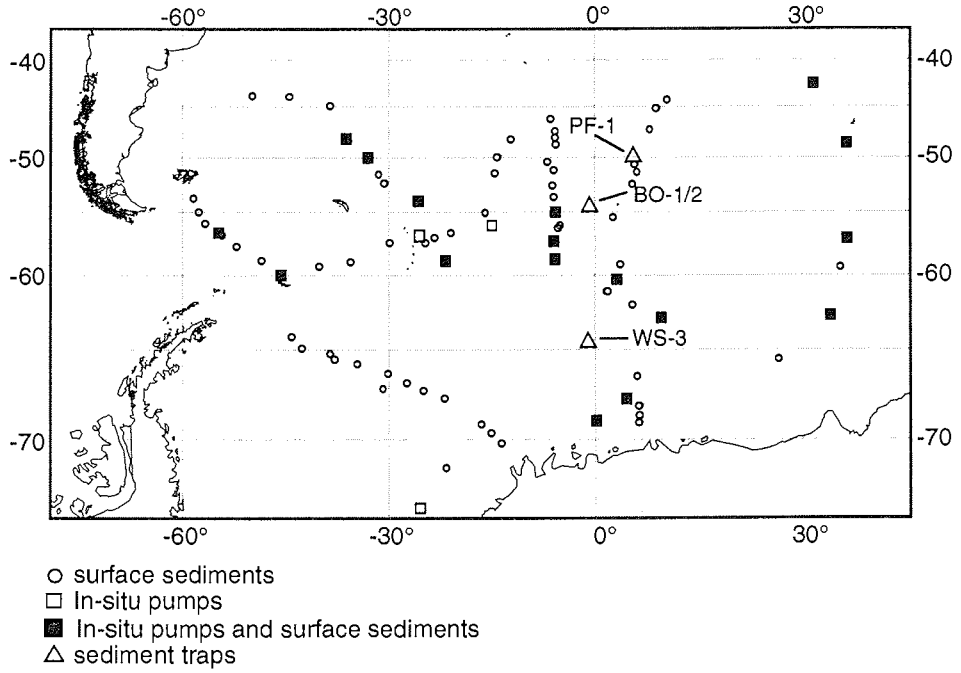

Fig.3-1: Map with sample locations.

At each pumping station 300-1400 liters of seawater were filtered in situ by several COSS-filtration systems through a 1μ nuclepore filter and two MnO_2-coated cartridges. A detailed description of the analytical procedures for the cartridges is given in Rutgers van der Loeff and Berger (1993). Briefly, cartridges were spiked with appropriate amounts of ^{229}Th and ^{233}Pa as yield tracers and leached on board under recirculation with a solution containing 0.02 N hydroxylammonium chloride, 0.07 N HNO_3 and 0.01 N HF. We found that the leaching procedure was not quantitative for Th (only 40-70% were leached from the cartridges) which prevented

an isotopic equilibrium between the ^{229}Th spike and the Th isotopes in the sample to be reached. Therefore natural ^{234}Th which is in radioactive equilibrium with its parent ^{238}U below a depth of 100m (Rutgers van der Loeff et al., 1997), was used as yield tracer for the calculation of dissolved ^{230}Th. The leaching procedure for ^{231}Pa was found to be quantitative. Collection efficiencies for ^{231}Pa and ^{230}Th are based on the activities of ^{231}Pa and ^{234}Th leached from the two cartridges in series (Mann et al., 1984), mostly ranged between 60 to 80% and 85 to 95%, respectively. Filters were dried (not weighed), spiked with the same yield tracers and digested in a microwave using a mixture of 10ml HNO_3 (65%), 2ml HF (40%), 1ml H_2O_2 (30%) and 2ml $HClO_4$ (70%). After digestion, Th and Pa were separated on anion exchange resin (AG1-X8, 100-200 mesh) and further treated according to Anderson and Fleer (1982). Pa was purified by the conventional TTA-extraction (Anderson and Fleer, 1982) except for the filters from expedition ANT XI/4, where an electroplating method was performed. Good results were obtained by the electroplating procedure using polypropylene rather than glass columns (Francois, pers. comm) for the separation of Pa from Th to prevent the release of silica.

The surface sediment samples were analyzed for ^{231}Pa, Th and U isotopes according to the following procedure. 0.5g of dry sediment was spiked with ^{233}Pa, ^{229}Th and ^{236}U, and digested in a mixture of 10ml HNO_3 (65%), 5ml HF (40%) and 5ml $HClO_4$ (70%). Th and U isotopes were separated, purified and electroplated according to Anderson and Fleer (1982). For Pa, the electroplating method was applied. After electroplating onto silver discs, activities of ^{231}Pa, Th and U isotopes were determined by alpha-, ^{234}Th and ^{233}Pa by beta-counting. Chemical yields for Pa were around 50% for the conventional TTA-extraction method (except for ANT IX/3 with only 10-30%). Higher chemical efficiencies for Pa (60-80%) were achieved by the new electroplating method. Chemical yields for Th and U were around 80% and 50-60%, respectively (except for a number of cartridges with Th-efficiencies <50% due to incomplete leaching, see above).

The tracers ^{236}U and ^{229}Th were calibrated with certified standard solutions prepared from pure U_3O_8 and ThO_2 (PTB-Braunschweig, uncertainty 2.5% (3σ)), respectively. For the calibration of the ^{233}Pa tracer a definite amount of tracer solution was evaporated on a platinum disc and beta counted. Calibrations were checked by replicate analysis of the uranium-bearing sediment standards DL-1a (Steger and Bowman, 1980) and UREM-11 (Hansen and Ring, 1983). Blank contributions for ^{231}Pa and ^{230}Th to the sediments were negligible but blanks contributed mostly around 2-5% to ^{231}Pa in the first and 3-25% in the second cartridge in series. ^{230}Th blanks contributed generally 2-8% (only one cartridge used). Contributions are highest for the suspended particulate matter with blanks for ^{231}Pa of 3-75% and 1-30% for ^{230}Th. Due to low chemical efficiency for Pa of the cartridges (only 10-30%) during ANT IX/3 blank contributions for ^{231}Pa were higher with 8-20% for the first and 14-70% for the second cartridge. Only data with blank contributions less than 50% were included in the results.

Measured activities of ^{230}Th and ^{231}Pa of the surface sediments were corrected for detrital, U-supported ^{230}Th and ^{231}Pa, which is assumed to be in secular equilibrium with the detrital ^{234}U and ^{235}U, respectively. For samples with a $^{234}U/^{232}Th$ ratio less

than 0.8, excess activities of ^{230}Th ($_{xs}^{230}Th$) and ^{231}Pa ($_{xs}^{231}Pa$) were calculated as follows:

$$_{xs}^{230}Th = {}^{230}Th_m - {}^{234}U \quad (2)$$

$$_{xs}^{231}Pa = {}^{231}Pa_m - 0.046 \cdot {}^{234}U \quad (3)$$

The notation (m) stands for measured activity and the factor 0.046 is the activity ratio of $^{235}U/^{234}U$ in detrital material. Sediments with $^{234}U/^{232}Th$ exceeding 0.8 were assumed to contain authigenic uranium and in those cases unsupported activities of ^{230}Th and ^{231}Pa were calculated using ^{232}Th (Anderson et al., 1983a):

$$_{xs}^{230}Th = {}^{230}Th_m - R \cdot {}^{232}Th_m \quad (4)$$

$$_{xs}^{231}Pa = {}^{231}Pa_m - 0.046 \cdot R \cdot {}^{232}Th \quad (5)$$

("R") designates the $^{238}U/^{232}Th$ ratio of average detrital material and is based on those samples with $^{234}U/^{232}Th$ less than 0.8. R has been found to vary with latitude, with values around 0.6 north of 60°S decreasing to the south to values between 0.3-0.4. These regional variations are included in the calculation of the unsupported activities. Ingrowth of ^{230}Th and ^{231}Pa from authigenic U can be excluded because of the young age of the sediments. Although the calculation of $_{xs}^{231}Pa$ and $_{xs}^{230}Th$ may overestimate or underestimate the supported activities for some of the samples, this does not significantly affect the conclusions drawn in this study because of the high $^{230}Th/^{232}Th$ ratio in most of the samples.

3.4 Results

An overview of $_{xs}^{231}Pa/_{xs}^{230}Th$ ratios of surface sediments throughout the Atlantic sector of the Southern Ocean is given in Table 3-1 and Fig.3-2. The ratios are surprisingly well correlated with latitude (Fig.3-3 a). As expected from the low primary productivity (Berger et al., 1987), lowest $_{xs}^{231}Pa/_{xs}^{230}Th$ ratios far below the production ratio of 0.093 are observed in sediments north of the Polar Front. The southward increase above the production ratio within ACC persists throughout the Weddell Sea, where values are mostly clustering around 0.15. Results of dissolved (<1µm) $^{231}Pa/^{230}Th$ are shown in Table 3-2 and Fig. 3-3 (b). The data designate a rough N-S decrease across the ACC, with lowest values occurring in the central Weddell Sea (Fig.3-3 b), where dissolved ^{230}Th accumulates relative to ^{231}Pa due to upwelling and ingrowth (Rutgers van der Loeff and Berger, 1993). $^{231}Pa/^{230}Th$ ratios on suspended particles (Table 3-2, Fig.3-3 c) show the same N-S trend as the surface sediments (Fig.3-3 a) with lowest values far below the production ratio in the northernmost stations, typical for open ocean environments (Anderson et al., 1983a; 1983b; Nozaki and Nakanishi, 1985) increasing strongly across the ACC to the south.

Table 3-1: Activities (dpm/g) of ^{234}U, ^{232}Th, ^{230}Th, ^{231}Pa, excess ^{231}Pa ($_{xs}^{231}Pa$), excess ^{230}Th ($_{xs}^{230}Th$) and $_{xs}^{231}Pa/_{xs}^{230}Th$ for all surface sediment samples (errors are 1σ propagated from counting statistics).

expedition	station	latitude	longitude	water depth (m)	depth (cm)	^{234}U	^{232}Th	^{230}Th	^{231}Pa	$_{xs}^{231}Pa$	$_{xs}^{230}Th$	$_{xs}^{231}P_{xs}^{230}Th$
ANT VIII/3	PS 1751	44° 29.3' S	10° 28.3' E	4770	0-2	0.68±0.04	1.19±0.10	33.19±0.94	2.39±0.10	2.38±0.10	32.51±0.96	0.074±0.004
	PS 1752	45° 37.2' S	09° 36.5' E	4507	0-5	0.47±0.03	1.02±0.05	28.16±0.55	1.94±0.07	1.92±0.07	27.69±0.59	0.070±0.003
	PS 1755	47° 47.3' S	07° 06.1' E	4263	1-2	0.58±0.03	0.79±0.06	30.09±0.78	2.29±0.09	2.29±0.09	29.52±0.80	0.078±0.004
	PS 1759	50° 09.2' S	05° 45.3' E	3717	0-5	0.62±0.03	0.43±0.04	14.57±0.42	1.28±0.05	1.28±0.05	14.31±0.49	0.089±0.004
	PS 1765	51° 49.9' S	04° 51.8' E	3749	0-5	0.60±0.03	0.26±0.03	8.82±0.22	1.07±0.04	1.07±0.04	8.67±0.27	0.123±0.006
	PS 1768	52° 35.5' S	04° 27.6' E	3276	1-2	0.75±0.06	0.27±0.04	8.65±0.30	0.97±0.05	0.97±0.05	8.49±0.38	0.114±0.008
	PS 1772	55° 27.5' S	01° 10.0' E	4136	1-2	0.74±0.10	1.06±0.07	10.96±0.28	1.55±0.06	1.55±0.06	10.23±0.45	0.152±0.009
	PS 1775	50° 57.1' S	07° 30.1' W	2516	0-5	0.51±0.03	0.81±0.04	27.93±0.50	2.40±0.09	2.40±0.09	27.42±0.55	0.088±0.004
	PS 1777	48° 13.9' S	11° 02.2' W	2556	0-1.5	n.d.	0.22±0.03	7.27±0.23	0.71±0.04	0.71±0.04	7.14±0.29	0.100±0.006
	PS 1779	50° 23.7' S	14° 04.5' W	3549	0-5	n.d.	0.56±0.04	11.72±0.26	1.06±0.04	1.05±0.04	11.39±0.32	0.093±0.005
	PS 1780	51° 41.0' S	15° 16.4' W	4258	0-5	0.92±0.06	0.75±0.05	10.34±0.28	1.49±0.06	1.49±0.06	9.89±0.34	0.151±0.008
	PS 1782	55° 11.4' S	18° 36.6' W	5016	0-5	0.86±0.08	0.30±0.03	7.84±0.25	1.19±0.05	1.18±0.05	7.66±0.30	0.155±0.008
ANT IX/2	PS 1954	64° 24.4' S	45° 48.2' W	4434	0.5-2	1.49±0.05	3.39±0.13	6.85±0.22	0.76±0.03	0.71±0.03	5.36±0.19	0.142±0.008
	PS 1955	64° 49.2' S	42° 30.2' W	4684	0-0.5	1.70±0.13	3.91±0.17	9.72±0.34	1.28±0.05	1.22±0.05	8.02±0.37	0.160±0.010
	PS 1957	65° 40.3' S	37° 44.6' W	4727	0-0.5	1.27±0.04	3.26±0.13	13.40±0.38	1.76±0.06	1.69±0.06	12.12±0.36	0.145±0.007
	PS 1959	65° 24.7' S	37° 54.8' W	4736	0-0.5	1.33±0.06	3.48±0.12	12.61±0.30	1.67±0.06	1.61±0.06	11.28±0.31	0.148±0.007
	PS 1961	65° 43.2' S	35° 26.9' W	4777	0.5-2	1.33±0.06	3.63±0.19	15.38±0.58	1.91±0.09	1.84±0.09	14.05±0.56	0.136±0.008
	PS 1964	66° 16.6' S	30° 17.8' W	4800	0.5-2	1.54±0.09	3.67±0.22	13.65±0.54	1.74±0.08	1.68±0.08	12.10±0.54	0.144±0.009
	PS 1966	66° 37.6' S	27° 07.5' W	4860	0-0.5	1.28±0.04	3.18±0.15	10.36±0.36	1.58±0.06	1.53±0.06	9.09±0.33	0.174±0.009
	PS 1968	67° 28.7' S	31° 06.6' W	4625	0-0.5	2.12±0.10	3.42±0.13	12.51±0.34	1.67±0.08	1.64±0.08	10.39±0.35	0.161±0.010
	PS 1974	67° 13.3' S	24° 08.8' W	4857	0.5-2	1.23±0.06	3.66±0.18	14.91±0.51	2.21±0.08	2.13±0.08	13.68±0.50	0.162±0.008
	PS 1976	67° 50.5' S	20° 50.7' W	4919	0.5-2	1.50±0.11	3.57±0.18	15.50±0.49	2.57±0.11	2.51±0.11	14.00±0.55	0.184±0.011
	PS 1978	68° 50.4' S	17° 53.6' W	4795	0.5-2	1.18±0.06	2.92±0.11	15.69±0.41	2.34±0.09	2.29±0.09	14.51±0.42	0.161±0.008
	PS 1979	69° 22.0' S	16° 29.8' W	4735	0.5-2	1.20±0.09	2.78±0.16	18.65±0.59	2.54±0.11	2.49±0.11	17.45±0.64	0.146±0.008
	PS 1981	70° 07.9' S	14° 15.2' W	4526	0.5-2	0.80±0.06	3.35±0.18	19.54±0.61	2.68±0.12	2.59±0.12	18.73±0.65	0.143±0.008
ANT IX/3	PS 1991	76° 24.8' S	30° 21.2' W	394	0-5	1.11±0.06	1.18±0.05	1.42±0.06	0.09±0.01	0.06±0.01	1.07±0.09	0.080±0.009
	PS 2011	71° 05.7' S	20° 46.8' W	4428	0-1	1.00±0.08	3.40±0.14	13.43±0.39	2.00±0.08	1.92±0.08	12.43±0.46	0.161±0.009
	PS 2039	69° 01.4' S	06° 13.7' E	2123	0-5	1.15±0.09	3.78±0.13	7.57±0.21	0.97±0.04	0.88±0.04	6.43±0.26	0.151±0.009
	PS 2040	68° 50.5' S	06° 14.1' E	2674	0-1	1.10±0.08	3.44±0.15	9.80±0.32	1.16±0.05	1.09±0.05	8.70±0.36	0.134±0.008
	PS 2049	69° 05.2' S	00° 53.4' E	3320	0-5	0.83±0.04	2.37±0.11	8.30±0.26	0.78±0.03	0.73±0.03	7.47±0.26	0.105±0.006
	PS 2052	66° 48.3' S	06° 15.8' E	4322	0-1	0.99±0.07	4.30±0.17	26.20±0.76	4.48±0.16	4.37±0.16	25.21±0.80	0.178±0.009
	PS 2055	68° 17.4' S	06° 14.9' E	3609	0-1.2	1.06±0.05	3.61±0.13	13.11±0.35	2.05±0.10	1.97±0.10	12.05±0.37	0.170±0.010
	PS 2072	60° 33.9' S	03° 57.6' E	5372	0-1	1.03±0.08	2.68±0.13	32.46±0.91	5.21±0.17	5.16±0.17	31.43±0.98	0.166±0.007
ANT X/5	PS 2254	43° 58.3' S	50° 06.4' W	5341	0-1	1.01±0.04	1.51±0.08	10.74±0.32	0.89±0.03	0.88±0.03	9.73±0.31	0.092±0.005
	PS 2256	44° 31.0' S	44° 27.1' W	5111	0-1	0.98±0.05	1.33±0.08	13.50±0.38	1.06±0.09	1.06±0.09	12.52±0.39	0.085±0.008
	PS 2257	45° 00.7' S	38° 32.5' W	4886	0-1	1.05±0.04	1.49±0.08	14.29±0.41	1.20±0.06	1.19±0.06	13.24±0.40	0.090±0.005
	PS 2262	48° 30.1' S	37° 00.3' W	5396	0-1	0.98±0.06	1.68±0.07	18.80±0.37	1.74±0.11	1.72±0.11	17.82±0.44	0.098±0.007
	PS 2269	50° 22.3' S	33° 14.7' W	4781	0-1	0.99±0.08	0.95±0.05	10.34±0.23	1.13±0.05	1.12±0.05	9.73±0.28	0.116±0.006

Table 3-1: (continued)

expedition	station	latitude	longitude	water depth (m)	depth (cm)	^{234}U	^{232}Th	^{230}Th	^{231}Pa	$_{xs}{}^{231}Pa$	$_{xs}{}^{230}Th$	$_{xs}{}^{231}Pa/_{xs}{}^{230}Th$
Ant X/5	PS 2271	51° 31.9' S	31° 22.3' W	3642	0-1	0.69±0.03	0.67±0.04	8.04±0.18	0.85±0.04	0.85±0.04	7.61 ±0.23	0.112±0.006
	PS 2273	52° 39.4' S	30° 33.1' W	3345	0-1	0.78±0.03	0.71±0.04	6.78±0.19	0.75±0.04	0.75±0.04	6.33±0.24	0.119±0.007
	PS 2276	54° 38.1' S	23° 57.3' W	4381	0-1	0.54±0.03	0.45±0.04	6.60±0.22	0.76±0.03	0.75±0.03	6.31 ±0.27	0.120±0.007
	PS 2280	56° 49.7' S	22° 19.5' W	4747	0-1	0.60±0.03	0.37±0.04	7.43±0.25	0.93±0.03	0.93±0.03	7.20±0.31	0.130±0.007
	PS 2283	59° 44.1' S	23° 16.5' W	4696	0-1	0.49±0.03	0.41±0.02	6.04±0.13	0.86±0.04	0.86±0.04	5.78±0.16	0.149±0.008
	PS 2288	57° 45.4' S	25° 20.2' W	3880	0-1	0.36±0.03	0.32±0.04	3.86±0.15	0.59±0.02	0.59±0.02	3.65±0.19	0.162±0.011
	PS 2299	57° 30.6' S	30° 14.1' W	3503	0-1	1.42±0.04	0.72±0.03	8.00±0.15	1.13±0.05	1.12±0.05	7.54±0.18	0.149±0.008
	PS 2307	59° 03.5' S	35° 34.6' W	2533	0-1	0.87±0.07	1.16±0.07	9.85±0.31	1.32±0.05	1.28±0.05	8.99±0.38	0.142±0.008
	PS 2312	59° 49.6' S	39° 42.3' W	1666	0-1	0.73±0.03	0.60±0.05	4.46±0.16	0.78±0.03	0.77±0.03	4.07 ±0.20	0.188±0.012
	PS 2320	60° 06.0' S	44° 50.8' W	5224	0-1	0.99±0.06	1.40±0.08	7.28±0.22	0.83±0.04	0.79±0.04	6.29±0.28	0.125±0.007
	PS 2331	59° 02.4' S	48° 59.6' W	3938	0-1	0.85±0.05	1.28±0.04	4.06±0.09	0.38±0.02	0.34±0.02	3.22±0.12	0.105±0.008
	PS 2334	57° 55.1' S	52° 00.0' W	4555	0-1	0.99±0.05	1.62±0.09	10.81±0.32	0.93±0.04	0.88±0.04	9.82±0.39	0.090±0.005
	PS 2336	57° 09.1' S	53° 59.3' W	4027	0-1	0.89±0.05	1.68±0.08	15.16±0.38	1.80±0.07	1.76±0.07	14.27±0.45	0.123±0.006
	PS 2339	56° 01.9' S	56° 56.6' W	4539	0-1	0.89±0.04	1.71±0.09	13.20±0.38	1.42±0.06	1.38±0.06	12.31 ±0.45	0.112±0.006
	PS 2342	55° 15.5' S	57° 59.1' W	4372	0-1	0.77±0.04	1.25±0.05	4.79±0.11	0.57±0.03	0.53±0.03	4.02±0.14	0.132±0.009
	PS 2353	53° 36.4' S	58° 58.6' W	1916	0-1	1.24±0.06	1.51±0.04	2.68±0.06	0.21±0.01	0.16±0.01	1.72±0.08	0.094±0.008
ANT X/6	PS 2361	55° 00.1' S	06° 02.8' W	3194	0-5	0.48±0.02	0.16±0.02	5.68±0.17	1.33±0.05	1.32±0.05	5.57±0.21	0.238±0.013
	PS 2362	53° 00.1' S	05° 59.9' W	2688	0-5	0.35±0.04	0.18±0.02	5.05±0.16	0.85±0.04	0.85±0.04	4.93±0.20	0.172±0.010
	PS 2363	48° 00.1' S	06° 00.1' W	4040	0-5	1.36±0.21	0.51±0.02	10.65±0.21	0.73±0.03	0.71±0.03	10.31 ±0.23	0.069±0.003
	PS 2364	56° 04.3' S	06° 50.6' W	4156	0-5	n.d.	0.46±0.03	8.13±0.28	1.03±0.04	1.01±0.04	7.81 ±0.31	0.130±0.008
	PS 2365	55° 00.5' S	06° 00.3' W	3117	0-5	0.51±0.03	0.13±0.02	5.03±0.19	1.27±0.04	1.26±0.04	4.94±0.22	0.256±0.015
	PS 2366	50° 59.9' S	06° 00.0' W	2060	0-5	0.40±0.02	0.39±0.03	3.92±0.14	0.55±0.03	0.54±0.03	3.66±0.17	0.147±0.010
	PS 2367	49° 00.0' S	06° 00.1' W	3715	0-5	0.58±0.03	0.47±0.04	10.32±0.29	0.85±0.03	0.84±0.03	10.00±0.33	0.084±0.004
	PS 2368	46° 52.3' S	05° 43.0' W	3756	0-0.5	0.36±0.02	0.46±0.03	10.41±0.24	0.57±0.03	0.56±0.03	10.05±0.28	0.055±0.003
	PS 2369	55° 51.1' S	05° 59.6' W	4059	0-5	0.43±0.02	0.58±0.03	8.09±0.16	1.24±0.04	1.22±0.04	7.66±0.19	0.159±0.007
	PS 2370	58° 29.2' S	05° 59.9' W	5039	0-5	0.36±0.04	0.69±0.03	11.99±0.25	1.65±0.08	1.63±0.08	11.63±0.28	0.140±0.008
	PS 2371	57° 03.3' S	06° 00.5' W	3660	0-5	0.63±0.03	0.38±0.03	7.87±0.25	1.35±0.05	1.34±0.05	7.61 ±0.29	0.176±0.009
	PS 2372	53° 59.8' S	06° 00.2' W	2341	0-5	0.36±0.03	0.22±0.01	6.15±0.12	0.57±0.03	0.56±0.03	6.00±0.14	0.094±0.005
	PS 2376	48° 30.1' S	06° 00.2' W	4091	0-5	0.59±0.02	0.88±0.05	14.43±0.39	1.20±0.04	1.17±0.04	13.83±0.44	0.085±0.004
ANT XI/4	PS 2562	43° 11.2´ S	31° 35.2´ E	5193	0-5	0.97±0.04	1.76±0.10	37.75±1.13	2.73±0.08	2.68±0.08	36.78±1.22	0.073±0.003
	PS 2575	59° 26.8´ S	03° 12.4´ W	5012	0-0.5	0.83±0.04	2.13±0.15	18.48±0.76	3.20±0.11	3.16±0.11	17.65±0.88	0.179±0.010
	PS 2577	61° 13.2´ S	02° 11.7´ E	5349	0-0.5	0.76±0.05	2.46±0.08	29.35±0.56	2.74±0.08	2.70±0.08	28.59±0.61	0.095±0.004
	PS 2578	62° 07.4´ S	05° 01.8´ E	5322	0-5	1.00±0.05	2.76±0.14	30.55±0.97	3.92±0.12	3.87±0.12	29.55±1.07	0.131±0.006
	PS 2579	62° 57.8´ S	07° 46.4´ E	5324	0-5	n.d.	4.26±0.11	16.61±0.47	2.51±0.10	2.43±0.10	14.90±0.51	0.163±0.009
	PS 2589	66° 00.1´ S	24° 58.6´ E	4641	0-5	n.d.	4.22±0.11	21.76±0.44	3.03±0.09	3.03±0.09	20.07±0.51	0.147±0.006
	PS 2600	63° 11.0´ S	34° 31.6´ E	5056	0-5	0.87±0.05	2.29±0.08	22.71±0.45	3.40±0.11	3.36±0.11	21.84±0.51	0.154±0.006
	PS 2602	60° 22.5´ S	36° 34.9´ E	5289	0-5	0.66±0.04	0.80±0.04	17.53±0.41	2.66±0.09	2.65±0.09	17.21 ±0.46	0.154±0.007
	PS 2604	57° 35.9´ S	38° 35.4´ E	5083	0-5	0.61±0.05	0.43±0.05	11.82±0.34	1.88±0.08	1.88±0.08	11.65±0.43	0.161±0.009
	PS 2611	49° 30.3´ S	38° 49.6´ E	4261	0-5	0.57±0.04	0.48±0.03	15.78±0.32	1.73±0.06	1.72±0.06	15.59±0.36	0.110±0.005

Table 3-2: Activities (dpm/m^3) of dissolved and particulate ^{230}Th and ^{231}Pa, dissolved and particulate ^{231}Pa/^{230}Th, and (^{230}Th/^{231}Pa)-fractionation factor (F) for the water column samples (errors are given as 1σ of propagated uncertainty of counting statistics and blank).

exped.	station	latitude	longitude	water depth (m)	depth (m)	^{230}Th$_{diss.}$	^{230}Th$_{part.}$	^{231}Pa$_{diss.}$	^{231}Pa$_{part.}$	^{231}Pa/^{230}Th dissolved	^{231}Pa/^{230}Th particulate	F-factor
ANT IX/3	PS 1999	73° 37.3' S	26° 07.0' W	3360	2100	1.237 ± 0.035	0.071 ± 0.006	0.386 ± 0.048	0.023 ± 0.006	0.313 ± 0.040	0.331 ± 0.082	0.94 ± 0.26
	PS 2049	69° 05.2' S	00° 53.4' E	3264	85	0.516 ± 0.0492	—	0.154 ± 0.034	—	0.298 ± 0.072		
					275	0.935 ± 0.052	—	0.228 ± 0.034	—	0.243 ± 0.038		
	PS 2054	67° 58.1' S	06° 15.0' E	3900	295	0.895 ± 0.027	—	0.242 ± 0.046	—	0.297 ± 0.058		
					2335	1.443 ± 0.025	0.062 ± 0.005	0.461 ± 0.076	0.021 ± 0.006	0.320 ± 0.053	0.339 ± 0.095	0.94 ± 0.31
	PS 2072	60° 33.9' S	03° 57.6' E	5370	160	0.821 ± 0.035	—	0.231 ± 0.041	—	0.281 ± 0.051		
					3900	1.771 ± 0.035	0.072 ± 0.005	0.421 ± 0.043	0.014 ± 0.003	0.238 ± 0.025	0.187 ± 0.043	1.27 ± 0.32
ANT X/5	PS 2262	48° 30.1' S	37° 00.3' W	5396	2500	0.660 ± 0.035	0.078 ± 0.012	0.299 ± 0.020	0.005 ± 0.002	0.461 ± 0.039	0.070 ± 0.029	6.62 ± 2.77
					4500	1.035 ± 0.044	0.233 ± 0.021	0.318 ± 0.018	0.008 ± 0.002	0.312 ± 0.022	0.032 ± 0.011	9.73 ± 3,40
	PS 2269	50° 24.0' S	33° 08.1' W	4744	500	0.365 ± 0.024	—	0.219 ± 0.018	—	0.599 ± 0.064		
	PS 2276	54° 38.1' S	23° 57.3' W	4450	500	0.483 ± 0.022	—	0.227 ± 0.014	—	0.465 ± 0.036		
					2000	1.013 ± 0.034	0.051 ± 0.009	0.276 ± 0.015	0.008 ± 0.002	0.272 ± 0.017	0.147 ± 0.042	1.85 ± 0.54
					3000	1.032 ± 0.033	0.136 ± 0.015	0.353 ± 0.035	0.019 ± 0.004	0.344 ± 0.031	0.139 ± 0.026	2.48 ± 0.52
					4000	0.940 ± 0.024	0.386 ± 0.020	0.327 ± 0.020	0.023 ± 0.005	0.348 ± 0.023	0.061 ± 0.011	5.75 ± 1.11
	PS 2283	59° 44.1' S	23° 16.5' W	4766	500	0.730 ± 0.030	—	0.272 ± 0.022	—	0.364 ± 0.033		
					2000	1.265 ± 0.046	0.109 ± 0.010	0.335 ± 0.017	0.017 ± 0.004	0.261 ± 0.016	0.152 ± 0.029	1.71 ± 0.34
					3000	1.132 ± 0.039	0.218 ± 0.021	0.310 ± 0.014	0.017 ± 0.004	0.272 ± 0.015	0.076 ± 0.014	3.60 ± 0.70
					4000	1.351 ± 0.043	0.195 ± 0.020	0.312 ± 0.024	0.025 ± 0.003	0.226 ± 0.019	0.130 ± 0.019	1.74 ± 0.29
	PS 2323	60° 13.4' S	44° 52.7' W	4598	500	0.999 ± 0.041	—	0.306 ± 0.022	—	0.276 ± 0.023		
					1500	1.3786 ± 0.068	0.140 ± 0.025	0.383 ± 0.022	0.017 ± 0.003	0.289 ± 0.023	0.119 ± 0.030	2.42 ± 0.55
					2500	1.154 ± 0.043	0.076 ± 0.019	0.349 ± 0.017	0.009 ± 0.002	0.301 ± 0.018	0.121 ± 0.039	2.48 ± 0.82
					3500	1.298 ± 0.043	0.152 ± 0.012	0.295 ± 0.015	0.014 ± 0.003	0.226 ± 0.013	0.090 ± 0.018	2.51 ± 0.53
	PS 2337	56° 38.0' S	54° 55.1' W	5106	3500	0.951 ± 0.030	0.197 ± 0.022	0.309 ± 0.020	0.014 ± 0.002	0.325 ± 0.023	0.070 ± 0.014	4.65 ± 0.99
ANT X/6	PS 2358	56° 59.6' S	23° 18.5' W	4910	3000	0.732 ± 0.019	0.132 ± 0.006	0.310 ± 0.016	0.011 ± 0.001	0.424 ± 0.023	0.086 ± 0.012	4.93 ± 0.73
					4000	1.125 ± 0.027	0.393 ± 0.028	0.335 ± 0.020	0.038 ± 0.003	0.298 ± 0.017	0.098 ± 0.009	3.04 ± 0.34
	PS 2359	56° 09.1' S	15° 25.5' W	4887	3000	1.002 ± 0.023	0.079 ± 0.006	0.350 ± 0.019	0.009 ± 0.001	0.350 ± 0.021	0.108 ± 0.019	3.24 ± 0.59
					4000	0.881 ± 0.032	0.148 ± 0.009	0.337 ± 0.015	0.016 ± 0.002	0.383 ± 0.022	0.110 ± 0.012	3.49 ± 0.43
	PS 2360	57° 44.7' S	06° 28.6' W	3480	2000	0.981 ± 0.033	0.049 ± 0.004	0.288 ± 0.022	0.007 ± 0.001	0.293 ± 0.024	0.146 ± 0.022	2.02 ± 0.35
					3000	1.074 ± 0.038	0.099 ± 0.007	0.361 ± 0.017	0.012 ± 0.002	0.336 ± 0.019	0.116 ± 0.018	2.88 ± 0.49
	PS 2369	55° 51.1' S	05° 59.6' W	3980	2500	0.923 ± 0.026	0.062 ± 0.006	0.291 ± 0.017	0.005 ± 0.001	0.315 ± 0.020	0.080 ± 0.023	3.93 ± 1.14
	PS 2370	58° 29.2' S	05° 59.9' W	4980	2500	1.259 ± 0.050	0.119 ± 0.014	0.394 ± 0.021	0.016 ± 0.003	0.313 ± 0.021	0.132 ± 0.027	2.38 ± 0.51
					4000	1.433 ± 0.055	0.286 ± 0.020	0.447 ± 0.019	0.036 ± 0.004	0.312 ± 0.017	0.126 ± 0.016	2.47 ± 0.34
ANT XI/4	PS 2562	43° 11.2´ S	31° 35.2´ E	5220	2700	0.593 ± 0.024	0.134 ± 0.005	0.311 ± 0.043	0.005 ± 0.002	0.524 ± 0.075	0.038 ± 0.017	13.75 ± 2.06
					4220	0.841 ± 0.034	0.193 ± 0.007	0.369 ± 0.022	0.008 ± 0.003	0.439 ± 0.031	0.044 ± 0.014	10.02 ± 3.20
	PS 2579	62° 57.8´ S	07° 46.4´ E	5324	1900	1.473 ± 0.099	0.049 ± 0.005	0.431 ± 0.022	0.011 ± 0.002	0.293 ± 0.025	0.225 ± 0.043	1.30 ± 0.27
					3500	1.737 ± 0.092	0.079 ± 0.006	0.510 ± 0.024	0.015 ± 0.002	0.293 ± 0.021	0.193 ± 0.033	1.52 ± 0.28
	PS 2600	63° 11.0´ S	34° 31.6´ E	5084	2000	1.245 ± 0.052	0.054 ± 0.005	0.385 ± 0.022	0.013 ± 0.002	0.309 ± 0.022	0.243 ± 0.039	1.27 ± 0.23
					3500	1.613 ± 0.064	0.101 ± 0.007	0.418 ± 0.020	0.021 ± 0.002	0.259 ± 0.016	0.202 ± 0.027	1.28 ± 0.19
	PS 2604	57° 35.9´ S	38° 35.4´ E	5120	300	0.491 ± 0.026	—	0.164 ± 0.015	—	0.346 ± 0.036		
					3500	1.073 ± 0.043	0.090 ± 0.009	0.366 ± 0.022	0.022 ± 0.003	0.341 ± 0.025	0.243 ± 0.040	1.40 ± 0.25
					4620	1.374 ± 0.067	0.204 ± 0.014	0.419 ± 0.021	0.029 ± 0.004	0.305 ± 0.022	0.144 ± 0.021	2.12 ± 0.15
	PS 2611	49° 30.3´ S	38° 49.6´ E	4290	2820	0.754 ± 0.031	0.101 ± 0.008	0.373 ± 0.029	0.004 ± 0.002	0.495 ± 0.044	0.075 ± 0.017	6.62 ± 1.58
					3790	0.993 ± 0.043	0.193 ± 0.017	0.437 ± 0.034	0.017 ± 0.002	0.441 ± 0.039	0.090 ± 0.014	4.88 ± 0.87

(—) count rate not sufficiently above background

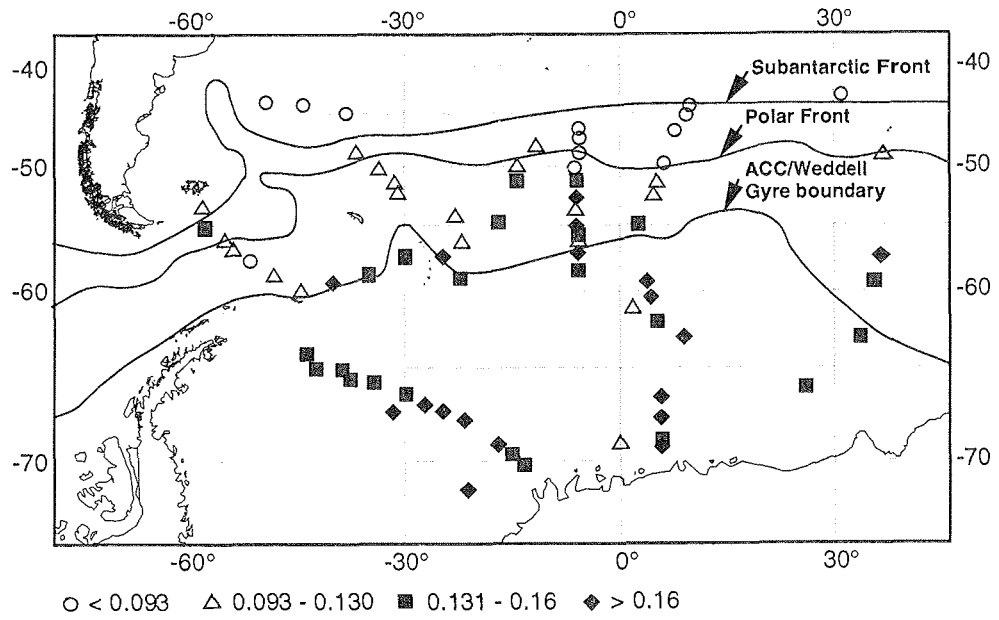

Fig.3-2: Overview of excess $^{231}Pa/^{230}Th$ ratios in surface sediments of the Atlantic sector of the Southern Ocean. The positions of the Subantarctic Front (SAF), the Polar Front (PF) and the ACC-Weddell Gyre boundary (AWB) according to Orsi et al. (1995) are also shown.

3.5 Discussion

3.5.1 Fractionation of ^{231}Pa and ^{230}Th in the Southern Ocean

As we have shown above, $_{xs}^{231}Pa/_{xs}^{230}Th$ ratios in surface sediments of the South Atlantic are characterized by a strong latitudinal gradient with high $_{xs}^{231}Pa/_{xs}^{230}Th$ ratios far above the production ratio south of the Polar Front, extending to the Antarctic continent. According to usual scavenging theory, throughout the oceans the depositional flux of ^{230}Th is assumed to almost equal its local rate of production in the water column with little net lateral advection (Anderson et al., 1983a; 1983b; Yu et al., 1996; Bacon et al., 1985; Francois et al., 1990). If this assumption also holds for the Southern Ocean, the high $_{xs}^{231}Pa/_{xs}^{230}Th$ ratios south of the Polar Front suggest that in addition to the local production, a considerable portion of the ^{231}Pa deposited in sediments south of Polar Front must have been supplied by lateral transport. The average $_{xs}^{231}Pa/_{xs}^{230}Th$ ratio of about 0.15 in surface sediments south of Polar Front would suggest a lateral contribution of ^{231}Pa to the sediment inventory of almost 40%. This model was applied to calculate the ^{231}Pa mass balance for the Southern Ocean (Yu et al., 1996). Assuming a mean $_{xs}^{231}Pa/_{xs}^{230}Th$ rain ratio of 0.17 they estimated that the depositional flux of ^{231}Pa throughout the entire Southern Ocean balances in situ production plus ^{231}Pa import from the Atlantic Ocean, suggesting this region to be an important sink for ^{231}Pa.

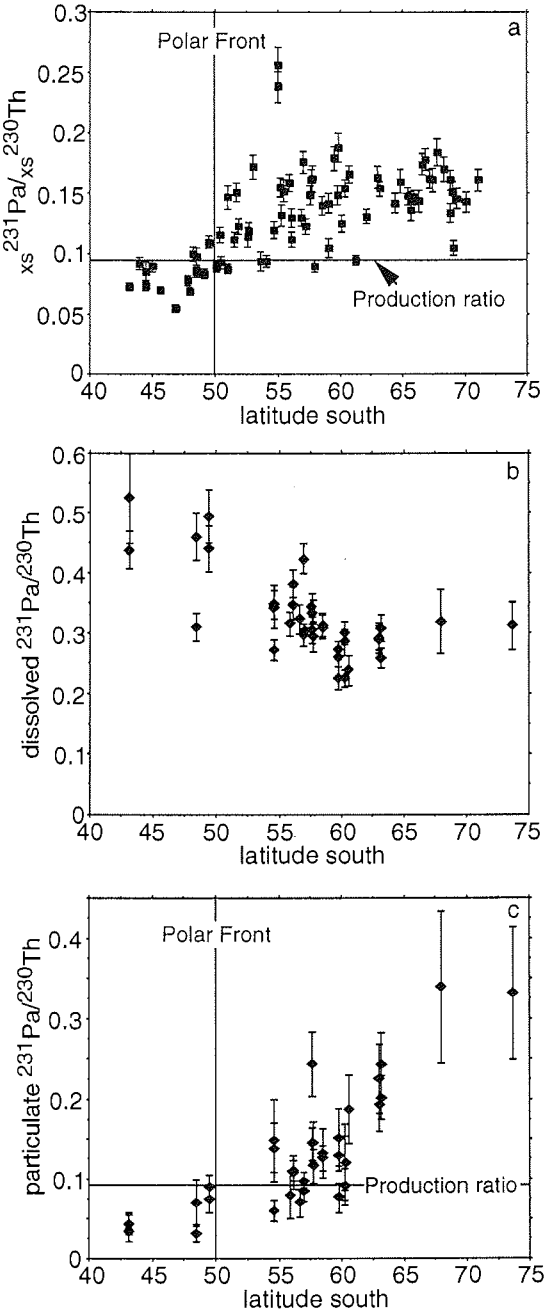

Fig.3-3 (a): Plot of excess $^{231}Pa/^{230}Th$ ratios in surface sediments of the South Atlantic versus latitude. (b): Dissolved (<1μm) and (c): particulate $^{231}Pa/^{230}Th$ ratios throughout the Atlantic sector of the Southern Ocean. Only samples in the depth interval from 1500m below the surface and 500m above the sea floor are shown. Error bars represent 1σ uncertainty propagated from counting statistics and blank.

Based on the fact that scavenging of ^{231}Pa in excess of its production in the water column is well known from high productivity regions at ocean margins (boundary scavenging), previous authors have hypothesized that this process might also occur in the Southern Ocean (Yu et al., 1996; DeMaster, 1979). They suggested that the enhanced scavenging of ^{231}Pa in the Southern Ocean south of the Polar Front primarily results from the high particle flux within the Antarctic Circumpolar Current (ACC). If this assumption holds, then we should expect a corresponding decrease of the $_{xs}^{231}Pa/_{xs}^{230}Th$ ratio in surface sediments south of the ACC (e.g. in the Weddell Sea), where particle fluxes are thought to be much lower than further north (Fischer et al., 1988; Wefer and Fischer, 1991). However, indistinguishable $_{xs}^{231}Pa/_{xs}^{230}Th$ ratios in surface sediments south of the ACC from those underlying the ACC are in conflict with this model.

The same conclusion can be drawn from the water column distributions of ^{231}Pa and ^{230}Th. While in an earlier study (DeMaster, 1981) the high $_{xs}^{231}Pa/_{xs}^{230}Th$ ratios in rapidly accumulating sediments underlying the ACC were hypothesized to result from quantitative stripping of the dissolved concentrations of ^{231}Pa and ^{230}Th from the water column because of the high particle flux, our data confirm recent results (Rutgers van der Loeff and Berger, 1993) and clearly indicate, that there is no significant depletion of either radionuclide in the water column within the ACC relative to the less productive regions to the north and south. Furthermore, the observed N-S decrease of dissolved $^{231}Pa/^{230}Th$ ratios across the ACC is in conflict to what should be expected from published scavenging models (Anderson et al., 1983a; 1983b; Bacon and Anderson, 1982). In the scenario described in Yu et al. (1996), namely the southward flow of NADW into the ACC, the dissolved $^{231}Pa/^{230}Th$ ratio of this water mass should increase as it enters the area of enhanced particle flux because of the preferential removal of ^{230}Th over ^{231}Pa.

Although total mass fluxes measured in sediment traps within the ACC, located at 50°S (PF-1) and 55°S (BO 1+2) with $38.3 g \cdot m^{-2} \cdot y^{-1}$ (Wefer and Fischer, 1991) and $53.1 g \cdot m^{-2} \cdot y^{-1}$ (Fischer and Wefer, unpublished), respectively (Table 3-3) exceed most values observed for the typical open ocean ($7\text{-}45 g \cdot m^{-2} \cdot y^{-1}$; Wefer, 1989), they are much lower than values occurring in upwelling regions at ocean margins (often$>100 g \cdot m^{-2} \cdot y^{-1}$; Yu, 1994; Wefer, 1991). At this mass flux in the ACC, it is not likely that ^{231}Pa is scavenged significantly above its rate of production in the water column (Yu, 1994). Consequently, the enhanced scavenging of ^{231}Pa within the ACC does not seem to result from an enhanced mass flux of particles, as postulated previously (Kumar et al., 1993; 1994; 1995; Lao et al., 1992a; 1992b; Francois et al., 1993; Yu, 1994), but is more likely explained by a N-S change in the Th/Pa fractionation factor (F). This is clearly illustrated in Fig.3-4, where F is plotted against latitude. North of 48°S high values of F around 10, typical for the open ocean (Anderson et al., 1983a; 1983b; Nozaki and Nakanishi, 1985), indicate a strong preference for the adsorption of Th on particles, while to the south F decreases gradually to relatively constant values between 1 and 2 south of 60°S. In theory, the strong N-S decrease of F may result either from a southward decrease in the scavenging efficiency of ^{230}Th, or from a respective increase in the scavenging efficiency of ^{231}Pa. However, as long as we do not have data on the activities of both radionuclides on a weight mass basis, and consequently on their distribution coefficients, or on their inventories in the sediment this question can not be answered. In line with general scavenging theory (Anderson et al., 1983a; 1983b;

Bacon et al., 1985; Bacon and Anderson, 1982) in the following we will therefore assume that the scavenging efficiency of ^{230}Th does not change with latitude.

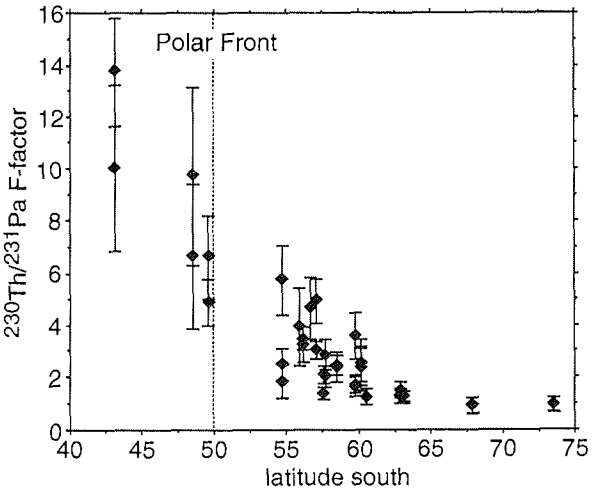

Fig.3-4: Latitudinal gradient of the Th/Pa-fractionation factor (F) in the South Atlantic. Errors as in Fig.3-3.

3.5.2 Effect of the composition of particles on F

The strong latitudinal gradient of F in the South Atlantic south of Polar Front can only be explained by a N-S change in the chemical composition of particulate matter, thus confirming recent speculations (Rutgers van der Loeff and Berger, 1993). Particles with a clear preference for the adsorption of ^{230}Th relative to ^{231}Pa are only observed north of 48°S, while to the south the abundance of a particulate phase with a high scavenging efficiency for ^{231}Pa increases, which dominates scavenging south of 60°S. Values of F close to 1 show that this particulate phase does not substantially fractionate ^{230}Th and ^{231}Pa. MnO_2 is thought not to fractionate ^{230}Th and ^{231}Pa (eg. Anderson et al., 1992), and scavenging by MnO_2 coated particles has been suggested to explain values of F around 1, found at ocean margins (e.g. in the Panama and Guatemala basins; Anderson et al., 1983b). Further evidence for unpreferential scavenging of ^{231}Pa and ^{230}Th comes from hydrothermal plumes, rich in Fe and Mn, emanating near mid ocean ridges (Shimmield and Price, 1988). Although MnO_2 coated cartridges do fractionate ^{230}Th and ^{231}Pa (based on the slightly higher collection efficiencies for ^{230}Th than for ^{231}Pa), this effect seems to be small and a N-S increase in the availability of MnO_2-coated particles in the water column could explain the N-S trend of F. Since we have no data on the Mn and Fe contents of suspended matter south of the Polar Front these possibilities cannot be further assessed. However, we are not aware of sources like hydrothermal activity that would cause a N-S increase in suspended Mn and Fe-oxyhydroxides.

Biogenic opal is also suggested to have a high affinity for the adsorption of ^{231}Pa, which is hypothesized on the basis of field observations (Kumar et al., 1995; Lao et al., 1992b; Rutgers van der Loeff and Berger, 1993; Yu et al., 1996; Taguchi et al., 1989; DeMaster, 1979) and laboratory experiments carried out by Anderson et al. (1992) who determined a F factor of 1.1, indicating that opal does not significantly fractionate ^{230}Th and ^{231}Pa. Available data on the composition of settling particles in the South Atlantic, based on sediment trap studies (Fischer et al., 1988; Wefer and Fischer, 1991) show a strong N-S increase in the content of biogenic opal contributing up to 70% of the total annual flux (Table 3-3). This N-S increase in the content of biogenic opal on sedimenting particles agrees well with the N-S breakdown of F, suggesting this phase to be a possible carrier for ^{231}Pa to the sediment, although data on the opal contents of suspended particulate are not available.

Consequently, to further investigate this question we have determined $^{231}Pa/^{230}Th$ ratios in sinking particles with high contents of biogenic opal (Tab.3-3). In Fig.3-5 these data (which will be discussed in more detail in chapter 4) are shown together with the dissolved $^{231}Pa/^{230}Th$ ratios measured at similar water depths (85-500m, Tab.3-2). Assuming that the sinking particles are representative for the suspended particles, and that they are in equilibrium with respect to exchange of dissolved ^{231}Pa and ^{230}Th, an estimation of F can be made. Although at the trap sites the dissolved concentrations of ^{231}Pa and ^{230}Th were not measured, it is obvious from Fig.3-5 that the dissolved $^{231}Pa/^{230}Th$ ratios are primarily determined by the geographic latitude, with high values of 0.6 at 50°S decreasing to relatively constant values of 0.25-0.30 south of 60°S. This well-established relationship can be used to assess the dissolved $^{231}Pa/^{230}Th$ ratios at the respective trap sites. Thus, at PF 1-4 and BO 1+2, F values were calculated based on the dissolved $^{231}Pa/^{230}Th$ ratios available at the same latitude, whereas for WS-3 an average value of 0.28±0.056 for the region south of 60°S was taken. F values show a slight N-S decrease from 1.86±0.43 at PF-1/4, over 1.35±0.17 at BO-1/2, to 1.01±0.23 at WS-3, coinciding with a respective increase in the content of biogenic opal of sinking particles from 40 to 70% (Tab.3-3), thus strongly supporting the hypothesis of unpreferential scavenging of ^{231}Pa and ^{230}Th by biogenic opal in the surface ocean. Based on these lines of evidence we suggest the high $^{231}Pa/^{230}Th$ ratios in surface sediments south of the Polar Front throughout the South Atlantic to result from enhanced scavenging of ^{231}Pa by biogenic opal, rather than from a high mass flux of particles.

Note that there is a general ocean-wide trend that the relative abundance of diatoms in the phytoplankton increases as primary productivity increases (Dymond and Lyle, 1985; Nelson et al., 1995), implying that high opal contents of particulate matter could be interpreted as a signal of high productivity. If so, in the Southern Ocean the $^{231}Pa/^{230}Th$ record of the surface sediments could still be a reliable tracer for export production. However, as can be seen from sediment trap data (Wefer and Fischer, 1991) in this region there is not such a relationship. At Maud Rise (WS-3 and WS-4) where annual mass fluxes vary by a factor of 14, opal contents of particles are indistinguishable (Wefer and Fischer, 1991). Furthermore, in the Western Weddell Sea (WS-1) where the mass flux has been shown to be extremely low (Fischer et al., 1988), opal contents of particles are highest reaching almost 80%.

Table 3-3: Opal contents and $_{xs}^{231}Pa/_{xs}^{230}Th$ ratios of sinking particles, and estimated F-factors.

trap	latitude	longitude	depth (m)	mass flux $g \cdot m^{-2} \cdot a^{-1}$	opal (%)	$_{xs}^{231}Pa/_{xs}^{230}Th$	$^{*}(^{231}Pa/^{230}Th)$ dissolved	F-factor
PF 1-4	50° 09.0' S	05° 46.4' E	700	38.3	40	0.322 ± 0.066	0.599 ± 0.064	1.86 ± 0.43
BO 1+2	54° 20.2' S	03° 20.2' W	450	53.1	62	0.344 ± 0.034	0.465 ± 0.036	1.35 ± 0.17
WS 3	64° 54.1' S	02° 33.8' W	360	33.7	70	0.278 ± 0.016	0.280 ± 0.058	1.01 ± 0.23

Data on mass flux and opal content of PF 1-4 and WS-3 are from Wefer and Fischer (1991), and of BO 1+2 from Wefer and Fischer (unpublished).

*interpolated from latitudinal gradient of dissolved $^{231}Pa/^{230}Th$ ratios
errors are 1σ propagated from counting statistics and blank.

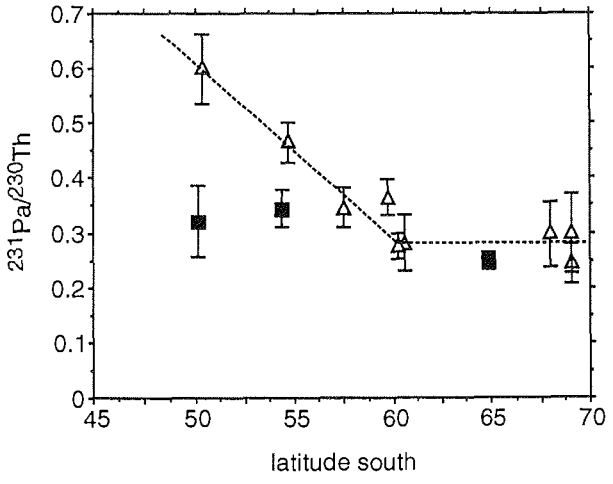

Fig.3-5: Plot of excess $^{231}Pa/^{230}Th$ ratios of sediment traps (filled squares) and dissolved (<1μm) $^{231}Pa/^{230}Th$ ratios (open triangles) measured in the depth interval between 85 and 500m, versus latitude. The stippled line indicates the N-S trend of dissolved $^{231}Pa/^{230}Th$ ratios. Errors as in Fig.3-3.

3.5.3 The $^{231}Pa/^{230}Th$ ratio as a paleoproductivity proxy

Our study in the South Atlantic has unequivocally revealed that south of the Polar Front the simple relationship between $^{231}Pa/^{230}Th$ ratio and particle flux is no more valid. In particular, the high $^{231}Pa/^{230}Th$ ratios measured in surface sediments throughout the Weddell Sea cannot be interpreted as a signal of high particle flux, because of the low particle flux of this region relative to the ACC, based on sediment trap data (Fischer et al., 1988; Wefer and Fischer, 1991). Although in the Western Weddell Sea, minimum particle fluxes of $8 g \cdot m^{-2} a^{-1}$, estimated from the flux of opal out of the sediment of $100 mmol \cdot m^{-2} a^{-1}$ (Schlüter et al., submitted), and the average opal content of sinking particles of 70-80% (Fischer et al., 1988; Wefer and Fischer, 1991), are much higher than the sediment trap results ($0.37 g \cdot m^{-2} a^{-1}$), values are still much lower than in the ACC (Schlüter et al., submitted). Thus, the

high $^{231}Pa/^{230}Th$ ratios observed are more likely explained by an increased adsorption of ^{231}Pa to biogenic opal, which contributes up to 80% of the total annual flux (Fischer et al., 1988). Consequently, in regions where the sedimenting flux is dominated by biogenic opal, the $^{231}Pa/^{230}Th$ ratio does not seem to be a reliable indicator for the mass flux of particles, although a definite conclusion in terms of a relationship between opal content and fractionation factor cannot yet be given.

The strong affinity of ^{231}Pa to opal has important implications for the use of the $^{231}Pa/^{230}Th$ ratio as a paleoproductivity-proxy in dated sediment cores, as changes with time in opal content of the sedimenting flux could have influenced the scavenging efficiency of ^{231}Pa (Kumar et al., 1995; Lao et al., 1992b). We suggest that predictions about particle fluxes from the $^{231}Pa/^{230}Th$ ratio can only be inferred, if high fluxes of biogenic opal to the sediment can be excluded. However, reliable data about the opal content of sedimenting particles can only be expected in regions of high bulk accumulation rates, where the preservation efficiency of opal is high. In contrast, in regions of very low bulk accumulation rates, biogenic opal can dissolve almost quantitatively at the sediment surface. This effect is well known throughout the Weddell Sea, where sinking particles are primarily composed of biogenic opal with up to 80% of the total flux (Fischer et al., 1988), while contents of opal in surface sediments are extremely low (<1% Schlüter, 1990). Although in this region most of the biogenic opal production is already recycled in the water column (Leynaert et al., 1993), the flux of dissolved silica out of the sediments ($100 mmol \cdot m^{-2} \cdot a^{-1}$ in the Central Weddell Sea, Schlüter, submitted) which can be regarded as a minimum estimate of the Si-flux to the seafloor, is still 12% of the production rate of biogenic opal in the surface water ($800 mmol \cdot m^{-2} \cdot a^{-1}$, Leynaert et al., 1993). With a bulk accumulation rate of $1 g \cdot cm^{-2} \cdot ka^{-1}$ and an opal content of less than 1% of the sediments, the burial rate of biogenic opal is estimated to be in the order of $1 mmol \cdot m^{-2} \cdot a^{-1}$, which illustrates that only 1% of the biogenic opal reaching the sea floor is buried. In contrast to the Weddell Sea, the flux and preservation of biogenic opal are much higher within the opal belt underlying the ACC, with burial rates of more than 60% of the primary production (Schlüter et al., submitted). Based on the constant $^{231}Pa/^{230}Th$ ratios in surface sediments throughout the South Atlantic south of the Polar Front, with opal contents varying from less than 1 to almost 80%, we suggest the primary opal-influenced $^{231}Pa/^{230}Th$ signal to be preserved in the sediment, even if recycling of opal in the surface sediment is almost quantitative.

Consequently, we suggest that the $^{231}Pa/^{230}Th$ ratio can not be applied as a reliable paleoproductivity-proxy in regions where the flux to the sediment has been dominated by opal. Variations of the $^{231}Pa/^{230}Th$ ratios through time normally interpreted in terms of changes in particle flux could solely result from changes in the content of biogenic opal on sinking particles. As every other proxy, the $^{231}Pa/^{230}Th$ ratio is affected by secondary factors, our results from the South Atlantic show again that reliable reconstructions of paleoproductivity can only be made if several independent proxies are used together.

4 Surface vs. deep-water scavenging of ^{231}Pa and ^{230}Th under high seasonality in mass flux: Implications for lateral distribution in the Atlantic Sector of the Southern Ocean

H.J. Walter*#, M.M. Rutgers van der Loeff*, H. Höltzen*, U.V. Bathmann* and G. Fischer&

*Alfred Wegener Institute for Polar and Marine Research, Bremerhaven, Germany
&Fachbereich Geowissenschaften, University of Bremen, Germany

4.1 Abstract

The scavenging of ^{231}Pa and ^{230}Th was investigated in the Atlantic Sector of the Southern Ocean by combining results from sediment trap and in-situ filtration studies. Even under extreme variations in particle flux, scavenging of ^{231}Pa and ^{230}Th is closely coupled with the annual cycle of particle fluxes. Extremely high particulate $_{xs}^{231}Pa/_{xs}^{230}Th$ ratios (>0.3), far above the production ratio of both radionuclides in the water column (0.093), are generated in the upper water column during short-time high-productivity events (plankton blooms) in austral summer. The high $_{xs}^{231}Pa/_{xs}^{230}Th$ signal is weakened during downward transport of the bloom particles in the water column by continuous exchange with suspended particles, which have a lower $_{xs}^{231}Pa/_{xs}^{230}Th$ ratio due to alteration and reequilibration with the dissolved phase. As upwelling causes a strong N-S increase of ^{230}Th and ^{231}Pa in surface waters, we have investigated whether a southward increase of scavenging from the upper ocean could possibly explain the N-S increase in the $_{xs}^{231}Pa/_{xs}^{230}Th$ ratios observed in Southern Ocean's surface sediments. Estimated contributions of ^{230}Th and ^{231}Pa from the upper ocean <700m to the buried flux in the sediment are relatively uniform with latitude, with values of <17% and <35%, respectively. This makes the upper water column unlikely as a source to explain the high $_{xs}^{231}Pa/_{xs}^{230}Th$ ratios in sediments south of the Polar Front. Rather, the latitudinal gradient of the sediments is a reflexion of the southward increase in the $_{xs}^{231}Pa/_{xs}^{230}Th$ ratio of suspended particles in the deep ocean which is still found to be the major source of ^{231}Pa and ^{230}Th to the sediment. Radionuclide fluxes are highly variable in the Southern Ocean with highest values far above the production rates of ^{230}Th and ^{231}Pa in the Bransfield Strait near King George, whereas within the Antarctic Circumpolar Current evidence for enhanced scavenging was only found for ^{231}Pa. In contrast, in the Weddell Sea fluxes for both radionuclides are strongly reduced. Long-term fluxes measured in sediment cores taken from the Central Weddell Gyre agree well with the sediment trap results, and suggest that the Weddell Sea is a source for both ^{230}Th and ^{231}Pa to surrounding oceans. The estimated export of ^{230}Th from the Weddell Sea of >50% of its production over the last 180ka has to be taken into account when applying ^{230}Th for paleoceanographic studies.

4.2 INTRODUCTION

In the last decade the natural radionuclides ^{230}Th and ^{231}Pa have become of increasing interest as proxies in the study of paleoceanographic processes. The $^{231}Pa/^{230}Th$ record of dated sediment cores can be used under certain circumstances (for a recent review see Walter et al., in press) to assess relative changes in bioproductivity of the ocean (Lao et al., 1992a; 1992b; Kumar et al., 1993; Francois et al., 1993; Yu, 1994; Kumar et al., 1995), and of water mass circulation (Yu et al., 1996; Moran et al., 1997). Both radionuclides are continuously produced in the water column by decay of their soluble U parents at an initial activity ratio of 0.093. After production they rapidly adsorb onto particle surfaces, and are removed from the water column on timescales of 5-40 years (^{230}Th) and 50-200 years (^{231}Pa) (Nozaki et al., 1981; Anderson et al., 1983a; 1983b; Nozaki and Nakanishi, 1985; Nozaki and Yamada, 1987; Huh and Beasley, 1987; Guo et al., 1995). Due to its short residence time, the flux to the seafloor of $_{xs}^{230}Th$ throughout the oceans almost equals its local rate of production in the water column (Anderson et al., 1983a; 1983b; Francois et al., 1990). In contrast, the longer oceanic residence time for ^{231}Pa allows this nuclide to be transported laterally over thousands of kilometres prior to scavenging, resulting in its preferential removal in regions of high particle flux. The different pathways of removal from the water column are reflected by high $^{231}Pa/^{230}Th$ ratios in oceanic surface sediments underlying high particle flux regions (e.g. equatorial Pacific, ocean margins), compared to low particle flux regions (e.g. the central gyres), where ratios are much lower (Yang et al., 1986; Walter et al., in press). This relationship between $^{231}Pa/^{230}Th$ ratio and mass flux forms the basis for its use as a paleoproductivity proxy. However, due to a N-S increase in the scavenging efficiency of ^{231}Pa relative to ^{230}Th in the Southern Ocean south of the Polar Front, the $^{231}Pa/^{230}Th$ record of surface sediments there does no more reflect total mass flux (Walter et al., 1997). In this previous paper we have explained the high $^{231}Pa/^{230}Th$ ratios found e.g. throughout the Weddell Sea, a region of very low particle fluxes (Fischer et al., 1988; Wefer and Fischer, 1991), by the high content of biogenic opal on sedimenting particles (>50%), for which a high affinity for ^{231}Pa is suggested (Taguchi et al., 1989; Anderson et al., 1992; Lao et al., 1992a; 1992b).

In this study an alternative scenario is discussed to explain the unusually high $^{231}Pa/^{230}Th$ ratios found in the Southern Ocean sediments, which, in addition to the high opal content of sinking particles, takes into account two aspects that make this region so different from other oceans: the high seasonality in primary production (El-Sayed and Taguchi, 1981; Smith and Nelson, 1986; Jacques, 1989; Leynaert et al., 1993), and the high radionuclide concentrations in the surface waters (Rutgers van der Loeff and Berger, 1993).

Time-series sediment trap deployments in the Southern Ocean have revealed extreme regional and temporal variations in sedimenting flux up to a factor 1000, in phase with the annual cycle of primary production in the euphotic zone (Wefer et al., 1988; Fischer et al., 1988; Wefer and Fischer, 1991). During open-water conditions in austral summer, short-term high flux pulses (opal content >50%) account for up to 95% of the total annual flux, whereas fluxes are negligible during sea ice coverage (Wefer et al., 1988; Wefer and Fischer, 1991). First results from a sediment trap deployed in the Bransfield Strait (Rutgers van der Loeff and Berger, 1991) have

shown, that the scavenging of ^{210}Pb and ^{230}Th is closely coupled to the particle flux, in line with observations at lower latitudes with less extreme seasonality (Bacon et al., 1985; Fisher et al., 1988; Colley et al., 1995). During such short events of high diatom productivity, both the mass flux and the high opal content of particles would favor enhanced scavenging rates of ^{231}Pa relative to ^{230}Th in the euphotic zone. The high initial $^{231}Pa/^{230}Th$ signal from the surface ocean would then be transported rapidly through the water column by fast sinking particles and be superimposed on the scavenging in deep waters.

Over most of the oceans, activities of ^{231}Pa and ^{230}Th in the surface waters (upper few hundred meters) are very low (eg. Anderson et al., 1983a; 1983b). Even quantitative stripping from this layer during a bloom period could not significantly contribute to their inventories in the sediment. This does not hold for the Southern Ocean, where concentrations of ^{230}Th and ^{231}Pa in surface waters show a strong N-S increase with latitude (Rutgers van der Loeff and Berger, 1993), as a result of deep upwelling of radionuclide-enriched water masses advected from the north with North Atlantic Deep Water (NADW) (Yu et al., 1996). Especially south of the ACC-Weddell Gyre Boundary (AWB), concentrations of ^{230}Th and ^{231}Pa in surface water can reach values usually observed only in the deep ocean, so that scavenging from this layer is expected to contribute much more to the burial flux to the sediment than elsewhere. Consequently, in contrast to other ocean regions, the upper water column in the Southern Ocean could have a significant imprint on the $^{231}Pa/^{230}Th$ signal in the sediment.

In this paper we discuss the hypothesis that upwelling of deep water enriched in ^{230}Th and ^{231}Pa and subsequent near-complete scavenging in surface waters during short time plankton blooms creates an effective pathway of nuclides, especially of ^{231}Pa, to the sediments in the South Atlantic south of the Polar Front. In order to determine export rates from the upper water column, activities of ^{230}Th and ^{231}Pa were measured in sinking particles collected by time-series sediment traps, deployed at various water depths throughout the South Atlantic (Fig.4-1). To evaluate the relative contributions of scavenging from upper and deeper water column, $^{231}Pa/^{230}Th$ ratios of settling particles were compared with those measured on suspended particles and in surface sediments (Walter et al., 1997). Furthermore, to find out whether the Weddell Sea is a source for ^{230}Th and ^{231}Pa to other regions in the Southern Ocean, short-term radionuclide fluxes derived from sediment traps, and long-term inventories in the underlying sediments were related to the production rates of both radionuclides in the water column.

4.3 Material and Methods

4.3.1 Sediment traps

Automated time-series sediment traps (types S/MT 230 & S/MT 233, described in Peinert et al. (1987), and MARK V & MARK VI, Honjo and Doherty (1988)) were deployed in the South Atlantic Sector of the Southern Ocean at the Polar Front (PF), north of the ACC-Weddell Gyre Boundary (BO), in the Northern (AWI 400) and Central (AWI 208) Weddell Sea, west of Maud Rise (WS) and in the Bransfield Strait (KG) south of King George Island (Fig.4-1). Experiments were conducted

during expeditions with R/V Polarstern, for details on mooring stations the reader is referred to the respective cruise reports PF/1 (Fütterer, 1989); PF/3, BO/1, AWI-400/0 and AWI-208 (Bathmann et al., 1992); BO/2 and AWI-400/1 (Spindler et al., 1993); AWI-208/1 (Augstein et al., 1991); KG-1 (Fütterer, 1984). At most moorings, two traps were deployed, one in the upper water column (360-1000m), and the other in the deep ocean (360-500m above the seafloor). Sampling periods ranged from 10 to 60 days, and except for BO/2 and AWI-400/1, a set of data from the complete annual cycle of seasonal flux changes was obtained. No such high resolution time-series data are available from PF-1, where as a result of a malfunction of the stepping motor a one year interval was collected in cup 4 (Table 4-1). Before and after deployment, $HgCl_2$ was added to minimize bacterial degradation (see Fischer and Wefer, 1991).

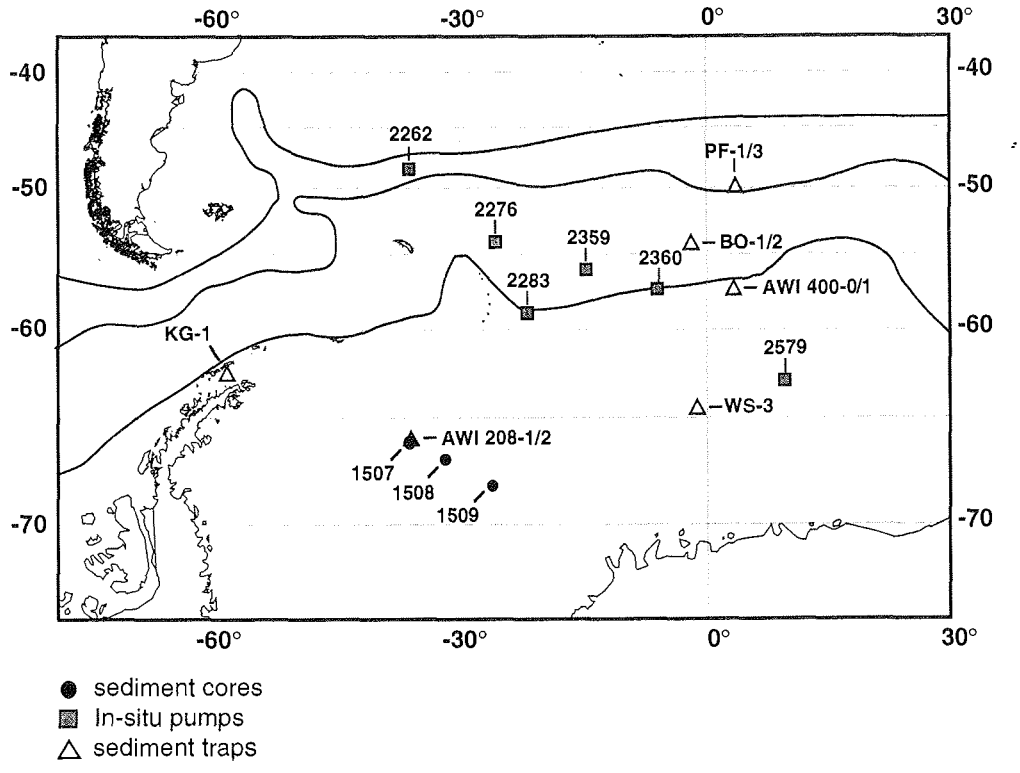

Fig.4-1: Map with sample locations. The lines represent the positions of the major oceanographic fronts after Orsi et al. (1995), from north to south: Subantarctic Front, Polar Front, ACC-Weddell Gyre boundary.

After recovery, samples were further treated according to Wefer et al. (1988; 1990; 1991). Briefly, after removing large swimmers and wet splitting, a split of the fraction <1mm was desalted, freeze-dried and weighed to obtain the total mass fluxes. The size fraction >1mm was negligible except at site BO1 during the austral spring sampling periods. Individual biogenic components (Table 4-3) were determined in

two different ways. Dried material from AWI 208 and AWI 400 was first treated with HCl to obtain the carbonate content from weight loss. Then the amount of organic matter was determined as combustable fraction at 550°C. A portion of material from the mooring sites PF, BO, WS and KG was treated with 6N HCl and measured in a CHN analyser for organic carbon. Carbonate contents were also measured in a CHN analyser using samples that have not been treated with HCl before analysis. Carbonate was calculated as follows (Carbonate = (C_{total} - C_{org}) * 8.33). Biogenic opal was determined by a leaching technique with NaOH at 85°C described in DeMaster (1981) and in Mueller and Schneider (1993), the latter method being an improvement of the manual sequential leaching technique of DeMaster (1981). The amount of lithogenic material was estimated as the difference between the sum of the individual biogenic components and the total mass flux (lithogenic flux = total flux - opal flux - carbonate flux - 2 * C_{org} flux). Splits obtained for analysis of ^{230}Th, ^{232}Th and ^{231}Pa mostly were 1/4 to 1/16 of the respective sampling interval, except for KG1o#1 and KG1u#1-2 (# represents the number of the collector, see Table 4-1) where only 1/256 was taken. The radionuclide measurements could not be performed on the same high time resolution as the particle flux (Fig.4-2 a,b). Deployment in shallow water depths, together with the extremely low particle fluxes over most of the year often required integration over a large time interval (up to a one year period) to achieve satisfactory count statistics for ^{231}Pa. 0.01-1g of dry sample were spiked with appropriate amounts of ^{233}Pa and ^{229}Th, and digested in the presence of HNO_3, HF and $HClO_4$. Th isotopes were separated, purified and electroplated according to Anderson and Fleer (1982), whereas Pa was analyzed using an electroplating procedure described in Francois et al. (1993). Chemical yields for Th and Pa mostly range from 85-95% and 50-70%, respectively.

4.3.2 Sediments

Two sediment cores (PS1507, PS1508) and a box corer (PS1509) from the central abyssal plain of the Weddell Sea, taken during Polarstern expedition ANT V/4 (Miller and Oerter, 1990), were selected to study long-term fluxes of ^{230}Th and ^{231}Pa. All locations are situated within the broad center of the Weddell Gyre, where circulation is sluggish (Pudsey et al., 1988) and measured bottom currents are very low with values <0.5cm/sec (Fahrbach et al., 1994; Fahrbach and Rohardt, pers. comm.). Apart from a few very localized channels, there is no evidence for erosional processes to occur in that region (Pudsey et al., 1988; Barker et al., 1988; Kuhn, pers. comm.). Sediments are predominantly hemipelagic muds, containing thin layers of distal turbidites ranging from a few mm up to several cm in thickness (Dieckmann, pers. comm.), which are derived from the southwest during periods of low sea level (Pudsey et al., 1988). Their occurrence is highest in core 1507 which is located closest to the continent, and decreases offshore. As such turbidites are more often found in the deeper parts of the cores (e.g. below a depth of 100cm in core 1507, probably reflecting isotope stage 6, see below), to minimize their influence, our investigation is restricted to the upper 100cm (Fig.4-3). Since the activities of $_{xs}^{231}$Pa and $_{xs}^{230}$Th in the turbidity layers are very low, they cannot contribute much to the mass balance of both radionuclides in the sediment.

Continuous samples of the cores, each representing a homogenized 1-5cm sediment slice, were taken for analysis of ^{231}Pa, U and Th isotopes. 0.5g of dry

sediment was spiked with ^{233}Pa, ^{229}Th and ^{236}U, and digested in the same way as the sediment trap samples. For U and Th the chemical procedure follows the description of Anderson and Fleer (1982). Chemical yields for Pa obtained by the electroplating method (Francois et al., 1993), often were very low (<10%), probably related to the precipitation of amorphous silicious compounds in the final stage of the digestion step after almost complete removal of $HClO_4$ by repeated washings with HNO_3. Better yields (45-60%) were obtained by a modified procedure based on the recovery of Pa that was lost on such silicious compounds (Geibert, in prep.). Chemical yields for Th were comparable to those obtained for the trap material. For U values ranged between 30 and 70%.

4.3.3 Calibrations and data reduction

Activities of ^{231}Pa, Th and U isotopes were determined by alpha-, ^{233}Pa by beta counting. The tracers ^{229}Th and ^{236}U were calibrated with a certified standard solution prepared from pure ThO_2 and U_3O_8 (PTB-Braunschweig, uncertainty 2.5%, (3σ)), respectively. To calibrate the ^{233}Pa tracer a weighed amount of tracer solution was evaporated on a platinum disc and beta counted. Calibrations were checked by repeated analysis of a uranium-bearing sediment standard, UREM-11 (Hansen and Ring, 1983). Blank contributions of ^{230}Th were negligible for the sediments but significant for the sediment trap material with values up to 14%. For ^{231}Pa blanks contributed 0.2-30% to the sediments and 1-27% to the trap material.

Measured activities of ^{230}Th and ^{231}Pa of the sediments were corrected for detrital, U-supported activities of ^{230}Th and ^{231}Pa using the following equations:

$$_{xs}{}^{230}Th = {}^{230}Th_m - {}^{234}U_m \quad (1)$$

$$_{xs}{}^{231}Pa = {}^{231}Pa_m - 0.046 * {}^{234}U_m \quad (2)$$

The notations (xs) designate unsupported and (m) measured activities, and the factor 0.046 is the $^{235}U/^{234}U$ activity ratio in detrital material. A correction for ingrowth of ^{230}Th and ^{231}Pa from authigenic uranium was not necessary, as $^{234}U/^{238}U$ ratios are always <1, and $^{234}U/^{232}Th$ ratios are invariably low with values <0.5.

For the sediment trap material detrital $^{230}Th/^{232}Th$ ratios (indicated by letter "R"), were estimated from $^{234}U/^{232}Th$ ratios measured in surface sediments (Walter et al., 1997) in the vicinity of the respective moorings. Corrections were made as follows:

$$_{xs}{}^{230}Th = {}^{230}Th_m - (R) * {}^{232}Th_m \quad (3)$$

$$_{xs}{}^{231}Pa = {}^{231}Pa_m - (R) * 0.046 * {}^{232}Th_m \quad (4)$$

Values of "R" were 0.7 at the Polar Front (PF) and Bouvet (BO), 0.6 at AWI 400, 0.4 at AWI 208, and 0.77-0.89 near King George (KG). Because of the high $^{230}Th/^{232}Th$ ratios (>20) in most of the samples, corrections generally were very small with 1-4% for ^{230}Th and less than 1% for ^{231}Pa. This does not hold for the trap deployed in the Bransfield Strait, where activities of ^{232}Th both in the upper and lower trap are very

high reaching 50-82% of the measured ^{230}Th activities. The strong influence of a lithogenic component at this location (Table 4-1) is suggested to result from resuspension of sediments derived from the adjacent shelf regions (Abelmann and Gersonde, 1991). If we assume that the resuspended sediment is of very old age so that its unsupported activities have already decayed, an upper limit for $_{xs}^{230}Th$ and $_{xs}^{231}Pa$ (Table 4-1, Fig.4-2 b) can be given. Note the strong influence in the uncertainty of the detrital $^{230}Th/^{232}Th$ ratio "R" on the calculation of unsupported fluxes at this location, especially for ^{230}Th. A lower limit for $_{xs}^{230}$ and $_{xs}^{231}Pa$ cannot be given, as the amount of unsupported activities in the resuspended sediment is not known.

4.4 RESULTS

4.4.1 Fluxes in the water column

Radionuclide data for the sediment trap material are listed in Table 4-1. Fluxes of ^{230}Th and ^{231}Pa are closely coupled with the annual cycle of total mass flux of particulate matter (Fig.4-2 a,b) confirming earlier results on ^{230}Th and ^{210}Pb (Rutgers van der Loeff and Berger, 1991). During the short peaks in particle flux occurring in austral summer, radionuclide fluxes are very high, followed by much lower fluxes over the rest of the year. $_{xs}^{231}Pa/^{230}Th$ ratios of the individual samples all exceed the production ratio of 0.093 with values spanning a wide range from 0.11 to 0.91 (Table 4-1).

In Table 4-2 total annual fluxes of ^{230}Th (F_aTh) and ^{231}Pa (F_aPa) are presented and are normalized to their expected fluxes (F_p) from production rates in the water column using the following equation

$$F_p = \beta * z \qquad (5)$$

where z is the water depth [m] and β is the production rate in the water column (β_{Th} = 0.0252; β_{Pa} = 0.00233 [dpm/m^3/y]). Apart from the moorings at KG, calculated F_a/F_p ratios for ^{230}Th are below 1, whereas for ^{231}Pa, ratios exceed 1 in most of the shallow traps (Table 4-2). Lowest ratios of F_a/F_p for both radionuclides are observed in the deep traps at moorings BO and AWI 400. Mean annual $_{xs}^{231}Pa/^{230}Th$ in the shallow traps are extremely high with values of 0.28-0.46. A N-S trend of increasing $^{231}Pa/^{230}Th$ ratios, as observed so clearly for the surface sediments and the suspended particles (Walter et al., 1997), is not seen. In 3 out of 4 mooring sites, $^{231}Pa/^{230}Th$ ratios in the deep traps are lower than in the shallow traps by almost a factor of 2 (Tables 4-1, 4-2). Values in the deep traps increase from 0.16 at the Polar Front (PF-3) to 0.27 south of the ACC-Weddell Gyre (AWI 400). In the deep trap from the Bransfield Strait (KG) an intermediate $^{231}Pa/^{230}Th$ ratio of 0.22 was measured. Note that the $^{231}Pa/^{230}Th$ ratios even for the deeper sediment traps are still much higher than those found in nearby surface sediments (Table 4-6, Walter et al., 1997). Data on the chemical composition of the sediment trap material are listed in Table 4-3. Opal is the dominant biogenic component on sinking particles, ranging from 40% at the Polar Front to 70% in the Weddell Sea.

Table 4-1: Mass fluxes, concentrations of ^{230}Th and ^{231}Pa and $_{xs}^{231}Pa/_{xs}^{230}Th$ ratios of the sediment trap samples.

sample	trap depth (m)	collection interval	days	mass flux (mg/m^2/d)	^{232}Th (dpm/g)	^{230}Th (dpm/g)	$_{xs}^{230}Th$ (dpm/g)	^{231}Pa (dpm/g)	$_{xs}^{231}Pa$ (dpm/g)	$^{231}Pa/^{230}Th$	$_{xs}^{231}Pa/_{xs}^{230}Th$
Polar Front 1. 50°09.0'S. 05°50'E. 3750m											
PF1o#1-3	700	15. Jan 87 - 16. Mar 87	60	229.7	0.008 ± 0.003	0.140 ± 0.009	0.134 ± 0.009	0.037 ± 0.005	0.036 ± 0.005	0.262 ± 0.040	0.271 ± 0.042
PF1o#4		16. Mar 87 - 12. Mar 88	361	84.3			0.200 ± 0.014		0.065 ± 0.013		0.322 ± 0.066
Polar Front 3. 50°07.6'S. 05°50'E. 3785m											
PF3o#1-17	614	10. Nov 89 - 23. Dec 90	408	149.1	0.007 ± 0.001	0.196 ± 0.009	0.191 ± 0.009	0.057 ± 0.003	0.057 ± 0.003	0.292 ± 0.020	0.298 ± 0.021
PF3u#1-2	3196	10. Nov 89 - 22. Dec 89	42	99.8	0.033 ± 0.016	2.977 ± 0.206	2.954 ± 0.206	0.331 ± 0.033	0.330 ± 0.033	0.111 ± 0.014	0.112 ± 0.014
PF3u#3	3196	22. Dec 89 - 12. Jan 90	21	333.1	0.043 ± 0.011	1.318 ± 0.075	1.288 ± 0.076	0.265 ± 0.026	0.263 ± 0.026	0.201 ± 0.023	0.204 ± 0.023
PF3u#4	3196	12. Jan 90 - 02. Feb 90	21	369.9	0.025 ± 0.007	1.310 ± 0.075	1.293 ± 0.075	0.229 ± 0.025	0.228 ± 0.025	0.174 ± 0.022	0.176 ± 0.022
PF3u#5	3196	02. Feb 90 - 23. Feb 90	21	46.3	0.028 ± 0.026	0.568 ± 0.082	0.548 ± 0.084	0.108 ± 0.048	0.107 ± 0.048	0.191 ± 0.089	0.196 ± 0.093
PF3u#6	3196	23. Feb 90 - 16. Mar 90	21	516.6	0.015 ± 0.005	0.817 ± 0.052	0.807 ± 0.052	0.149 ± 0.015	0.148 ± 0.015	0.182 ± 0.021	0.184 ± 0.022
PF3u#7-17	3196	16. Mar 90 - 23. Dec 90	282	21	0.009 ± 0.009	0.243 ± 0.034	0.237 ± 0.035	0.036 ± 0.008	0.035 ± 0.008	0.147 ± 0.039	0.150 ± 0.041
Bouvet 1. 54°20.6'S. 03°22.6'W. 2734m											
BO1o#1	450	28. Dec 90 - 20. Jan 91	23	333.5	0.008 ± 0.003	0.163 ± 0.011	0.157 ± 0.012	0.042 ± 0.006	0.041 ± 0.006	0.256 ± 0.040	0.264 ± 0.042
BO1o#2	450	20. Jan 91 - 12. Feb 91	23	457.9	0.001 ± 0.002	0.105 ± 0.009	0.104 ± 0.009	0.032 ± 0.004	0.032 ± 0.004	0.309 ± 0.043	0.311 ± 0.044
BO1o#3	450	12. Feb 91 - 07. Mar 91	23	1277.3	0.006 ± 0.002	0.057 ± 0.006	0.053 ± 0.006	0.019 ± 0.003	0.019 ± 0.003	0.339 ± 0.064	0.362 ± 0.071
BO1o#4	450	07. Mar 91 - 30. Mar 91	23	471.7	0.003 ± 0.002	0.084 ± 0.007	0.081 ± 0.007	0.031 ± 0.004	0.031 ± 0.004	0.365 ± 0.056	0.375 ± 0.058
BO1o#5	450	30. Mar 91 - 22. Apr 91	23	494.2	0.002 ± 0.002	0.066 ± 0.006	0.064 ± 0.006	0.027 ± 0.004	0.027 ± 0.004	0.415 ± 0.072	0.425 ± 0.075
BO1o#6-20	450	22. Apr 91 - 01. Apr 92	345	43.8	0.051 ± 0.004	0.131 ± 0.006	0.095 ± 0.007	0.032 ± 0.003	0.031 ± 0.003	0.248 ± 0.027	0.325 ± 0.041
BO1u#1*	2194	28. Dec 90 20. Jan 91	23	554.9							
BO1u#2	2194	20. Jan 91 - 12. Feb 91	23	674.4	0.011 ± 0.002	0.398 ± 0.012	0.390 ± 0.012	0.171 ± 0.010	0.170 ± 0.010	0.429 ± 0.029	0.437 ± 0.030
BO1u#3-20	2194	12. Feb 91 - 01. Apr 92	414	7.4	0.037 ± 0.008	0.100 ± 0.012	0.074 ± 0.013	0.069 ± 0.013	0.068 ± 0.013	0.688 ± 0.150	0.911 ± 0.224
Bouvet 2. 54°20.8'S. 03°23.6'W. 2695m											
BO2o#1-20	456	15. May 92 - 01. Dec 92	200	55.4	0.021 ± 0.003	0.250 ± 0.013	0.235 ± 0.013	0.097 ± 0.005	0.097 ± 0.005	0.389 ± 0.029	0.411 ± 0.032
BO2u#1-12	2183	15. May 92 - 12. Sep 92	120	29.9	0.030 ± 0.005	0.544 ± 0.027	0.523 ± 0.027	0.223 ± 0.013	0.222 ± 0.013	0.410 ± 0.031	0.425 ± 0.033
AWI-400/0. 57°18'S. 04°07'E. 4467m											
400/0u#1	3700	26. Mar 91 - 25. Apr 91	30	148.2	0.063 ± 0.011	2.056 ± 0.100	2.018 ± 0.100	0.530 ± 0.029	0.528 ± 0.029	0.258 ± 0.019	0.262 ± 0.019
400/0u#2	3700	25. Apr 91 - 09. Jun 91	45	53.3	0.042 ± 0.014	2.076 ± 0.130	2.050 ± 0.130	0.726 ± 0.052	0.725 ± 0.052	0.350 ± 0.033	0.354 ± 0.034
400/0u#3	3700	09. Jun 91 - 24. Jul 91	45	8.1	0.050 ± 0.064	3.010 ± 0.251	2.980 ± 0.254	0.982 ± 0.106	0.980 ± 0.106	0.326 ± 0.045	0.329 ± 0.045
400/0u#4-13	3700	24. Jul 91 - 04. Apr 92	255	0.5	0.009 ± 0.034	1.228 ± 0.152	1.223 ± 0.154	0.353 ± 0.139	0.353 ± 0.139	0.288 ± 0.119	0.289 ± 0.120
400/0u#14	3700	04. Apr 92 - 10. May 92	36	19.2	0.207 ± 0.052	6.003 ± 0.344	5.879 ± 0.345	1.192 ± 0.099	1.186 ± 0.099	0.199 ± 0.020	0.202 ± 0.021
AWI-400/1. 57°37.6'S. 04°03.2'E. 4495m											
400/1o#1-2	450	15. May 92 - 04. Jun 92	20	100.9	0.011 ± 0.012	0.294 ± 0.038	0.287 ± 0.039	0.133 ± 0.021	0.132 ± 0.021	0.452 ± 0.091	0.461 ± 0.095
400/1o#3-4	450	04. Jun 92 - 24. Jun 92	20	45.8	0.028 ± 0.019	0.440 ± 0.049	0.423 ± 0.050	0.172 ± 0.035	0.172 ± 0.035	0.392 ± 0.090	0.406 ± 0.095
400/1o#5-19	450	24. Jun 92 - 01. Dec 92	160	7.1	0.025 ± 0.012	0.369 ± 0.037	0.354 ± 0.037	0.194 ± 0.032	0.193 ± 0.032	0.525 ± 0.100	0.546 ± 0.106
400/1u#1-2	3048	15. May 92 - 04. Jun 92	20	74.7	0.055 ± 0.018	1.719 ± 0.111	1.686 ± 0.112	0.623 ± 0.048	0.621 ± 0.048	0.362 ± 0.036	0.368 ± 0.037
400/1u#3-4	3048	04. Jun 92 - 24. Jun 92	20	41.4	0.034 ± 0.023	1.894 ± 0.116	1.873 ± 0.117	0.594 ± 0.059	0.593 ± 0.059	0.314 ± 0.037	0.316 ± 0.037
400/1u#5	3048	24. Jun 92 - 04. Jul 92	10	156.9	0.029 ± 0.021	0.455 ± 0.051	0.438 ± 0.052	0.084 ± 0.022	0.083 ± 0.022	0.184 ± 0.053	0.190 ± 0.055
400/1u#6-7	3048	04. Jul 92 - 24. Jul 92	20	24.7	0.110 ± 0.054	1.790 ± 0.183	1.724 ± 0.186	0.388 ± 0.066	0.385 ± 0.066	0.217 ± 0.043	0.224 ± 0.045
400/1u#8-12	3048	24. Jul 92 - 12. Sep 92	50	5.9	0.130 ± 0.082	3.120 ± 0.277	3.042 ± 0.282	0.610 ± 0.097	0.607 ± 0.097	0.196 ± 0.036	0.199 ± 0.037

* no sample available for radionuclide analysis

Table 4-1: continued

sample	trap depth(m)	collection interval	days	mass flux (mg/m^2/d)	^{232}Th (dpm/g)	^{230}Th (dpm/g)	$_{xs}^{230}$Th (dpm/g)	^{231}Pa (dpm/g)	$_{xs}^{231}$Pa (dpm/g)	^{231}Pa/^{230}Th	$_{xs}^{231}$Pa/$_{xs}^{230}$Th
Weddell Sea 3. 64°54.1'S. 02°33.8'W. 5053m											
WS3#1-2	360	16. Jan 88 - 17. Feb 88	32	260.3	0.011 ± 0.004	0.144 ± 0.013	0.140 ± 0.013	0.055 ± 0.006	0.055 ± 0.006	0.381 ± 0.052	0.392 ± 0.054
WS3#3	360	17. Feb 88 - 04. Mar 88	16	647.5	0.003 ± 0.001	0.167 ± 0.011	0.166 ± 0.011	0.057 ± 0.005	0.057 ± 0.005	0.340 ± 0.037	0.342 ± 0.037
WS3#4-20	360	04. Mar 88 - 04. Feb 89	336	50.1	0.005 ± 0.001	0.313 ± 0.015	0.311 ± 0.015	0.072 ± 0.004	0.072 ± 0.004	0.231 ± 0.017	0.232 ± 0.017
AWI-208/1. 65°56.2'S. 36°30.2'W. 4710m											
208/1#1-6	1090	05. Oct 89 - 03. Jan 90	90	8.2	0.016 ± 0.023	1.058 ± 0.091	1.051 ± 0.091	0.231 ± 0.053	0.231 ± 0.053	0.219 ± 0.053	0.220 ± 0.054
208/1#7-9	1090	03. Jan 90 - 17. Feb 90	45	44.3	0.036 ± 0.034	0.688 ± 0.116	0.674 ± 0.117	0.183 ± 0.021	0.182 ± 0.021	0.266 ± 0.054	0.271 ± 0.056
208/1#10-11	1090	17. Feb 90 - 18. Apr 90	60	53.5	0.018 ± 0.008	1.246 ± 0.073	1.239 ± 0.073	0.363 ± 0.030	0.363 ± 0.030	0.291 ± 0.029	0.293 ± 0.029
208/1#12-13	1090	18. Apr 90 - 17. Jun 90	60	18.4	0.008 ± 0.013	1.209 ± 0.087	1.205 ± 0.087	0.385 ± 0.048	0.385 ± 0.048	0.318 ± 0.046	0.319 ± 0.046
208/1#14	1090	17. Jun 90 - 16. Aug 90	60	16.4	0.011 ± 0.017	1.787 ± 0.129	1.783 ± 0.129	0.407 ± 0.066	0.407 ± 0.066	0.228 ± 0.041	0.228 ± 0.041
208/1#15-17	1090	16. Aug 90 - 14. Nov 90	90	1.8	0.741 ± 0.146	2.162 ± 0.245	1.866 ± 0.252	0.796 ± 0.166	0.783 ± 0.166	0.368 ± 0.087	0.419 ± 0.105
AWI-208/1. 65°56.2'S. 36°30.2'W. 4710m											
208/2#2	1090	29. Dec 90 - 28. Jan 91	30	7.4	0.039 ± 0.064	1.301 ± 0.196	1.285 ± 0.198	0.201 ± 0.076	0.200 ± 0.076	0.154 ± 0.063	0.156 ± 0.064
208/2#3	1090	28. Jan 91 - 27. Feb 91	30	83.6	0.008 ± 0.006	0.803 ± 0.045	0.800 ± 0.045	0.171 ± 0.020	0.171 ± 0.020	0.213 ± 0.028	0.213 ± 0.028
208/2#4	1090	27. Feb 91 - 29. Mar 91	30	171.7	0.007 ± 0.004	1.139 ± 0.063	1.137 ± 0.063	0.206 ± 0.021	0.206 ± 0.021	0.181 ± 0.021	0.181 ± 0.021
208/2#5	1090	29. Mar 91 - 28. Apr 91	30	236.5	0.001 ± 0.002	0.661 ± 0.039	0.661 ± 0.039	0.165 ± 0.012	0.165 ± 0.012	0.250 ± 0.024	0.250 ± 0.024
208/2#6	1090	28. Apr 91 - 28. May 91	30	66.5	0.023 ± 0.013	0.734 ± 0.050	0.725 ± 0.050	0.132 ± 0.019	0.132 ± 0.019	0.181 ± 0.029	0.182 ± 0.030
208/2#7-9	1090	28. May 91 - 26. Aug 91	90	6.6	0.009 ± 0.017	1.023 ± 0.094	1.019 ± 0.095	0.165 ± 0.046	0.165 ± 0.046	0.161 ± 0.048	0.162 ± 0.048
208/2#10-11	1090	26. Aug 91 - 25. Oct 91	60	12.5	0.022 ± 0.018	2.694 ± 0.155	2.685 ± 0.155	0.375 ± 0.064	0.375 ± 0.064	0.139 ± 0.025	0.140 ± 0.025
208/2#12-16	1090	25. Oct 91 - 23. Mar 92	150	3.1	0.045 ± 0.031	2.040 ± 0.144	2.022 ± 0.144	0.311 ± 0.076	0.310 ± 0.076	0.152 ± 0.039	0.153 ± 0.039
208/2#17	1090	23. Mar 92 - 22. May 92	60	67.4	0.001 ± 0.003	0.134 ± 0.014	0.133 ± 0.014	n.d.			
208/2#18	1090	22. May 92 - 21. Jul 92	60	60.3	0.007 ± 0.004	0.424 ± 0.025	0.422 ± 0.025	0.073 ± 0.011	0.073 ± 0.011	0.172 ± 0.028	0.173 ± 0.028
208/2#19	1090	21. Jul 92 - 19. Sep 92	60	4.6	0.030 ± 0.041	0.745 ± 0.110	0.733 ± 0.111	n.d.			
King George 1. 62°15.4'S. 57°31.7'W. 1952m											
KG-1o#0	494	01. Dec 83 - 30. Dec 83	30	**							
KG-1o#1	494	31. Dec 83 - 30. Jan 84	30	1559	0.320 ± 0.026	0.478 ± 0.035	0.213 ± 0.041	0.082 ± 0.011	0.070 ± 0.011	0.172 ± 0.026	0.330 ± 0.082
KG-1o#2-3	494	30. Jan 84 - 30. Mar 84	60	55.3	0.655 ± 0.044	0.903 ± 0.056	0.360 ± 0.067	0.110 ± 0.012	0.085 ± 0.012	0.122 ± 0.015	0.237 ± 0.056
KG-1o#8-12	494	28. Jun 84 - 25. Nov 84	150	67.3	2.533 ± 0.318	3.084 ± 0.418	0.982 ± 0.494	n.d.			
KG1u#1-2	1588	01. Dec 83 - 30. Jan 84	60	1741.5	1.056 ± 0.064	1.564 ± 0.093	0.687 ± 0.107	0.189 ± 0.012	0.148 ± 0.013	0.121 ± 0.011	0.216 ± 0.038
KG1u#5-6	1588	30. Mar 84 - 29. May 84	60	32	0.399 ± 0.030	0.799 ± 0.046	0.468 ± 0.052	0.140 ± 0.017	0.125 ± 0.017	0.176 ± 0.024	0.268 ± 0.047

Errors are given as 1σ of propagated uncertainty of counting statistics and blank
- = count rate not sufficiently above background
** instrument failure

Table 4-2: Annual mass fluxes, concentrations, fluxes (F_a) and expected fluxes (F_p) of $_{xs}{}^{230}Th$ and $_{xs}{}^{231}Pa$, and mean $_{xs}{}^{231}Pa/_{xs}{}^{230}Th$ ratios for the sediment trap samples.

sample	depth (m)	collection interval	days	mass flux# (g/m^2)	mass flux ($g/m^2/y$)	mean $_{xs}{}^{230}Th$ (dpm/g)	F_a(Th) $dpm/m^2/y$	F_p(Th) $dpm/m^2/y$	F_a/F_p(Th)	mean $_{xs}{}^{231}Pa$ (dpm/g)	F_a(Pa) $dpm/m^2/y$	F_p(Pa) $dpm/m^2/y$	F_a/F_p(Pa)	mean $_{xs}{}^{231}Pa/_{xs}{}^{230}Th$
Bouvet 1	450	28. Dec 90 - 01. Apr 92	460	84.91	67.38	0.081 ± 0.003	5.47 ± 0.20	11.34	0.48 ± 0.02	0.028 ± 0.002	1.85 ± 0.11	1.05	1.77 ± 0.10	0.339 ± 0.023
	2194	20. Jan 91 - 01. Apr 92	437	18.57	15.51	0.338 ± 0.010	5.24 ± 0.16	55.29	0.095 ± 0.003	0.153 ± 0.009	2.38 ± 0.14	5.12	0.46 ± 0.03	0.454 ± 0.030
Bouvet 1*	2194	28. Dec 90 - 01. Apr 92	460	31.33	24.86	-	(8.9)		(0.16)		(3.98)		(0.78)	0.411 ± 0.032
Bouvet 2	456	15. May 92 - 01. Dec 92	200	11.09		0.235 ± 0.013				0.097 ± 0.005				0.425 ± 0.033
	2183	15. May 92 - 12. Sep 92	120	3.59		0.523 ± 0.027				0.222 ± 0.013				
Weddell Sea 3	360	16. Jan 88 - 03. Feb 89	384	35.52	33.76	0.229 ± 0.008	7.72 ± 0.27	9.07	0.85 ± 0.03	0.064 ± 0.003	2.15 ± 0.09	0.84	2.56 ± 0.11	0.278 ± 0.016
AWI 208/1	1090	05. Oct 89 - 14. Nov 90	405	8.19	7.38	1.157 ± 0.046	8.54 ± 0.34	27.47	0.31 ± 0.01	0.324 ± 0.017	2.39 ± 0.13	2.54	0.94 ± 0.05	0.280 ± 0.019
AWI 208/2	1090	29. Dec 90 - 19. Sep 92	630	26.72	15.48	0.753 ± 0.018	11.65 ± 0.28	27.47	0.42 ± 0.01	0.139 ± 0.006	2.15 ± 0.10	2.54	0.85 ± 0.04	0.185 ± 0.010
AWI 400/0	3700	26. Mar 91 - 10. May 92	411	8.04	7.14	2.390 ± 0.075	17.07 ± 0.53	93.24	0.18 ± 0.01	0.655 ± 0.024	4.68 ± 0.17	8.63	0.54 ± 0.02	0.274 ± 0.013
AWI 400/1	450	15. May 92 - 01. Dec 92	200	4.07		0.336 ± 0.025				0.159 ± 0.016				0.472 ± 0.058
	3048	15. May 92 - 12. Sep 92	120	4.68		1.389 ± 0.052				0.411 ± 0.022				0.296 ± 0.019
King George 1	494	31. Dec 83 - 25. Nov 84	330	60.20	66.59	0.350 ± 0.089	23.31 ± 5.92	12.45	1.87 ± 0.48	n.d.				
King George 1*	494	01. Dec 83 - 25. Nov 84	360	(117)	(119)	-	(33.5)	12.5	(2.69)					
	1588	01. Dec 83 - 25. Nov 84	360	107.7	109.2	0.675 ± 0.105	73.71 ± 11.3	40.02	1.84 ± 0.28	0.146 ± 0.013	16.0 ± 1.35	3.71	4.31 ± 0.36	0.217 ± 0.038
Polar Front 1	700	15. Jan 87 - 11. Mar 88	421	44.21	38.33	0.181 ± 0.010	6.93 ± 0.39	17.64	0.39 ± 0.02	0.056 ± 0.009	2.15 ± 0.36	1.63	1.32 ± 0.22	0.310 ± 0.055
Polar Front 3	614	10. Nov 89 - 23. Dec 90	408	60.82	54.41	0.191 ± 0.009	10.39 ± 0.48	15.47	0.67 ± 0.03	0.057 ± 0.003	3.09 ± 0.16	1.43	2.16 ± 0.11	0.298 ± 0.021
	3196	10. Nov 89 - 23. Dec 90	408	36.9	33.01	1.141 ± 0.036	37.66 ± 1.18	80.54	0.47 ± 0.01	0.185 ± 0.009	6.10 ± 0.31	7.46	0.82 ± 0.04	0.162 ± 0.010

*estimated from total mass flux (BO/1) and expected total mass flux (KG/1, Wefer et al., 1988). see text for details.
#per total sampling time

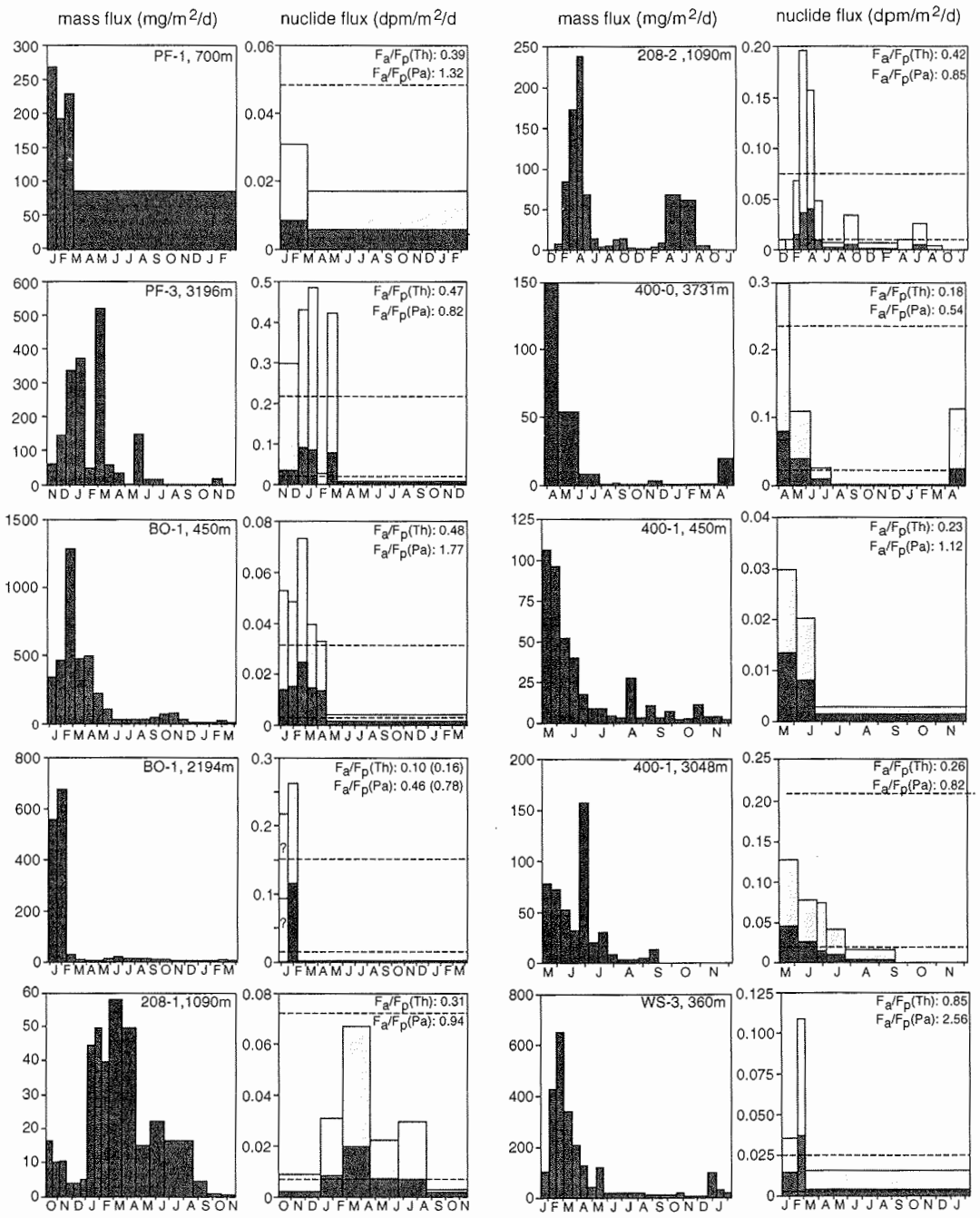

Fig.4-2 (a): Seasonality in particle flux, and in fluxes of $_{xs}^{230}$Th (light shaded) and $_{xs}^{231}$Pa (dark shaded) at the respective trap moorings. The stippled lines are the expected fluxes of $_{xs}^{230}$Th (upper line) and $_{xs}^{231}$Pa (lower line) from their respective production rates. The F_a/F_p ratios in brackets at BO-1, 2194m are corrected for the expected activities from mass flux of cup 1, for which no radionuclide determination was made (see text for details).

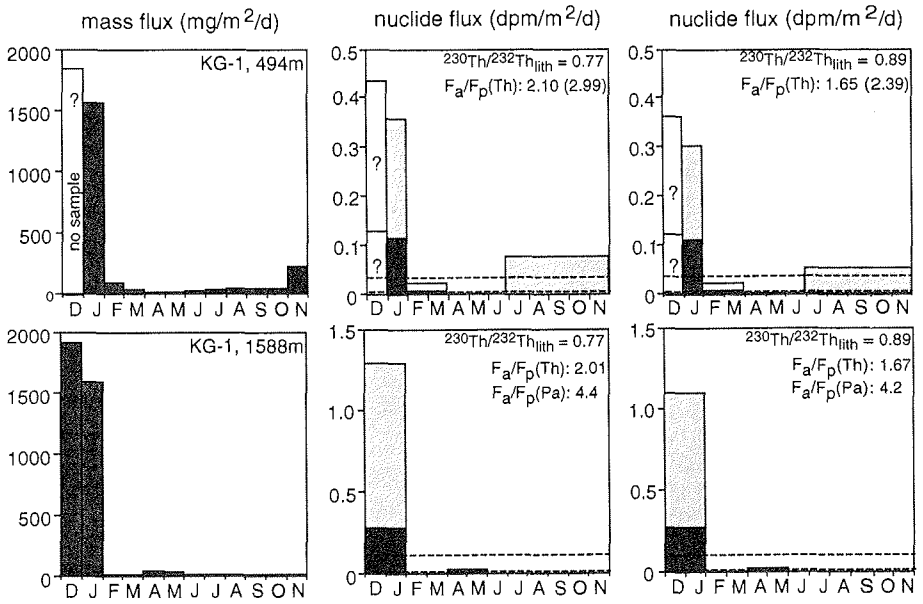

Fig.4-2 (b): Seasonality in particle flux, and in fluxes of $_{xs}^{230}$Th and $_{xs}^{231}$Pa measured at the mooring site KG. Note the large influence in the uncertainty of the detrital ^{230}Th/^{232}Th ratio on the calculation of excess activities of ^{230}Th and ^{231}Pa (see text for details). Shaded areas and stippled lines as in Fig.4-2 (a). The F_a/F_p ratios in brackets in the shallow trap are corrected values including expected activities from estimated mass flux for cup 1 (see text for details).

Although opal data for the locations AWI 400 and AWI 208 are not available, the small lithogenic influence (based on ^{232}Th data) and the low carbonate content (7-21%) show that fluxes must be dominated by opal there as well.

4.4.2 Fluxes to the seafloor

We derive the burial rates of $_{xs}^{230}$Th and $_{xs}^{231}$Pa in the Weddell Sea from their inventories in the sediment cores. The corresponding age model is based on the depth distributions of both radionuclides (Fig.4-3). Activities of $_{xs}^{230}$Th and $_{xs}^{231}$Pa in the three cores show similar patterns of minima and maxima with variations up to an order of magnitude, confirming earlier results (Francois et al., 1993; Frank et al., 1995; Frank 1996). The $_{xs}^{231}$Pa/$_{xs}^{230}$Th ratio roughly follows exponential decay with depth (Rosholt et al., 1961; Faure, 1986), according to the equation

$$_{xs}(^{231}Pa/^{230}Th)_m = {}_{xs}(^{231}Pa/^{230}Th)_o * \exp[(\lambda^{230}Th - \lambda^{231}Pa)_t \qquad (6)$$

where m and o refer to the measured and initial $_{xs}^{231}$Pa/$_{xs}^{230}$Th ratios, t [a] is the time elapsed since deposition of the sediment, and λ^{230}Th and λ^{231}Pa are the decay constants [y^{-1}] of ^{230}Th and ^{231}Pa, respectively. Corresponding average sediment accumulation rates range from 2.7-4.8mm/ka (Table 4-4).

Table 4-3: Mean annual composition of the sediment trap material (based on total sampling time).

	depth (m)	% opal	% Corg	% carb	% POM	% lith	reference
BO-1	450	63.2	3.2	14.0		17.0	this study
BO-1*	2194	65.6	1.7	4.8		26.2	this study
BO-2	456	60.5	4.1	16.7		11.5	this study
	2183	53.4	4.7	18.3		18.9	this study
WS-3	360	70.3	6.6	8.3		8.3	this study
208-1	1090	n.d.	n.d.	12.7	21.3	n.d.	this study
208-2	1090	n.d.	n.d.	21.1	n.d.	n.d.	this study
400-0	3700	n.d.	n.d.	7.3	9.5	n.d.	this study
400-1	450	n.d.	n.d.	13.1	n.d.	n.d.	this study
	3048	n.d.	n.d.	17.8	n.d.	n.d.	this study
KG-1	494	43.1	3.3	3.8		32.9	Wefer et al. (1988)
	1588	36.2	2.2	4.9		49.9	Wefer et al. (1988)
PF-1	700	40.1	7.5	26.5		11.3**	Wefer and Fischer (1991)
PF-3	614	47.9	6.3	21.4		18.5	this study
PF-3*	3196	39.6	13.3	22.0		n.d.	this study

*mean values based on BO1u#1+2, and PF3u#1-6, which represent 90% and 84% of the total mass flux, respectivtly (during rest of the year not enough material collected for analysis of its chemical composition)
**this study

An independent approach to derive average sedimentation rates was performed for the cores PS1507 and PS1508 by using their maxima and minima in the radionuclide profiles for a stratigraphic classification (Frank et al., 1995). In a sediment core from the continental margin of the southeastern Weddell Sea these authors found strong variations in the radionuclide concentrations, resembling the glacial/interglacial pattern of $\delta^{18}O$ stratigraphy with the most drastic increase in the activity of initial $_{xs}^{230}Th$ from very low values during isotope stage 6 to very high values in isotope stage 5e. Similar radionuclide profiles have also been found in other cores adjacent to the Weddell Sea, which led Frank et al. (1995) to suggest that radioisotope stratigraphy may be a useful tool to date sediment cores in areas where lack of carbonate prevents the establishment of a $\delta^{18}O$ stratigraphy. Applying their observations to our cores, the well-pronounced peaks at 37.5cm (1507) and 32.5cm (1508) could indeed reflect interglacial isotope stage 5e, and the low $_{xs}^{230}Th$ concentrations underneath stage 6. Sediment accumulation rates can then be determined either by assuming that the $_{xs}^{230}Th$ maxima represent the maximum productivity in stage 5e (120ka; Martinson et al., 1987), or that the minima at 57.5cm (1507) and 42.5cm (1508) mark the termination of stage 6 (130ka; Martinson et al., 1987). Average sediment accumulation rates obtained from $^{231}Pa/^{230}Th$ decay are in the range of the values obtained from radioisotope stratigraphy (Fig.4-3, Table 4-4). However, the difficulty in determining the transition from stage 6 to 5e from the ^{230}Th and ^{231}Pa activities results in a relatively large uncertainty in the calculation of average accumulation rates by the radiostratigraphic method (20-30% lower when based on the ^{230}Th maxima than when based on the minima, indicated by the shaded areas in Fig.4-3), which does not allow to unequivocally verify Frank's hypothesis. Anyhow, the $_{xs}^{231}Pa/_{xs}^{230}Th$ method of age determination provides an

Table 4-4: Observed (I_a) and expected (I_e) inventories of ^{230}Th and ^{231}Pa, average sediment accumulation rates, and extrapolated initial $_{xs}^{231}Pa/_{xs}^{230}Th$ ratios of the sediment cores.

core	latitude	longitude	water depth (m)	depth interval (cm)	$\Sigma xs^{230}Th$ obs. (I_aTh) dpm/cm^2	$\Sigma xs^{231}Pa$ obs. (I_oPa) dpm/cm^2	$_{xs}Pa/_{xs}Th$ acc.rate cm/ka	radioisotope stratigraphy acc.rate (cm/ka)	$\Sigma xs^{230}Th$ exp. (I_eTh) dpm/cm^2	$\Sigma xs^{231}Pa$ exp. (I_ePa) dpm/cm^2	I_aTh/I_eTh	$I_aPa/I_ePa.$	initial $_{xs}^{231}Pa/_{xs}^{230}Th$
1507	68°37.5' S	24°00.7' W	4771	0-77.5	447	28.3	0.43		1057	51.1	0.43	0.55	0.119
1507*				0-37.5	286	22.6		0.31	874	48.2	0.33	0.47	0.133
1507**				0-57.5	396	27.2		0.44	912	48.9	0.43	0.56	0.119
1508	67°00.0' S	32°21.5' W	4678	0-37.5	335	24.7	0.27		860	47.2	0.39	0.52	0.125
1508*				0-32.5	319	24.2		0.27	857	47.2	0.37	0.51	0.129
1508**				0-42.5	343	24.7		0.33	894	47.9	0.38	0.52	0.125
1509	66°00.3' S	37°22.1' W	4700	0-42.5	265	24.0	0.48		721	43.7	0.37	0.55	0.138

(*) and (**) are estimates based on radioisotope stratigraphy calculated in two different ways, first by assuming that the maxima in the radionuclide profiles at 37.5cm (1507) and 32.5cm (1508) represent the maximum productivity in isotope stage 5e (120ka;*), and second that the respective minima at 57.5cm and 42.5cm mark the boundary between isotope stage 6 and 5e (130ka;**). See text for details.

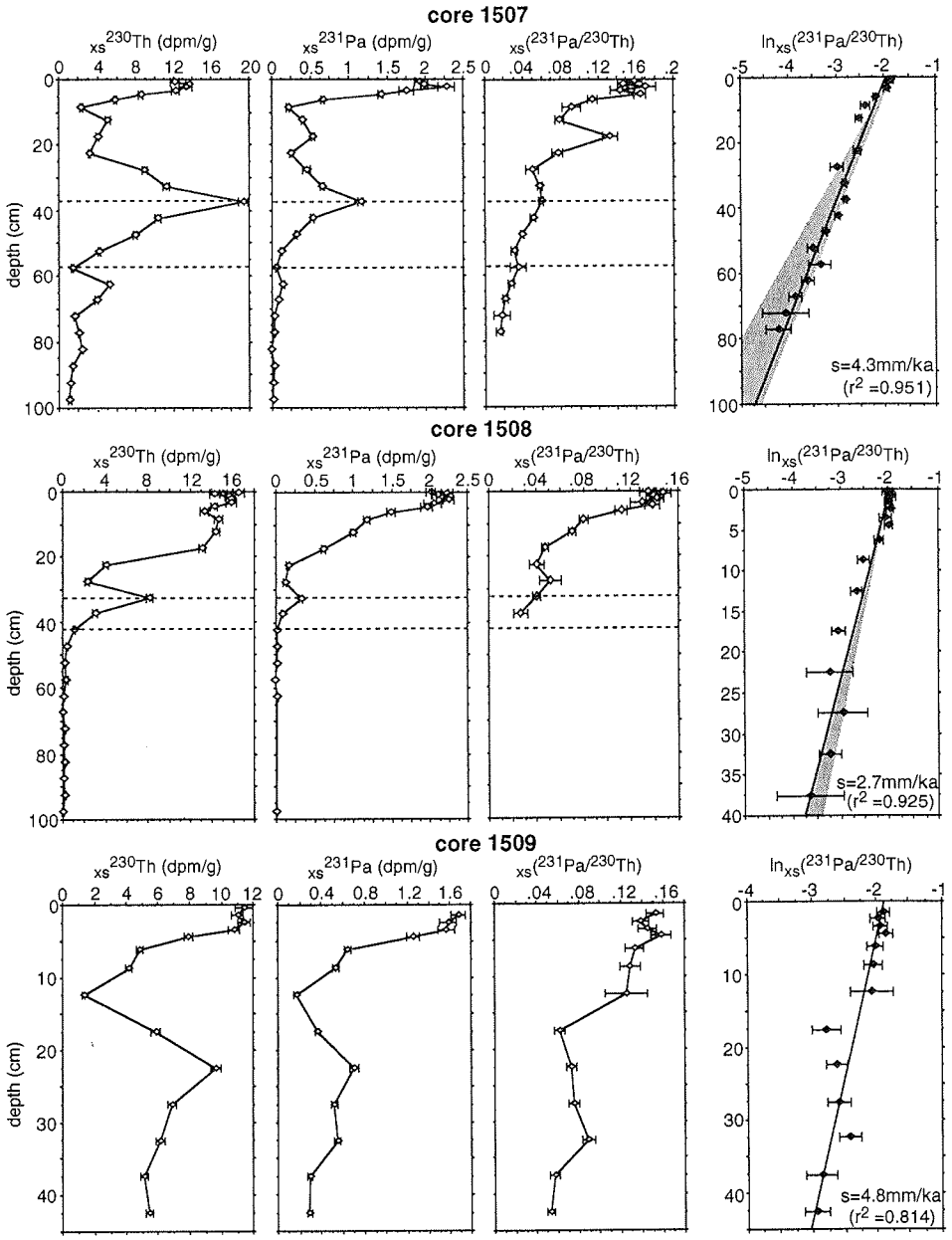

Fig.4-3: Plot of $_{xs}{}^{230}Th$, $_{xs}{}^{231}Pa$, and the $_{xs}{}^{231}Pa/_{xs}{}^{230}Th$ activity ratio of the sediment cores PS1507, PS1508 and PS1509 versus core depth. Average sediment accumulation rates were determined by the linear decrease of $ln(_{xs}{}^{231}Pa/_{xs}{}^{230}Th)$ with core depth (right row). The cores 1507 and 1508 were independently dated by radioisotope stratigraphy in two different ways (indicated by the stippled lines), first by assuming that the maxima at 37.5cm (1507) and 32.5cm (1508) represents the maximum productivity in isotope stage 5e (120ka, upper line), and second that the respective minima at 57.5cm and 42.5cm mark the boundary between isotope stages 6 and 5e (130ka, lower line). The shaded area represents the difference of the two radiostratigraphic approaches.

independent tool to determine average sediment accumulation rates in sediments of high latitudes where contents of biogenic carbonate are negligible.

In order to compare the results of the sediments with those of the traps, inventories (I_a [dpm/cm^2]) of $_{xs}^{230}$Th in each core were calculated by summing up to a depth x [cm] the product of $_{xs}^{230}$Th activity [dpm/g] and dry bulk density (D) [g/cm^3]. For $_{xs}^{231}$Pa the calculation is similar. These data are then compared with the expected inventories (I_e) of both radionuclides (Table 4-4), calculated from their theoretical flux (F_p) from the water column in time interval (t), corresponding to the depth x, according to the equation

$$I_e = \int_0^t F_p * \exp[-\lambda t]\, dt \qquad (7)$$

The salient feature in Table 4-4 is that for all cores the observed inventories of both ^{230}Th and ^{231}Pa are invariably low with only 33-43% and 47-55% of the expected values, respectively. Again, for the cores PS1507 and PS1508 the relatively good agreement of the two independent age determinations is documented by the similarity of the ratios I_a/I_e for both radionuclides. Extrapolated initial depositional $_{xs}^{231}$Pa/$_{xs}^{230}$Th ratios of 0.12-0.14 during the last 90-180ka are almost indistinguishable from the ratios measured in recent sediments (0.13-0.16).

4.5 Discussion

4.5.1 Seasonality in the flux of ^{230}Th and ^{231}Pa

In order to better understand the reasons for the high $_{xs}^{231}$Pa/^{230}Th ratios found in Southern Ocean's surface sediments south of the Polar Front, here the response of scavenging of ^{231}Pa and ^{230}Th to seasonal variations in particle flux and particle composition is investigated. From the sediment trap results it can be seen that fluxes of ^{231}Pa and ^{230}Th are closely coupled with the annual cycle of particle fluxes, with 75-95% of their annual fluxes occurring during short periods of high particle flux in austral summer, ranging in duration from 6 to 13 weeks (Fig.4-2). Radionuclide fluxes generally are linearly correlated with mass flux (Bacon et al., 1985; Lao et al., 1993; Colley et al., 1995). This correlation holds even under these extreme variations in particle flux. Correlation coefficients (R^2) for ^{231}Pa and ^{230}Th with mass flux for the individual moorings are 0.79-0.999 and 0.75-0.98, respectively, which implies that scavenging is not limited by the production rates of the two radionuclides in the water column.

Sediment traps deployed for at least one year in different oceanic settings with a 16-fold variation in particle flux between low an high productivity regions (Yu, 1994) have shown that annual fluxes of ^{230}Th change much less than those of ^{231}Pa in response to variations in annual particle flux, resulting in a strong positive correlation between $_{xs}^{231}$Pa/$_{xs}^{230}$Th and mass flux. If her findings are also valid on a shorter time scale (e.g. weeks), then particulate $_{xs}^{231}$Pa/$_{xs}^{230}$Th ratios during periods of high particle fluxes should strongly exceed those of low flux periods.

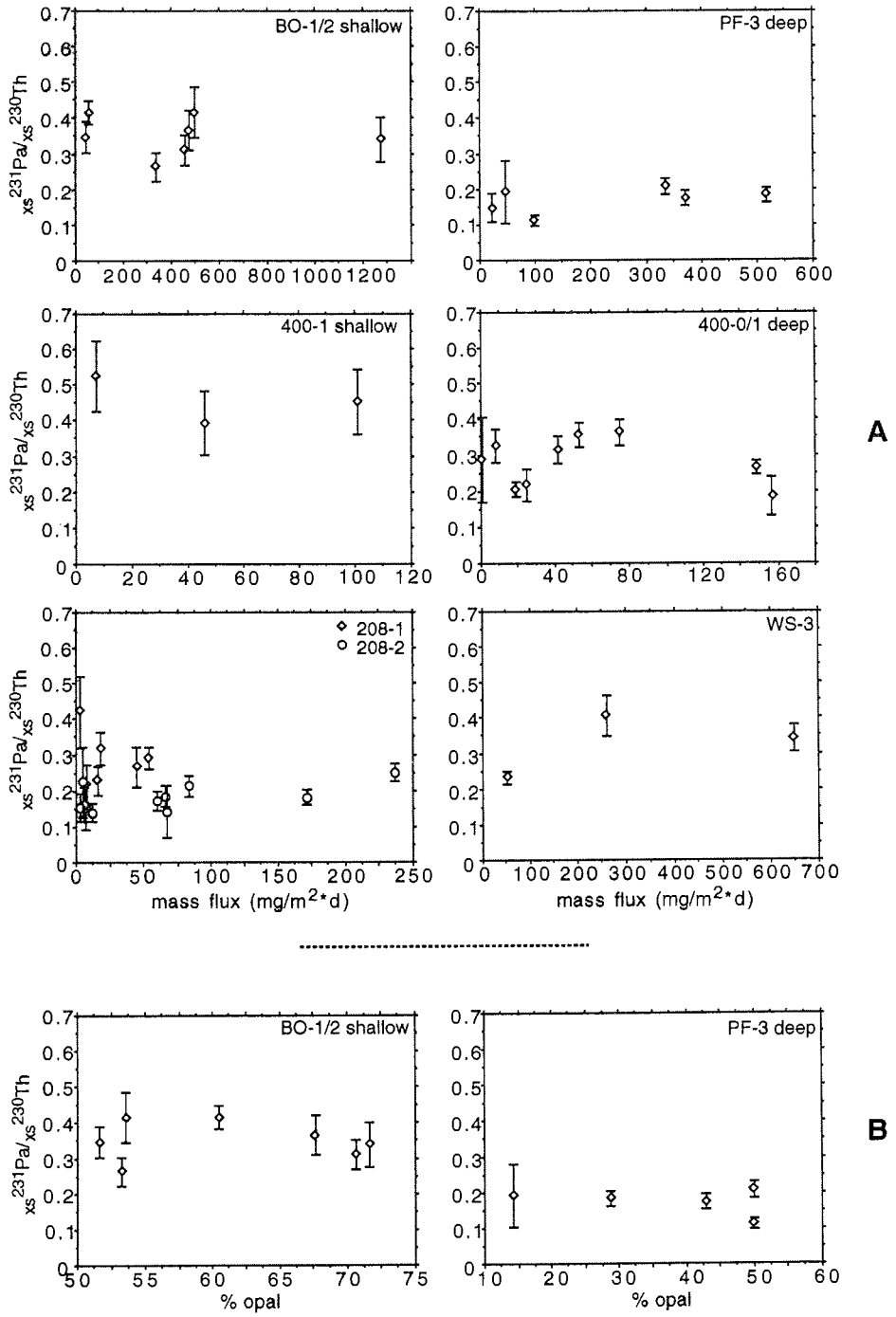

Fig.4-4: $^{231}Pa/^{230}Th_{xs}$ ratios (a) as a function of mass flux (upper 6 diagrams), and (b) as a function of the content of opal (lower 2 diagrams) of material collected in sediment traps.

However, such a relationship is not seen in our data (Fig.4-4 a). $_{xs}^{231}Pa/_{xs}^{230}Th$ ratios of the traps are independent from seasonal fluctuations in total mass flux. Additionally, we might expect a positive correlation of the particulate $_{xs}^{231}Pa/_{xs}^{230}Th$ ratio with increasing content of biogenic opal on sinking particles, but evidence for such a relationship was not found either (Fig.4-4 b).

4.5.1.1 Adsorption rates in the deep ocean

Fractionation between dissolved and particulate phases is believed to take place during adsorption to fine suspended particles, rather than during the seasonally varying aggregation process (Bacon and Anderson, 1982; Bacon et al., 1985; Nozaki et al., 1981; 1987). Consequently, enhanced scavenging of ^{231}Pa relative to ^{230}Th during a plankton bloom would require that both adsorption of the dissolved radionuclides on colloids and their subsequent coagulation to larger filterable particles (Honeyman and Santschi, 1989) is rapid on a seasonal time scale. We use the "dissolved" (<1µm) and "particulate" (>1µm) fractions of ^{230}Th and ^{234}Th, measured on a N-S transect across the ACC into the Weddell Sea during Polarstern expedition ANT XI/4, to calculate rate constants for adsorption (k_1) and desorption (k_2) [y^{-1}] for ^{230}Th in the deep South Atlantic (>1300m), by combining the following equations (Bacon and Anderson, 1982):

$$k_1 * Cd^{234} = (\lambda^{234} + k_2)\, Cp^{234} \qquad (8)$$

$$k_1 * Cd^{230} = k_2 * Cp^{230} \qquad (9)$$

where Cd and Cp are the dissolved and particulate activities of ^{234}Th and ^{230}Th, and λ^{234} is the radioactive decay constant of ^{234}Th (10.41 y^{-1}). Values for k_1 are 0.3-0.55 y^{-1} within the ACC north of 50°S, and decrease to the south by a factor of four, with lowest values around 0.1 in the Weddell Sea (Fig.4-5). According to the relationship between k_1 and the concentration of suspended matter (e.g. Bacon et al., 1982; Rutgers van der Loeff et al., 1997) the N-S decrease of k_1 implies a reduced particle concentration in the deep waters of the Weddell Sea compared to the ACC. Such a trend is not seen for k_2 with values ranging from 0.6 to 3 a^{-1} (Fig.4-5). These values of k_1 and k_2 correspond to a residence time of ^{230}Th with respect to adsorption on suspended particles of 1.8-10 years, and to a regeneration time of particulate Th of 0.3-1.6 years. Although for ^{231}Pa such a calculation cannot be made, k_1 and k_2 can be roughly estimated from the $^{230}Th/^{231}Pa$ fractionation factor (F), which in adsorption equilibrium is given by

$$F = \frac{(^{230}Th/^{231}Pa)_{part}}{(^{230}Th/^{231}Pa)_{diss}} = \frac{k_1}{k_2}(Th) \,/\, \frac{k_1}{k_2}(Pa) \qquad (10)$$

As values of F measured in the Southern Ocean are always >1 (Table 4-5), even throughout the Weddell Sea (Walter et al., 1997), and as we have no reason to assume that $k_2(Pa) > k_2(Th)$, we suggest that the adsorption rate constant for ^{231}Pa be slower than for ^{230}Th. Such long adsorption rates suggest that, at least in

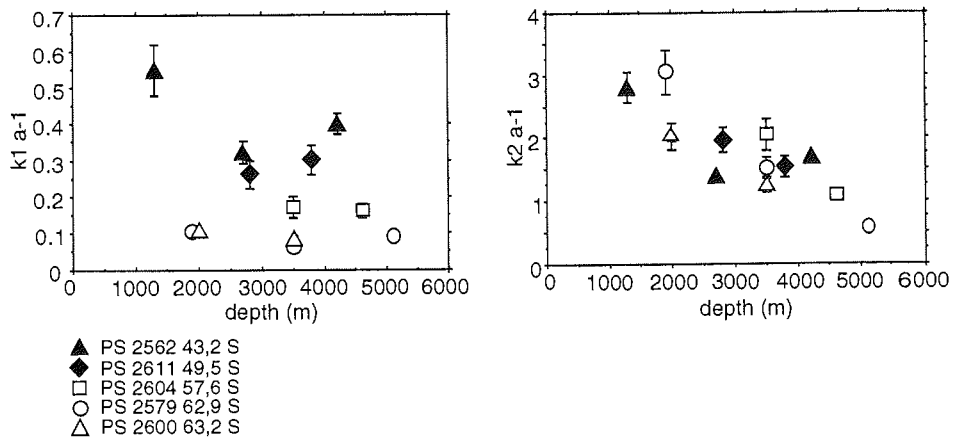

Fig.4-5: Average adsorption rate constants and desorption rate constants (d^{-1}) calculated according to Bacon and Anderson (1982) as a function of water depth and latitude north (filled symbols) and south (open symbols) of the Polar Front.

the deep South Atlantic, the $^{231}Pa/^{230}Th$ ratio cannot respond to fluctuations in mass flux and composition of particulate matter on a time scale of weeks to months.

4.5.1.2 Adsorption rates in the surface ocean

Reaction times are much faster in the surface ocean (e.g. Coale and Bruland, 1985; Bruland and Coale, 1986; Cochran et al., 1993; Guo et al., 1995). This has been well demonstrated by a study of Rutgers van der Loeff et al. (1997), carried out in the euphotic zone (upper 100m) of the South Atlantic (47-57°S). k_1 values for ^{234}Th during the development of an intensive plankton bloom increased from 0.0018 (d^{-1}) at the beginning of the bloom to 0.0298 (d^{-1}) at its maximum, corresponding to residence times of dissolved ^{234}Th with respect to uptake ranging from 1.5 years to 33 days. Using the argument given above for deep waters, these values can also be taken as minimum residence times of dissolved ^{231}Pa (assuming F >1). Although based on only a few data, these findings imply that the residence times of dissolved ^{231}Pa and ^{230}Th in the surface ocean during a plankton bloom are short enough to enable a high $^{231}Pa/^{230}Th$ signal on particles to be established. The $^{231}Pa/^{230}Th$ signal would then reflect both the high concentrations of particles and their high content of biogenic opal, often exceeding 70%. The constant high $^{231}Pa/^{230}Th$ ratio in the shallow traps throughout the year implies that desorption in low-flux periods (e.g. by mineralization of the organic matter) does not affect the $^{231}Pa/^{230}Th$ ratio of the bloom particles. Consequently, the residual particles would carry their high $^{231}Pa/^{230}Th$ signal from the spring bloom throughout the whole year, consistent with the sediment trap results (Fig.4-4 a,b). However, data on the residence times of dissolved and particulate ^{231}Pa and ^{230}Th in the euphotic zone during the development of a plankton bloom are needed to verify this speculation.

4.5.2 Change of the high $^{231}Pa/^{230}Th$ signature during transit through the water column

4.5.2.1 Continuous exchange with suspended particles

We now investigate how the high particulate $^{231}Pa/^{230}Th$ signal generated in the upper water column is likely to be transferred to the sediment. Two possible scenarios are considered: rapid transport without any modification of the bloom particles through the water column, and continuous exchange with radionuclide bearing phases in the deeper water column during their downward transport. Fig. 4-6 illustrates that the $^{231}Pa/^{230}Th$ ratios measured on suspended particles in the deep Southern Atlantic (Walter et al., 1997) generally are much lower (2-4 fold) than the ratios found in shallow sediment traps at similar latitudes. Consequently, any exchange of the bloom particles with suspended particles in the deeper water column would result in a lowering of their initial $^{231}Pa/^{230}Th$ signature. We do see such a trend at the sites PF, AWI-400 and KG, where the $^{231}Pa/^{230}Th$ ratios of material collected in the deeper traps are lower by almost a factor 2 than in the shallow traps (Fig.4-6). This observation implies that the particles found in the shallow traps do not make their way to the deeper water column without passing through several cycles of aggregation and disaggregation, by which material from the deeper water column is taken up. Our results thus corroborate earlier findings by Bacon et al. (1985), namely that the downward transport of the seasonal influence affects scavenging rates of ^{230}Th and ^{231}Pa both at the surface as well as at depth. Moreover, as concentrations of ^{230}Th and ^{231}Pa on suspended particles increase with water depth (e.g. Bacon and Anderson, 1982; Anderson et al., 1983a; 1983b), any exchange between the suspended and sinking particle reservoirs should be reflected by higher concentrations of ^{230}Th and ^{231}Pa of material collected in the deep traps compared to the shallow traps. As such a trend is seen at all moorings, this further constrains the conclusions drawn from the $^{231}Pa/^{230}Th$ ratios.

In order to verify the hypothesis of a continuous exchange of the bloom particles with deep suspended particles, we have compared the $^{231}Pa/^{230}Th$ ratios of the scavenging increment between upper and lower trap with the values measured on deep suspended particles. Because of the large uncertainty in the collection efficiency of the deep traps (see below), it is not possible to determine the $^{231}Pa/^{230}Th$ ratios of this incremental scavenging by comparing fluxes from the upper and lower trap. Alternatively, it can be estimated from differences in the concentrations of ^{230}Th and ^{231}Pa between upper and lower trap. Such an approach, however, requires that the bloom particles are not chemically altered during their downward transport in the water column. Incremental $^{231}Pa/^{230}Th$ ratios calculated in this way are higher than the respective ratios found on suspended particles (Table 4-5), which is in contrast to our expectations. This discrepancy can have two causes: First, the bloom particles might have experienced significant alteration, e.g. by remineralization of labile biogenic particles, which would cause an increase in the concentrations of ^{230}Th and ^{231}Pa on the remaining more resistent particles. Consequently, the values for the estimated scavenging increment must be considered as maximum values. Second, the data for the suspended particles which are all obtained from water depths >1900m are not representative for the shallower waters. This can be deduced from the increase with

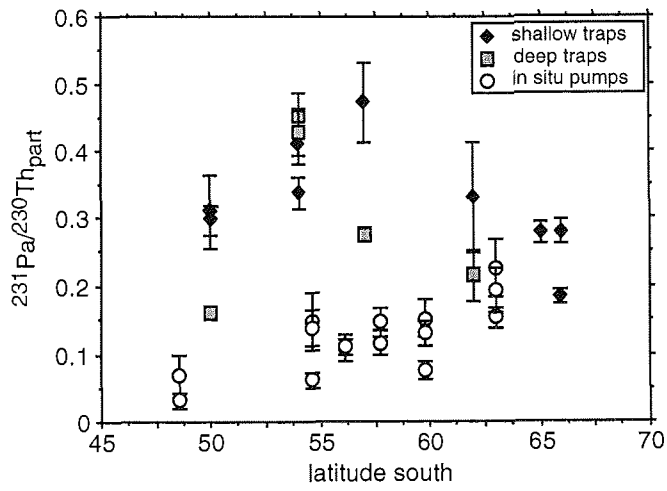

Fig.4-6: Comparison between $_{xs}^{231}Pa/_{xs}^{230}Th$ ratios of sinking particles collected in shallow and deep sediment traps, and suspended particles obtained by large volume filtration of seawater.

water depth of the $^{230}Th/^{231}Pa$ F-factor (Table 4-6), reflecting an increase in the scavenging preference of ^{230}Th over ^{231}Pa with increasing age (or alteration) of the suspended particles. Therefore, the $^{231}Pa/^{230}Th$ ratios of the suspended >1900m in table 4-5 must be regarded as minimum values for the shallower water depths. If we take into account these two sources of error in our simple approach (apart from the site BO, see below), deep scavenging can indeed be described as a continuous exchange of the bloom particles with the suspended particles during their downward transport in the water column.

Table 4-5: Comparison of $^{231}Pa/^{230}Th$ ratios of sediment trap material, suspended particles, and surface sediments, and estimated $^{231}Pa/^{230}Th$ ratios for the scavenging increment between upper and lower trap.

site	depth m	$_{xs}^{230}Th$ dpm/g	$_{xs}^{231}Pa$ dpm/g	sinking particles >1900m	suspended particles	surface sediments	incremental scavenging
PF 3	614	0.191 ± 0.009	0.057 ± 0.003	0.298 ± 0.021	0.07 - 0.10	0.08 - 0.10	0.13
	3196	1.148 ± 0.036	0.186 ± 0.009	0.162 ± 0.010			
BO 1	450	0.081 ± 0.003	0.028 ± 0.002	0.339 ± 0.023	0.13 - 0.15	0.24 - 0.26	0.43
	2194	0.338 ± 0.010	0.153 ± 0.009	0.454 ± 0.030			
BO 2	456	0.235 ± 0.013	0.097 ± 0.005	0.411 ± 0.032	0.13 - 0.15	0.24 - 0.26	0.49
	2183	0.523 ± 0.027	0.222 ± 0.013	0.425 ± 0.033			
400/1	450	0.336 ± 0.025	0.159 ± 0.016	0.472 ± 0.058	0.12 - 0.15	0.13 - 0.18	0.23
	3048	1.389 ± 0.052	0.411 ± 0.022	0.296 ± 0.019			
KG 1	494	0.213 ± 0.044	0.070 ± 0.011	0.330 ± 0.082	?	?	0.16
	1588	0.683 ± 0.105	0.148 ± 0.013	0.217 ± 0.038			

Table 4-6: Dissolved and particulate $_{xs}^{231}Pa/_{xs}^{230}Th$ ratios, and $^{230}Th/^{231}Pa$ F-factors of water column samples (taken from Walter et al., 1997, and unpublished results "*").

station	latitude	longitude	water depth	depth	($^{231}Pa/^{230}Th$) dissolved	($^{231}Pa/^{230}Th$) particulate	$^{230}Th/^{231}Pa$ F-factor
PS 2262	48° 30.1' S	37° 00.3' W	5396	2500	0.461 ± 0.039	0.070 ± 0.029	6.62 ± 2.77
				4500	0.312 ± 0.022	0.032 ± 0.011	9.73 ± 3.40
PS 2276	54° 38.1' S	23° 57.3' W	4450	2000	0.272 ± 0.017	0.147 ± 0.042	1.85 ± 0.54
				3000	0.344 ± 0.031	0.139 ± 0.026	2.48 ± 0.52
				4000	0.348 ± 0.023	0.061 ± 0.011	5.75 ± 1.11
PS 2359	56° 09.1' S	15° 25.5' W	4887	3000	0.35 ± 0.021	0.108 ± 0.019	3.24 ± 0.59
				4000	0.383 ± 0.022	0.110 ± 0.012	3.49 ± 0.43
PS 2360	57° 44.7' S	06° 28.6' W	3480	2000	0.293 ± 0.024	0.146 ± 0.022	2.02 ± 0.35
				3000	0.336 ± 0.019	0.116 ± 0.018	2.88 ± 0.49
PS 2283	59° 44.1' S	23°16.5' W	4766	2000	0.261 ± 0.016	0.152 ± 0.029	1.71 ± 0.34
				3000	0.272 ± 0.015	0.076 ± 0.014	3.60 ± 0.70
				4000	0.226 ± 0.019	0.130 ± 0.019	1.74 ± 0.29
PS 2579	62° 57.8´ S	07° 46.4´ E	5324	1900	0.293 ± 0.025	0.225 ± 0.043	1.30 ± 0.27
				3500	0.293 ± 0.021	0.193 ± 0.033	1.52 ± 0.28
				*5100	0.280 ± 0.018	0.153 ± 0.014	1.83 ± 0.21

4.5.2 2 Speciality of the mooring site BO

BO is different from all other mooring sites, as the $^{231}Pa/^{230}Th$ signal measured in the deep traps is similar to those in the upper traps (Table 4-2). Estimated $^{231}Pa/^{230}Th$ ratios for the incremental scavenging calculated from the difference in concentrations between upper and lower trap are extremely high with values >0.4 (Table 4-5), far higher than those found on suspended particles (0.15) at nearby pumping stations. This makes a continuous exchange of the bloom particles with suspended particles from the deeper water column, as observed for the other mooring sites, unlikely. As the increase with depth in the concentration of ^{231}Pa and ^{230}Th on particles, in addition to uptake of deeper suspended particles, may also result from mineralization or dissolution of labile biogenic components, the similarity of the $^{231}Pa/^{230}Th$ ratios in the deep and shallow trap might rather reflect lack of uptake of the bloom particles of suspended particles during sinking. This would imply that the primary surface signal has survived down to the deep ocean. Such an interpretation is further supported by the very high $^{231}Pa/^{230}Th$ ratios found in nearby surface sediments of 0.25-0.26, among the highest ever observed in the Southern Ocean (Kumar et al., 1995; Yu et al., 1996; Walter et al., 1997). The occurrence of material in the size fraction >1mm (probably reflecting remnants of large aggregates; Fischer, pers. comm.), might indeed indicate accelerated sinking at this location. However, since there is no evidence for a larger contribution of ^{231}Pa from the upper water column to the sediment than at the other trap sites (see last chapter), further investigation is needed to better understand the unusually high $^{231}Pa/^{230}Th$ signature of particles trapped in deep waters at this site.

4.5.2.3 Discrepancy in $^{231}Pa/^{230}Th$ ratio between deep traps and surface sediments

The $^{231}Pa/^{230}Th$ ratios in surface sediments at all mooring sites are still lower than the values measured in the deep traps (Table 4-5), suggesting continued exchange of the already altered bloom particles with suspended particles of a more and more increased scavenging preference of ^{230}Th over ^{231}Pa with water depth. Consequently, when the final particles reach the sea floor, their original high $^{231}Pa/^{230}Th$ signature from the surface ocean is strongly diminished, although values still exceed the production ratio of 0.093. Additionally, some ^{231}Pa may be released during dissolution of opal at the seafloor. This continuous modification of the primary $^{231}Pa/^{230}Th$ signal in the water column and probably at the sediment surface does not allow a reliable prediction of depositional fluxes and of initial $^{231}Pa/^{230}Th$ ratios to be made from sediment traps deployed in the upper water column, where the influence of the primary high productivity signal is overwhelming.

4.5.3 Regional variability in the flux of ^{230}Th and ^{231}Pa in the water column

Total annual mass fluxes measured in sediment traps span a wide range from >100 g/m²/y in the Bransfield Strait, through 54-67 g/m²/y within the ACC, to 7-15 g/m²/y in the Weddell Sea (Table 4-2). The high mass flux measured near Maud Rise of 33.8 g/m²/y cannot be taken as representative for the Weddell Sea because of its local high bioproductivity, related to doming of warm deep water forming the Maud Rise polynya (Comiso and Gordon, 1987). According to the relationship between mean annual particle flux and mean annual radionuclide flux (Lao et al., 1993; Yu, 1994), as well as from the southward enrichment of the concentrations of ^{230}Th and to a lesser extent of ^{231}Pa in the water column (Rutgers van der Loeff and Berger, 1993), we should expect large regional differences in the flux of ^{231}Pa and ^{230}Th. As the traps were not deployed in the same water depth, we use the annual fluxes of ^{230}Th and ^{231}Pa normalized to their respective production rates, $F_a/F_p(Th)$ and $F_a/F_p(Pa)$, (Table 4-2), in order to compare regional radionuclide fluxes. As expected from the high mass flux, highest scavenging rates are documented from the mooring deployed at KG, with F_a/F_p ratios of 1.8 for ^{230}Th and 4.3 for ^{231}Pa, implying a strong boundary scavenging effect, much more pronounced for ^{231}Pa than for ^{230}Th (Lao et al., 1992a; 1992b; 1993; Anderson et al., 1994). Within the ACC (sites PF and BO), F_a/F_p ratios are lower with only 0.4-0.7 for ^{230}Th and 1.3-2.2 for ^{231}Pa. At Maud Rise, F_a/F_p ratios for ^{230}Th (0.85) and ^{231}Pa (2.6) strongly exceed the values measured in the Central Weddell Sea, with only 0.31-0.42 and 0.85-0.94, respectively.

The shortfall in collection of ^{230}Th in the ACC and in the Weddell Sea is in contrast to the results obtained from a recent compilation of a large number of sediment traps deployed in various oceanographic settings (Francois, 1990; Yu, 1994). These authors found that the F_a/F_p ratio for ^{230}Th is almost independent from the total mass flux of particles, ranging from 0.9 at the lowest annual mass fluxes measured of only 10mg/m²/y, to a maximum of 1.5 in high particle flux regions with annual fluxes far above 100mg/m²/y. Hence, according to Yu's findings, at the mass

fluxes measured in the Weddell Sea (7-15mg/m^2/y) and in the ACC (54-67mg/m^2/y), strongly reduced scavenging of ^{230}Th should not be expected. Moreover, the ACC receives a large amount of ^{230}Th advected from the north with NADW (Yu et al., 1996), so that we might expect that scavenging of ^{230}Th in this high particle flux region would rather exceed its production rate ($F_a/F_p>1$).

4.5.3.1 Evaluation of sediment trap collection efficiencies

It is now to be investigated to what extent the low F_a/F_p ratios for ^{230}Th found in traps within the ACC and in the Weddell Sea may result from undertrapping of the downward flux of ^{230}Th. Unfortunately, the model for quantifying sediment trap efficiencies by combining information on ^{231}Pa/^{230}Th ratios both in the water column and on settling particles (Bacon et al., 1985) is not applicable in the Southern Ocean, because of the strong N-S advection of NADW (Francois et al., submitted). Therefore, only a qualitative assessment of possible collection biases at the mooring sites can be given. Monthly averaged current velocities measured at site PF are high reaching values of more than 10cm/s in the upper 300m and up to 8cm/s in 600-700m (Fig.4-7; Fahrbach and Rohardt, pers. comm.). Current speeds at this magnitude may introduce a hydrodynamic bias to the collection of fast-settling particles in the shallow sediment traps (Baker et al., 1988; Gust et al., 1994). Similar current velocities have been measured close to the ACC/Weddell Boundary (AWI-400) and near Maud Rise (WS-3), so that a current-induced bias in the trap efficiency for the shallow traps at all these sites cannot be excluded. Strong undertrapping might also explain the extremely low F_a/F_p ratios observed in the deep traps at BO (0.16?) and AWI-400 (0.18), far lower than the values in the upper traps, although monthly averaged current velocities decrease with increasing water depth (Fig.4-7).

At all other mooring sites, however, a current-induced bias in the collection efficiency is not expected to be large, since current velocities are much lower (Fig.4-7, KG-1; Fischer, pers. comm.), with lowest values (<2.5cm/s) recorded from the traps deployed in the center of the Weddell Gyre (AWI-208). Therefore, the low F_a/F_p ratios of 0.4 found in the Central Weddell Sea imply a reduced scavenging efficiency of ^{230}Th. From the relationship between F_a/F_p ratio and mass flux (Yu, 1994), we should not expect a value far below 0.9. However, our low F_a/F_p ratios of 0.4 can be understood by considering that the mean residence time of water in the Weddell Gyre is only 35 years (Rutgers van der Loeff and Berger, 1993), comparable to the scavenging residence time for ^{230}Th, so that a large amount of the ^{230}Th produced in the Weddell Sea is not deposited there, but is exported to other regions by horizontal advection.

Although further investigation is needed until a reliable estimate of trap efficiencies in the Southern Ocean can be made, for the remainder of the discussion we assume that the traps deployed in the Bransfield Strait and in the Central Weddell Sea (AWI-208) have a collection efficiency of about 100%, whereas those moored at the Polar Front, at Bouvet and at Maud Rise undertrap the downward flux of particles, so that their calculated F_a/F_p ratios must be regarded as minimum values. As we do not have an explanation for the extremely low F_a/F_p ratios found in the

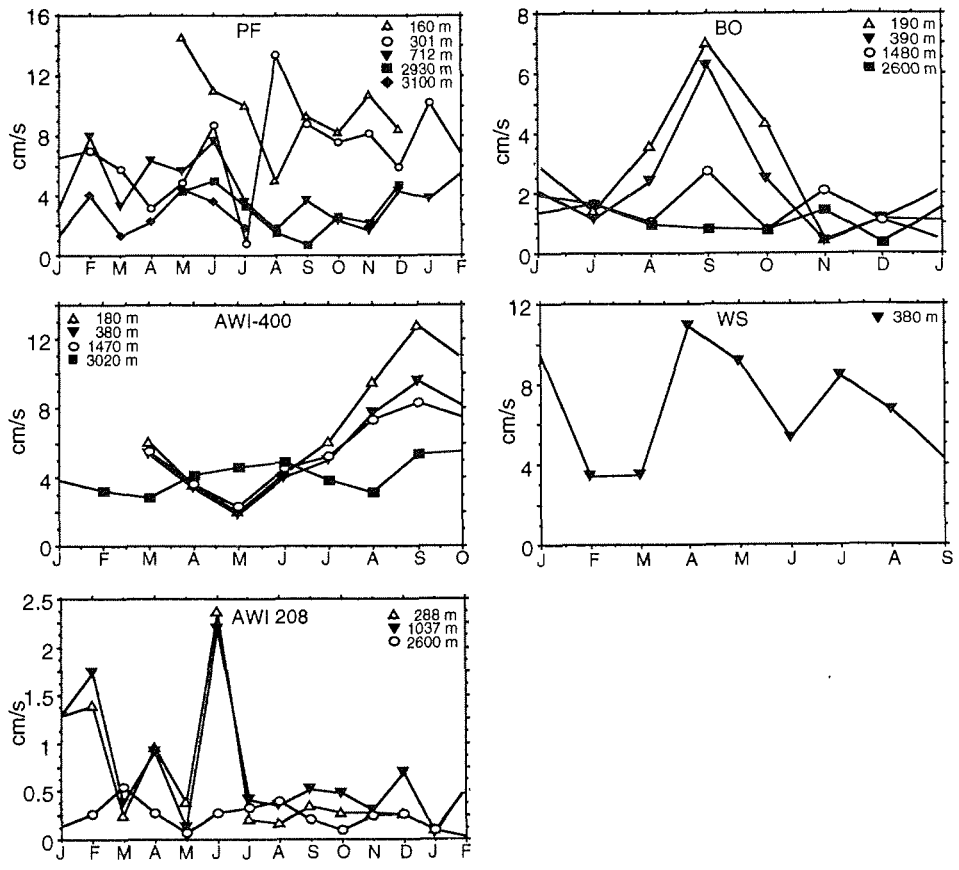

Fig.4-7: Monthly averaged current speeds measured in different water depths at the respective trap moorings (Fahrbach and Rohardt, unpublished data).

deep traps at Bouvet and AWI 400, these data are not used in the following interpretation.

4.5.3.2 Sources and sinks of ^{231}Pa and ^{230}Th

The sediment trap fluxes measured in the upper water column (<1100m) of the Southern Ocean thus imply, that the ACC is a strong sink for ^{231}Pa, especially if we take into account that the values for $F_a/F_p(Pa)$ of 1.3-2.2 measured at the Polar Front and at Bouvet are lower limits. This interpretation is consistent with the stong advective import of dissolved ^{231}Pa into the ACC derived from the Atlantic (Yu et al., 1996), and by the high ^{231}Pa inventories found in sediments underlying the ACC (DeMaster, 1979). In contrast, the low Fa/Fp ratios in the Central Weddell of ^{230}Th (<40%), and to a lesser extent for ^{231}Pa (<90%), show this region to be a strong source for ^{230}Th and a small source for ^{231}Pa. Within the Weddell Sea, the Maud Rise polynya is a local sink for ^{231}Pa and probably also for ^{230}Th. The very high

F_a/F_p ratios for ^{231}Pa >4 and ^{230}Th >1.6 in the Bransfield strait show that this local high productivity area is a strong sink for both radionuclides, and thus behaves as a typical ocean margin (e.g. Anderson et al., 1983b; 1990; 1994; Lao et al., 1992a; 1992b).

4.5.4 The Weddell Sea, a source for ^{230}Th and ^{231}Pa: Evidence from sediment traps and long-term sediment record

Previous authors have interpreted the high $_{xs}^{231}Pa/_{xs}^{230}Th$ ratios far above their production ratio of 0.093, found in sediments of the Southern Ocean, as evidence for enhanced scavenging of ^{231}Pa, which would make this region an important sink for the deposition of ^{231}Pa transported by advection with NADW (DeMaster, 1979; Yu et al., 1996). This assumption is reasonable in the ACC, where particle fluxes are high (Table 4-2), so that scavenging of ^{230}Th is expected to be equal or even higher than its local rate of production in the water column (DeMaster, 1979; Yu et al., 1996). However, south of the ACC/Weddell Gyre boundary where particle fluxes are much lower, a high $_{xs}^{231}Pa/^{230}Th$ signal in the sediment does no more necessarily mean that scavenging of ^{231}Pa is enhanced, which is illustrated by the sediment cores investigated from the Central Weddell Sea (Table 4-4). Despite their high $^{231}Pa/^{230}Th$ ratios of 0.12-0.14, averaged over the last 90-180ka, inventories of ^{230}Th and ^{231}Pa in this time interval only reach 33-43% and 47-55% of their expected inventories from production in the water column, respectively (remember that 40% and 87% of their respective production were found in the sediment traps). These findings suggest that the Weddell Sea is a net source for both radionuclides. This implies that over the last 180ka about half of the ^{230}Th and ^{231}Pa produced in the Weddell Sea must have been advected to other regions of the Southern Ocean prior to scavenging, where particle fluxes are much higher, such as the ACC (Table 4-2).

For ^{230}Th, the long-term results coincide with those of the three year sediment trap deployment (site 208) at 1000m water depth (40% of the production), whereas for ^{231}Pa, the trap values (87% of the production) are higher. As we have seen above, the high $^{231}Pa/^{230}Th$ signal at 1090m is altered during downward transport in the water column by continuous uptake of particles with an increased scavenging preference of ^{230}Th over ^{231}Pa. Based on the measured fluxes at 1090m, the $_{xs}^{231}Pa/^{230}Th$ ratio in the surface sediment of 0.15 (core 1508) yields upper and lower limits for the fluxes of ^{230}Th ($40\%<x<74\%$) and ^{231}Pa ($46\%<x<87\%$), respectively, to the seafloor. If the change in the scavenging efficiency with water depth is much less pronounced for ^{230}Th than for ^{231}Pa, then the depositional fluxes of both radionuclides are close to the lower limit and thus are in very good agreement with the sediment record.

Our results agree with those of an earlier study carried out in the Eastern Weddell Sea by Rutgers van der Loeff and Berger (1993), which was based on the water column enrichments of ^{230}Th and ^{231}Pa in the Eastern Weddell Sea. The authors explained the reduced scavenging rate of ^{230}Th by the short mean residence time of water in the Weddell Gyre of 35 years, comparable to the scavenging residence time of ^{230}Th. As the scavenging residence time for ^{231}Pa in the Weddell Sea is

similar to that of ^{230}Th, as can be deduced from the measured values of F between 1 and 2 (Walter et al., 1997), the findings of Rutgers van der Loeff (1993) may also account for the low scavenging rates for ^{231}Pa. Their modeling makes the deposition rate of ^{230}Th, and to a lesser extent of ^{231}Pa, sensitive to changes in the circulation time of water in the Weddell Gyre, that may have occurred in the past. E.g., a much longer residence time of water in the gyre during glacial times, as might have resulted from a strongly reduced formation rate of Weddell Sea deep waters, would, despite the low particle fluxes, possibly allow more ^{230}Th and ^{231}Pa to be deposited in the Weddell Sea. The low concentrations of ^{230}Th and ^{231}Pa during glacials, and the low mean ^{230}Th and ^{231}Pa inventories in the sediment cores suggest that over most of the last 180ka the circulation pattern cannot have deviated that much from that of the modern Weddell Sea.

4.5.4.1 Implications for the use of the ^{230}Th constant flux model in the Southern Ocean

The reduced scavenging efficiency of ^{230}Th in the Weddell Sea also has consequences for the calculation of vertical rain rates based on the ^{230}Th constant flux model. For a description of this model see Bacon (1984) and Suman and Bacon (1989). Briefly, it is assumed that the flux of ^{230}Th to the seafloor within a basin is constant and equals its rate of production from ^{234}U in the water column. The activity of $_{xs}^{230}Th$ in the surface sediment is then inversely proportional to the total mass flux, and decay corrected $_{xs}^{230}Th$ can be used as a reference against which the flux of other sedimentary components can be estimated. According to this model, the low ^{230}Th inventories (33-43%) in the Weddell Sea cores would be regarded as evidence for strong sediment winnowing at this location (57-67% of their original inventary being deposited elsewhere), so that ^{230}Th-normalized vertical rain rates of sedimentary components like C_{org}, biogenic opal or biogenic Ba, would be overestimated by up to a factor of 3. On the other hand, enhanced burial fluxes of ^{230}Th (>100% of its production), as assumed for the ACC, which receives a large amount of ^{230}Th advected from the Atlantic and probably from the Weddell Sea, would be regarded as indication for sediment focussing and would thus lead to underestimate vertical rain rates. Consequently, we suggest that in the Southern Ocean the application of the ^{230}Th constant flux model is limited not only in the Weddell Sea, but also in the ACC.

4.5.5 Shallow vs. deep scavenging of ^{230}Th and ^{231}Pa

As we have seen above, the $^{231}Pa/^{230}Th$ signal buried in sediments of the Southern Ocean contains both a high $^{231}Pa/^{230}Th$ bloom component (>0.3) generated in the upper water column during short plankton blooms, and a lower $^{231}Pa/^{230}Th$ component from the deep ocean (<0.2, dependent on water depth and latitude, see Table 4-6), represented by the suspended particles. An increase with latitude in the contribution of the bloom component, as might result from the strong increase in the concentrations of ^{230}Th and ^{231}Pa in surface waters (Rutgers van der Loeff and Berger, 1993), could thus explain the N-S increase in the $_{xs}^{231}Pa/_{xs}^{230}Th$ of sediments south of the Polar Front. In order to test this hypothesis, annual fluxes of

^{230}Th and ^{231}Pa in the shallow traps were normalized to a constant water depth of 700m (normalized flux = measured flux/mooring depth * 700m). These values were then compared with expected fluxes to the sediment, calculated from production in the water column (in the Weddell Sea 40% of this value). Such a N-S trend in the surface contribution of the fluxes of ^{230}Th and ^{231}Pa to the sediment is not seen (Table 4-7). Instead, contributions for ^{230}Th are more or less independent from latitude, whereas for ^{231}Pa highest values are observed in the ACC at PF-1 (50°S) with up to 40% of the flux to the seafloor produced in the upper 700m. Note, that the estimated sediment contributions for the sites in the ACC (PF, BO) may be biased to some extent because of the uncertainty in the trap efficiency and in the depositional flux of ^{230}Th in this region. Despite the high surface concentrations, in the Weddell Sea, the export rates of ^{231}Pa from the upper 700m only amount to about 20% of the expected flux to the sediment. Hence, the salient result of this rough estimate is that, throughout the Southern Ocean, the sediment seems to receive a more or less constant contribution of ^{230}Th and ^{231}Pa from the surface ocean. This observation leads us to conclude that it is not the episodic export of ^{230}Th and ^{231}Pa from the surface ocean by fast sinking particles carrying a high ^{231}Pa/^{230}Th signal that accounts for the latitudinal gradient of the $_{xs}^{231}$Pa/$_{xs}^{230}$Th ratio of surface sediments. It is more likely explained by the N-S increase in the ^{231}Pa/^{230}Th ratio of the standing stock of suspended particles (Table 4-5), which is the major source of ^{230}Th and ^{231}Pa to the sediment with contributions >700m water depth of >80% and >60%, respectively, as deduced from Table 4-7.

Table 4-7: Export rates of ^{230}Th and ^{231}Pa from the upper water column (0-700m), and their estimated contributions to the sediment at the trap sites arranged in order of latitude

site	latitude south	700m normalized flux		expected flux		estimated sediment contribution from <700m	
		^{230}Th dpm/m^2/y	^{231}Pa dpm/m^2/y	^{230}Th dpm/m^2/y	^{231}Pa dpm/m^2/y	^{230}Th %	^{231}Pa %
PF-1	50°09.0'	6.9*	2.2*	95	8.8	7	24
PF-3	50°07.6'	11.8*	3.5*	94	8.8	12	40
BO-1	54°20.6'	8.7*	2.9*	69	17.1	13	17
208-1	65°56.2'	5.5	1.6	52	7.1	13	24
208-2	65°56.2'	7.5	1.4	52	7.1	17	21
WS-3	64°54.1'	15.0	4.2	127	19	12	22

* uncertainties in trap efficiency and depositional flux of ^{230}Th are not considered. Expected fluxes for ^{230}Th were calculated from production in the water column, assuming a scavenging rate of 100% (except for the site 208 of only 40%). For ^{231}Pa expected fluxes are calculated as follows:

$^{231}Pa_{exp} = {}^{230}Th_{exp}/0.093 * {}_{xs}^{231}Pa/{}_{xs}^{230}Th$ sediment

We have recently shown (Walter et al., 1997), that the increase in the particulate ^{231}Pa/^{230}Th ratio with latitude results from a N-S decrease in the ^{230}Th/^{231}Pa F-factor, which we related to a corresponding increase in the opal content of sinking particles. Here we show (Table 4-3) that the opal content of sinking particles collected in the shallow traps increase from 40-47% at the Polar Front (50°S) to 70% in the Weddell Sea (65°S). Moreover, apart from the mooring Bouvet, opal

contents of sinking particles collected in the deep traps are 20% lower compared to those in the upper traps (sites PF-3 and KG-1, Table 4-3). This observation implies that the suspended particles taken up in the deeper water column must be chemically different from the initial bloom particles. Probably these deep suspended particles represent ancient bloom particles, that have experienced dissolution of opal in the water column (Leynaert et al., 1993). Continuous reequilibration between sinking particles, suspended particles and the dissolved phase could thus account for the observed increase in the $^{230}Th/^{231}Pa$ F-factor with water depth (Table 4-6).

These new data add to the argument that the N-S decrease of the F-factor is likely to reflect an increased portion of opal on suspended particles with latitude. Consequently, episodic aggregation of the suspended particles from this large reservoir, triggered by short events of high particle flux in the euphotic zone, could explain the high $_{xs}^{231}Pa/_{xs}^{230}Th$ ratios found in sediments south of the Polar Front, rather than an increased export from the upper ocean, which was shown to generate an insufficient flux.

4.6 CONCLUSIONS

In the Southern Ocean, fluxes of ^{231}Pa and ^{230}Th measured in sediment traps are closely coupled with the annual cycle of particle fluxes, with 75-95% of their annual fluxes occurring during short periods of high particles fluxes in austral summer, ranging in duration from 6-13 weeks. Enhanced scavenging of ^{231}Pa relative to ^{230}Th during the bloom, caused by the high particle flux and the high content of biogenic opal, is reflected by extremely high mean $_{xs}^{231}Pa/_{xs}^{230}Th$ ratios (0.28-0.46) of sinking particles collected in the shallow sediment traps. Lack of reequilibration of these bloom particles with the dissolved phase during low flux periods is suggested to explain the invariability of the $_{xs}^{231}Pa/_{xs}^{230}Th$ ratio in the shallow traps with seasonal changes in mass flux and composition of particles.

A comparison of both the concentrations of ^{231}Pa and ^{230}Th and the $_{xs}^{231}Pa/_{xs}^{230}Th$ ratios of shallow and deep traps indicates that the particles collected in the deep traps do not represent particles from the upper ocean that have settled through the water column without modification. Rather, during their downward transport in the water column, the bloom particles continuously exchange with suspended particles from the deeper ocean, so that their $_{xs}^{231}Pa/_{xs}^{230}Th$ signature at every depth reflects an integrated signal from the overlying water column. The particles suspended in the deep waters have obtained their lower $^{231}Pa/^{230}Th$ signature by equilibration with the dissolved phase during their long residence time in the water column. Consequently, until a particle reaches the sea floor, its high initial $_{xs}^{231}Pa/_{xs}^{230}Th$ signature from the surface ocean is strongly diminished.

In the Weddell Sea scavenging rates of ^{230}Th and ^{231}Pa are strongly reduced. The long-term sediment record for the Central Weddell Sea integrating over the last 180ka agrees well with the 3 year sediment trap deployment, which implies that the Weddell Sea is a net source for ^{230}Th and ^{231}Pa. The low average depositional fluxes for ^{230}Th (33-43%) in the cores limit here the application of the ^{230}Th constant

flux model to predict vertical rain rates of biogenic components in the past. This may also hold for the ACC, where fluxes of ^{230}Th and ^{231}Pa are predicted to surpass their production rates in the water column. Strong boundary scavenging is manifested in the Bransfield Strait with 45% of ^{230}Th and 77% of the ^{231}Pa supplied by lateral transport.

Lack of a southward increasing export of ^{230}Th and ^{231}Pa from the upper water column (700m) makes the upper ocean unlikely as a significant source to account for the high $_{xs}^{231}Pa/_{xs}^{230}Th$ ratios observed in sediments south of the Polar Front. Rather, these are explained by the N-S increase in the $^{231}Pa/^{230}Th$ ratio of suspended particles in the entire water column, presumably caused by an increased content of opal. Despite the extreme seasonality and the strong advective enrichment of radionuclides in the upper water column, even in the Southern Ocean the deep water is found to be the major source of ^{230}Th and ^{231}Pa to the sediment.

5 Acknowledgements

First of all, I would especially like to thank my supervisor Michiel Rutgers van der Loeff. This work would have never been completed in this form without his constant support, his creative ideas, and his encouragement throughout the last three years. Discussions with Michiel were always exciting and encouraging. Many of the scientific ideas were created during our numerous running excursions.

I would also like to thank Prof. Dieter Fütterer for his support and for his confidence in our small geochemistry group. He promoted writing of the thesis in this cumulative form and provided the first expert opinion. Special thanks go to Prof. Augusto Mangini (Heidelberger Akademie der Wissenschaften) for the second expert opinion.

Heike Höltzen is acknowledged for teaching me all she knows about sample preparation procedures, her patience, and her constant help in the lab. She provided me with encouragement during the writing of this thesis and made everyday work a pleasant experience.

I am grateful to Roger Francois (Department of Marine Chemistry and Geochemistry, Woods Hole) for providing radionuclide data of Holocene sediments from the equatorial Pacific, and for his constructive comments on the review article (chapter 3). Gerhard Fischer (Fachbereich Geowischenschaften, Universität Bremen) and Ulrich Bathmann are thanked for the sediment trap material, and for the unpublished data on mass fluxes and chemical composition of the sinking particles. Eberhard Fahrbach and Gerhard Rohardt supplied the current data. Bernhard Dieckmann carried out grain size analyses of the sediment cores. Gerhard Kuhn provided the data on dry bulk density of the cores. I would also like to thank Andreas Michel for his assistance on expedition ANT IX/3, and Michael Schlüter for deploying the in-situ-pumps on expedition ANT X/5. Thanks also go to Walter Geibert for his help with the radiochemical analyses.

I am very much indebted to the captains and crews of RV Polarstern. Without their help the comprehensive data set of this study would never have been obtained.

This work also benefitted from the constructive reviews of the manuscripts by Jan Scholten (Geologisch-Paläontologisches Institut der Universität Kiel), Bradley Moran (Graduate School of Oceanography, University of Rhode Island), Bob Anderson (Lamont-Doherty Earth Observatory of Columbia University) and Mike Bacon (Department of Marine Chemistry and Geochemistry, Woods Hole).

Finally I wish to thank all the collegues in the departments of geochemistry and chemistry.

References

Abelmann, A. and Gersonde, R. (1991): Biosiliceous particle flux in the Southern Ocean. Mar. Chem. 35, 503-536.

Altabet, M.A. and Francois, R. (1994): The use of nitrogen isotopic ratio for the reconstruction of past changes in surface ocean nutrient utilization. In: Carbon Cycling in the Glacial Ocean: Constraints on the Ocean's Role in Global Change. Zahn, R., Pedersen, T.F., Kaminski, M.A. and Labeyrie, L. (eds.). NATO ASI Series, Vol. 17, 281-306.

Anderson, H.L., Francois, R. and Moran, S.B. (1992): Experimental evidence for differential adsorption of Th and Pa on different solid phases in seawater. EOS 73 no. 43S: 270.

Anderson, R.F. (1981): The marine geochemistry of thorium and protactinium. Ph.D. Thesis. WHOI, Woods Hole, MA, 287pp.

Anderson, R.F. and Fleer, A.P. (1982): Determination of natural actinides and plutonium in marine particulate material. Analyt. Chem. 54, 1142-1147.

Anderson, R.F., Bacon, M.P. and Brewer, P.G. (1983a): Removal of ^{230}Th and ^{231}Pa from the open ocean. Earth Planet. Sci. Lett. 62, 7-23.

Anderson, R.F., Bacon, M.P. and Brewer, P.G. (1983b): Removal of ^{230}Th and ^{231}Pa at ocean margins. Earth Planet. Sci. Lett. 66, 73-90.

Anderson, R.F., Lao, Y., Broecker, W.S., Trumore, S.E., Hofmann, H.J. and Wolfi, W. (1990): Boundary scavenging in the Pacific Ocean: a comparison of ^{10}Be and ^{231}Pa. Earth Planet. Sci. Lett. 96, 287-304.

Anderson, R.F., Fleisher, M.Q., Biscaye, P.E., Kumar, N., Dittrich, B., Kubik, P. and Suter, M. (1994): Anomalous boundary scavenging in the Middle Atlantic Bight: evidence from ^{230}Th, ^{231}Pa, ^{10}Be and ^{210}Pb. Deep-Sea Res. II, 41, 537-561.

Augstein, E., Bagriantsev, N. and Schenke, H.W. (1991): The Expedition Antarktis VIII/1-2, 1989 with the Winter Weddell Gyre Study of Research Vessels "Polarstern" and "Akademik Fedorov". Reports on Polar Research 84, 1-134.

Bacon, M.P., Rosholt JN (1982): Accumulation rates of Th-230, Pa-231, and some transition metals on the Bermuda Rise. Geochim. Cosmochim. Acta 46, 651-666.

Bacon, M.P. and Anderson, R.F. (1982): Distribution of thorium isotopes between dissolved and particulate forms in the deep sea. J. Geophys. Res. 87, 2045-2056.

Bacon, M.P. (1984): Glacial to interglacial changes in carbonate and clay sedimentation in the Atlantic ocean estimated from Th-230 measurements. Isot. Geosci. 2, 97-111.

Bacon, M.P., Huh, C.-A., Fleer, A.P. and Deuser, W.G. (1985): Seasonality in the flux of natural radionuclides and plutonium in the deep Sargasso Sea. Deep-Sea Res. 32, 273-286.

Bacon, M.P. (1988): Tracers of chemical scavenging in the ocean: boundary effects and large scale chemical fractionation. Philosoph. Trans. Roy. Soc. London A, 320, 187-200.

Bacon, M.P., Huh, C.A. and Moore, R.M. (1989): Vertical profiles of some natural radionuclides over the Alpha Ridge, Arctic Ocean. Earth Planet. Sci. Lett. 95, 15-22.

Baker, E.T., Milburn, H.B. and Tennant, D.A. (1988): Field assessment of sediment trap efficiency under varying flow conditions. J. Mar. Res. 46, 573-592.

Bareille, G.M., Labracherie, M., Labeyrie, L., Pichon, J.J. and Turon, J.L. (1991): Biogenic silica accumulation rate during the Holocene in the southeastern Indian Ocean. Mar. Chem. 35, 537-552.

Barker, P.F., Kennett, J.P. and Scientific Party (1988): Weddell Sea Paleoceanography: Preliminary Results of ODP LEG 113. Paleogeogr. Paleoclimat. Paleoecol. 67, 75-102.

Barnola, J.M., Raynaud, D., Korotkevich, Y.S. and Lorius, C. (1987): Vostok ice core provides 160,000-year record of atmospheric CO_2. Nature 329, 408-414.

Barnola, J.M., Pimienta, P., Raynaud, D. and Korotkevich, Y.S. (1991): CO_2-climate relationship as deduced from the Vostok ice core: A re-examination based on new measurements and on a re-evaluation of the air dating. Tellus, 43 (B), 83-90.

Bathmann, U., Schulz-Baldes, M., Fahrbach, E., Smetacek, V. and Hubberten, H.-W. (1992): The Expedition ANT IX/1-4 of RV "Polarstern" 1990/1991. Reports on Polar Research 100, 1-403.

Bathmann, U., Smetacek, V., de Baar, H., Fahrbach, E. and Krause, G. (1994): The expeditions Antarktis X/6-8 of RV "Polarstern" in 1992-93. Berichte zur Polarforschung 135, 1-236.

Berger, W.H. (1973): Deep-sea carbonates: Pleistocene dissolution cycles. J. Foraminiferal Res. 3, 187-195.

Berger, W.H., Fisher, K., Lai, C., Wu, G. (1987): Ocean productivity and organic carbon flux, part 1: Overwiev and maps of primary production and export production. - SIO Reference Series 87-30, Scripps Institution of Oceanography, 67pp.

Berger, W.H., Smetacek, V.S. and Wefer, G. (1989): Ocean productivity and paleoproductivity - an overwiev. In: Berger, W.H., Smetacek, V.S. and Wefer, G. (eds.), Productivity of the oceans: Present and past, J. Wiley and Sons Ltd. New York, 1-34.

Berner, W., Oeschger, H. and Stauffer, B. (1980): Information on the CO_2 cycle from ice core studies. Radiocarbon 22, 227-235.

Bonn, W.J. (1995): Biogenic opal and barium: Indicators for late Quaternary changes in productivity at the Antarctic continental margin, Atlantic Sector. Ph.D. Thesis. Reports on Polar Research 180, 1-186.

Boyle, E.A. (1988): Cadmium: chemical tracer of deep-water paleoceanography. Paleoceanogr. 3, 471-489.

Boyle, E.A. (1992): Cadmium and $\delta^{13}C$ paleochemical ocean distributions during the stage 2 glacial maximum. Ann. Rev. Earth Planet. Sci. Lett. 20, 245-287.

Boyle, E.A. (1994): A comparison of carbon isotopes and cadmium in the modern and glacial maximum ocean: can we account for the discrepancies?. In: Carbon Cycling in the Glacial Ocean: Constraints on the Ocean's Role in Global Change. Zahn, R., Peterson, T.F., Kaminski, M.A. and Labeyrie, L. (eds.), NATO ASI Ser., Ser. 1, vol. 17, Springer Verlag, Berlin, Heidelberg, 167-193.

Boyle, E. (1996): Deep water distillation. Nature 379, 679-680.

Broecker, W.S. (1979): A revised estimate for the radiocarbon age of North Atlantic deep water. J. Geophys. Res. 84, 3218-3226.

Broecker, W.S. and Peng, T.-H. (1982): Tracers in the sea, 690 pp., Lamont-Doherty Geological Observatory, Columbia University.

Bruland, K.W. and Coale, K.H. (1986): Surface water $^{234}Th/^{238}U$ disequilibria: spatial and temporal variations of scavenging rates within the Pacific Ocean. In: Dynamic processes in the chemistry of the upper ocean, J.D. Burton, P.G. Brewer and R. Chesselet, editors, Plenum Press, New York, pp. 159-172.

Calvert, S.E., Nielsen, B. and Fontugne, M.R. (1992): Evidence from nitrogen isotope ratios for enhanced productivity during formation of eastern Mediterranean sapropels. Nature 359, 223-225.

Charles, C.D. and Fairbanks, R.G. (1990): Glacial to interglacial changes in the isotopic gradient of the Southern Ocean surface water. In: Geological History of the Polar Oceans. Arctic versus Antarctic. Bleil, U. and Tiede, J. (eds.), Kluwer Academic, Norwell, Mass., 519-538.

Charles, C.D., Froelich, P.N., Zibello, M.A., Mortlock, R.A. and Morely J.J. (1991): Biogenic opal in the Southern Ocean sediments over the last 450,000 years: Implications for surface waters chemistry and circulation. Paleoceanogr. 6 (6), 697-728.

Chen, J.H., Edwards, R.L., Wasserburg G.J (1986): ^{238}U, ^{234}U and ^{232}Th in seawater. Earth Planet. Sci. Lett. 80, 241-251.

Chen, J.H., Edwards, R.L., Wasserburg, G.J. (1992): Mass spectrometry and applications to uranium-series disequilibrium. In: Ivanovich M. Harmon R.S. (eds.), Uranium Series Disequilibria: Applications to Environmental Problems. Second edition, London, Clarendon, pp 174-206.

Cheng, H., Edwards, R.L., Goldstein, S.J. (1996): Pa-231 dating of carbonates using TIMS techniques. EOS, Trans. Amer. Geophys. Union 77, S168.

Coale, K.H. and Bruland, K.W. (1985): ^{234}Th:^{238}U disequilibria within the California current. Limnol. and Oceanogr. 30, 22-33.

Cochran, J.K., Krishnaswami, S. (1980): Radium, thorium, uranium and ^{210}Pb in deep-sea sediments and sediment pore waters from the north equatorial Pacific. Amer. J. Sci. 280, 849-889.

Cochran, J.K. (1992): The oceanic chemistry of the U- and Th-series nuclides. In: M. Ivanovich M. Harmon R.S. (eds.) Uranium Series Disequilibria: Applications to Environmental Problems. Second edition, London, Clarendon, pp. 334-395.

Cochran, J.K., Buesseler, K.O., Bacon, M.P. and Livingston, H.D. (1993): Thorium isotopes as indicators of particle dynamics in the upper ocean: Results from the JGOFS North Atlantic Bloom Experiment. Deep-Sea. Res. II, 40, 1569-1595.

Colley, S., Thomson, J. and Newton, P.P. (1995): Detailed ^{230}Th and ^{232}Th and ^{210}Pb fluxes recorded by the 1989/1990 BOFS sediment trap time-series at 48°N, 20°W. Deep-Sea Res. I, 42, 833-848.

Comiso, J.C. and Gordon, A.L. (1987): Recurring polynyas over the Cosmonaut Sea and the Maud Rise. J. Geophys. Res. 92 (C3), 2819-2833.

Dehairs, F., Chesselet, R. and Jedwab, J. (1980): Discrete suspended particles of barite and the barium cycle in the open ocean. Earth Planet. Sci. Lett. 49, 528-550.

DeMaster, D.J. (1979): The marine budgets of silica and 32-Si. Ph.D. Thesis, 308pp., Yale University, New Haven.

DeMaster, D.J. (1981): The supply and accumulation of silica in the marine environment. Geochim. Cosmochim. Acta 45, 1715-1732.

Dymond, J. and Lyle, M. (1985): Flux comparisons between sediments and sediment traps in the eastern tropical Pacific: Implications for atmospheric CO_2 variations during the Pleistocene. Limnol. Oceanogr. 30, 699-712.

Dymond, J., Suess, E. and Lyle, M. (1992): Barium in deep-sea sediment: A geochemical indicator of paleoproductivity. Paleoceanogr. 7, 163-181.

El-Sayed, S.Z. and Taguchi, S. (1981): Primary production and standing crop of phytoplankton along the ice-edge in the Weddell Sea. Deep-Sea Res. 28, 1017-1032.

Emerson, S., and Hedges, J.L. (1988): Processes controlling the organic carbon content of open ocean sediments. Paleoceanogr. 3 (5), 621-634.

Eppley, R. and Peterson, B.J. (1979): Particulate organic matter flux and planktonic new production in the deep ocean. Nature 282, 677-680.

Fahrbach, E., Rohardt, G., Schroeder, M. and Strass, V. (1994): Transport and structure of the Weddell Gyre. Ann. Geophysicae 12, 840-855.

Faure, G. (1986): Principles of Isotope Geology. Second edition, John Wiley & Sons, 589pp.

Fischer, G., Fütterer, D., Gersonde, R., Honjo, S., Osterman, D. and Wefer, G. (1988): Seasonal variability of particle flux in the Weddell Sea and its relation to ice cover. Nature 335, 426-428.

Fischer G. and Wefer G. (1991): Sampling, preparation and analysis of marine particulate matter. In: The Analysis and Characterization of Marine Particles, D.C. Hurd and D.W. Spencer (editors). Geophysical Monograph Series, 63, pp. 391-397.

Fisher N.S., Cochran J.K, Krishnaswami S. and Livingston H.D. (1988) Predicting the oceanic flux of radionuclides on sinking biogenic debris. Nature, 355, 622-625.

Francois, R., Bacon, M.P.and Suman, D.O. (1990): Thorium-230 profiling in deep-sea sediments: high-resolution records of flux and dissolution of carbonate in the equatorial Atlantic during the last 24,000 years. Paleoceanogr. 5, 761-787.

Francois, R., Altabet, M.A. and Burckle, L.D. (1992): Glacial to interglacial changes in surface nitrate utilization in the Indian sector of the Southern Ocean as recorded by sediment $\delta^{15}N$. Paleoceanogr. 7, 589-606.

Francois, R., Bacon, M.P., Altabet, M. and Labeyrie, L.D. (1993): Glacial/Interglacial changes in sediment rain rate in the SW Indian sector of subantarctic waters as recorded by ^{230}Th, ^{231}Pa, U and $\delta^{15}N$. Paleoceanogr. 8, 611-629.

Francois, R., Honjo, S., Manganini, S.J., and Ravizza, G.E. (1995): Biogenic barium fluxes to the deep sea: Implications for paleoproductivity reconstruction. Global Biogeochem. Cycles 9, 289-303.

Francois, R., Altabet, M.A., Yu, E.-F., Sigman, D.M., Bacon, M.P., Frank, M., Bohrmann, G., Bareille, G., Labeyrie, L.D.: Contribution of Southern Ocean upper water column stratification to the glacial decrease in atmospheric CO_2 (submitted to Nature).

Frank, M., Eckhardt, J.-D., Eisenhauer, A., Kubik, P.W., Dittrich-Hannen, B., Segl, M., Mangini, A. (1994): Beryllium 10, thorium 230, and protactinium 231 in Galapagos microplate sediments: Implications of hydrothermal activity and paleoproductivity changes during the last 100,000 years. Paleoceanogr. 9, 559-578.

Frank, M. (1995): Reconstruction of Late Quaternary environmental conditions applying natural radionuclides ^{230}Th, ^{10}Be, ^{231}Pa and ^{238}U: A study of deep-sea sediments from the eastern sector of the Antarctic Circumpolar Current System. Ph.D. Thesis. Reports on Polar Research 186, 1-136.

Frank, M., Eisenhauer, A., Bonn, W.J., Walter, P., Grobe, H., Kubik, P.W., Dittrich-Hannen, B. and Mangini, A. (1995): Sediment redistribution versus paleoproductivity change: Weddell Sea Margin sediment stratigraphy for the last 250,000 years deduced from $^{230}Thex$, ^{10}Be and biogenic barium profiles. Earth Planet. Sci. Lett. 136, 559-573.

Fütterer, D. (1984): The Expedition Antarktis-II of RV "Polarstern" 1983/84. Report of Legs 1, 2 and 3. Reports on Polar Research 18, 1-92.

Fütterer, D. (1989): The Expedition Antarktis-VI of RV "Polarstern" 1987/88. Reports on Polar Research 58, 1-267.

German, C.R., Fleer, A.P., Bacon, M.P., Edmond, J.M. (1991): Hydrothermal scavenging at the Mid-Atlantic Ridge: radionuclide distributions. Earth Planet. Sci. Lett. 105, 170-181.

Gersonde, R. (1993): The expedition Antarktis X/5 of RV "Polarstern" in 1992. Berichte zur Polarforschung 131, 1-167.

Guo, L., Santschi, P., Baskaran, M. and Zindler, A. (1995): Distribution of dissolved and particulate ^{230}Th and ^{232}Th in seawater from the Gulf of Mexico and off Cape Hatteras as measured by SIMS. Earth Planet. Sci. Lett. 133, 117-128.

Gust, G., Michaels, A.F., Johnson, R., Deuser, W.G. and Bowles, W. (1994): Mooring line motions and sediment trap hydromechanics: in situ intercomparison of three common deployment designs. Deep-Sea. Res. I, 41, 831-857.

Hansen, R.G. and Ring, E.J. (1983): The preparation and certification of a uranium reference material, Randburg, Council of Mineral Technology, Report M84, 8pp.

Honeyman, B.D. and Santschi, P.H. (1989): A Brownian-pumping model for oceanic trace metal scavenging: evidence from Th isotopes. J. Mar. Res. 47, 951-992.

Honjo, S. (1982): Seasonality and interaction of biogenic and lithogenic particulate flux at the Panama Basin. Science 218, 883-884.

Honjo, S, and Doherty, K.W. (1988): Large aperture time-series sediment traps; design objectives construction and application. Deep-Sea. Res. 35, 133-149.

Huh, C.-A., Zahnle, D.L., Small, L.F., Noshkin, V.E. (1987): Budgets and behaviour of uranium and thorium series isotopes in Santa Monica Basin sediments. Geochim. Cosmochim. Acta 51, 1743-1754.

Huh, C.-A. and Beasley, T.M. (1987): Profiles of dissolved and particulate thorium isotopes in the water column of coastal Southern California. Earth Planet. Sci. Lett. 85, 1-10.

Jacques, G. (1989): Primary production in the open Antarctic Ocean during the austral summer. A review. Vie Milieu 39, 1-17.

Jumars, P.A., Altenbach, A.V., De Lange, G.J., Emerson, S.R., Hargrave, B.T., Muller, P.J., Prahl, F.G., Reimers, C.E., Steiger, T. and Suess, E. (1989). Transformation of seafloor arriving fluxes into the sedimentary record. In: Productivity of the Oceans: Present and Past. Berger, W.H., Smetacek, V.S. and Wefer, G. (eds.). Wiley, NY, 291-311.

Keigwin, L.D. and Boyle, E.A. (1989): Late Quaternary paleochemistry of high latitude surface waters. Paleogeogr. Paleoclimatol. Paleooecol. 73, 85-106.

Keir, R.S. (1990): Reconstructing the ocean carbon system variation during the last 150.000 years according to the antarctic nutrient hypothesis. Paleoceanogr. 5, 253-276.

Klinkhammer, G. and Palmer, M.R. (1991): Uranium in the oceans, where it goes and why. Geochim. Cosmochim. Acta 55, 1799-1806.

Knox, F. and McElroy, B. (1984): Changes in atmospheric CO_2: Influence of the marine biota at high latitude. J. Geophys. Res. 89, 4629-4637.

Ku, T.-L. (1965): An evaluation of the $^{234}U/^{238}U$ method as a tool for dating pelagic sediments. J. Geophys. Res. 70, 3457-3474.

Ku, T.-L. (1966): Uranium series disequilibrium in deep-sea sediments. Ph.D. Thesis, Columbia University, New York.

Ku, T.-L., Bischoff J.L., Boersma A. (1972): Age studies of Mid-Atlantic Ridge sediments near 42 degrees N and 20 degrees N. Deep-Sea-Res. and Oceanogr. Abstr. 19, 3, 233-247.

Kumar, N., Gwiazda, R., Anderson, R.F. and Froelich, P.N. (1993): $^{231}Pa/^{230}Th$ ratios in sediments as a proxy for past changes in Southern Ocean productivity. Nature 362, 45-48.

Kumar, N. (1994): Trace metals and natural radionuclides as tracers of ocean productivity. Ph.D. Thesis, Columbia University, New York, 317pp.

Kumar, N., Anderson, R.F., Mortlock, R.A., Froelich, P.N., Kubik, P., Dittrich-Hannen, B. and Suter, M. (1995): Increased biological productivity and export production in the glacial Southern Ocean. Nature 378, 675-680.

Lao, Y., Anderson, R.F. and Broecker, W.S. (1992a): Boundary scavenging and deep-sea sediment dating: constraints from excess ^{230}Th and ^{231}Pa. Paleoceanogr. 7, 783-798.

Lao, Y., Anderson, R.F., Broecker, W.S., Trumbore, S.E., Hofmann, H.J. and Wolfi, W. (1992b): Transport and burial rates of ^{10}Be and ^{231}Pa in the Pacific Ocean during the Holocene period. Earth Planet. Sci. Lett. 113, 173-189.

Lao, Y., Anderson, R.F., Broecker, W.S., Hofmann, H.J. and Wolfi, W. (1993): Particulate fluxes of ^{230}Th, ^{231}Pa and ^{10}Be in the northeastern Pacific Ocean. Geochim. Cosmochim. Acta 57, 205-217.

Ledford-Hoffmann, P.A., DeMaster, D.J. and Nittrouer, C.A. (1986): Biogenic-silica accumulation in the Ross Sea and the importance of Antarctic-continental-shelf deposits in the marine silica budgets. Geochim. Cosmochim. Acta 50, 2099-2110.

Legeleux, F. (1994): Relations entre particules marines et message sédimentaire: flux de matière dans la colonne d'eau et transformations a l'interface eau-sédiment dans l'ocean atlantique tropical du nord-est. Ph.D. Thesis, University of Paris, 232pp.

Lehnaert, A., Nelson, D.M., Queguiner, B. and Treguer, P. (1993): The silica cycle in the Antarctic Ocean: is the Weddell Sea atypical?. Mar. Ecol. Prog. Ser. 96, 1-15.

Levitus, S., Conkright, M.E., Reid, J.L., Najjar, R.C. and Mantyla, A. (1993): Distribution of nitrate, phosphate and silicate in the world oceans. Progress in Oceanography 31, 245-273.

Mangini, A., Sonntag, C. (1977): ^{231}Pa dating of deep-sea cores via ^{227}Th counting. Earth Planet. Sci. Lett. 37, 251-256.

Mangini, A., Dieter-Haas, L. (1983): Excess Th-230 in sediments off NW Africa traces upwelling in the past. In: Coastal upwelling: its sedimentary records, Plenum, New York, pp. 455-470.

Mangini, A., Kühnel, U. (1987): Depositional history in the Clarion-Clipperton zone during the last 250,000 years; ^{230}Th and ^{231}Pa methods. Geol. Jahrb. D, 87, 105-121.

Mann, D.R., Surprenant, L.D. and Casso, S.A. (1984): In situ chemisorption of transuranics from seawater. Nuclear Instruments and Methods in Physics Research, 223, 235-238.

Martin, J.H., Knauer, G.A., Karl, D.M. and Broenkow, W.W. (1987): VERTEX: Carbon cycling in the northeast Pacific. Deep Sea Res. 34, 267-285.

Martin, J.H. (1990): Glacial-Interglacial CO_2 change: The iron hypothesis, Paleoceanogr. 5, 1-13.

Martinson, D.G., Pisias, N.G., Hays, D.J., Imbrie, J., Moore, T.C. and Shackleton, N.J. (1987): Age dating and the orbital theory of the ice ages: development of a high resolution 0 to 300.000-year chronostratigraphy. Quaternary Research 27, 1-29.

Miller, H. and Oerter, H. (1990): The Expedition Antarktis-V of RV "Polarstern" 1986/1987. Reports on Polar Research 57, 1-207.

Moran, S.B., Hoff, J.A., Buesseler, K.O., Edwards, R.L. (1995): High precision ^{230}Th and ^{232}Th in the Norwegian Sea and Denmark by thermal ionization mass spectrometry. Geophys. Res. Lett. 22, 2589-2592.

Moran, S.B., Hoff, J.A., Edwards, R.L., Charette, M.A., Landing, W.M.: Distribution of ^{230}Th in the Labrador Sea and its relation to ventilation. Earth Planet. Sci. Lett. (in press).

Mortlock, R.A., Charles, C.D., Froelich, P.N., Zibello, M.A., Salzmann, J., Hays, J.D. and Burckle, L.H. (1991). Evidence for lower productivity in the Antarctic Ocean during the last glaciation. Nature 351, 220-223.

Müller, P.J., Mangini, A. (1980): Organic carbon decomposition rates in sediments of the Pacific manganese nodule belt dated by ^{230}Th and ^{231}Pa. Earth Planet. Sci. Lett. 51, 94-114.

Müller P.J. and Schneider R. (1993): An automated leaching method for the determination of opal, in sediments and particulate matter. Deep Sea Res. 40, 425-444.

Nelson, D.M., Tréguer, P., Brzezinski, M., Leynaert, A. and Quéguiner, B. (1995): Production and dissolution of biogenic silica in the ocean: Revised global estimates, comparison with regional data and relationship to biogenic sedimentation. Glob. Biochem. Cycles 9, 359-372.

Nozaki, Y., Horibe, Y. and Tsubota, H. (1981): The water column distributions of thorium isotopes in the western North Pacific. Earth Planet. Sci. Lett. 54, 203-216.

Nozaki, Y. and Nakanishi, T. (1985): ^{231}Pa and ^{230}Th profiles in the open ocean water column. Deep-Sea Res. 32, 1209-1220.

Nozaki, Y. and Yamada, M. (1987): Thorium and protactinium isotope distributions in waters of the Japan Sea. Deep-Sea Res. 34, 1417-1430.

Nürnberg, C.C. (1995): Bariumfluß und Sedimentation im südlichen Südatlantik, Hinweise auf Produktivitätsänderungen im Quartär. Ph.D. Thesis, 117pp., Univ. Kiel, Germany.

Orsi, A.H., Whitworth III, Th. and Nowlin, Jr. (1995): On the meridional extent and fronts of the Antarctic Circumpolar Current. Deep-Sea Res. 42, 641-673.

Peinert R., Bathmann U., v.Bodungen B., and Noji T. (1987): The impact of grazing on spring phytoplankton growth and sedimentation in the Norwegian Current. In: E.T. Degens E.T., Honjo S. and Izdale E. (editors). Particle flux in the ocean. Mitt. Geol.-Pal. Inst. Univ. Hamburg, SCOPE/UNEP Sonderb. 62: 149-164.

Pudsey, C.J., Barker, P.F. and Hamilton, N. (1988): Weddell Sea abyssal sediments: A record of the Antarctic Bottom Water flow. Mar. Geol. 81, 289-314.

Rosholt, J.N., Emiliani, C., Geiss, J., Koczy, F.F and Wangersky, P.J. (1961): Absolute dating of deep-sea cores by the $^{231}Pa/^{230}Th$ method. J. Geol. 69, 162-185.

Rutgers van der Loeff, M.M. and Berger, G.W. (1991): Scavenging and particle flux: seasonal and regional variations in the Southern Ocean (Atlantic sector). Mar. Chem. 35, 553-568.

Rutgers van der Loeff, M.M. and Berger, G.W. (1993): Scavenging of ^{230}Th and ^{231}Pa near the Antarctic Polar Front in the South Atlantic. Deep-Sea Res. 40, 339-357.

Rutgers van der Loeff, M.M., Friedrich, J. and Bathmann, U.V. (1997): Carbon export during the Spring Bloom at the Antarctic Polar Front, determined with the natural tracer ^{234}Th. Deep-Sea Res. II, 44, 457-478.

Sarmiento, J.L. and Toggweiler, J.R. (1984): A new model for the role of the oceans in determining atmospheric pCO_2. Nature 308, 621-624.

Schlüter, M. (1990): Early diagenesis of orcanic carbon and opal in sediments of the southern and western Weddell Sea. Geochemical analyses and modelling. Berichte zur Polarforschung 73, 156pp.

Schlüter, M., Rutgers van der Loeff, M.M., Holby, O., Kuhn, G.: Silica cycle in surface sediments of the South Atlantic (submitted to Deep Sea Research).

Schmitz, W., Mangini, A., Stoffers, P., Glasby, G.P., Plueger, W.L. (1986): Sediment Accumulation rates in the Southwestern Pacific Basin and Aitutaki passage. Marine Geology 73, 181-190.

Scholten, J.C., Rutgers van der Loeff, M.M. and Michel, A. (1995): Distribution of ^{230}Th and ^{231}Pa in the water-column in relation to the ventilation of the deep Arctic basins. Deep-Sea Res. II, 42, 1519-1531.

Shimmield, G.B., Murray, J.W., Thomson, J., Bacon, M.P., Anderson, R.F., Price, N.B. (1986): The distribution and behaviour of ^{230}Th and ^{231}Pa at an ocean margin, Baja California, Mexico. Geochim. Cosmochim. Acta 50, 2499-2507.

Shimmield, G.B., Price, N.B. (1988): The scavenging of U, of ^{230}Th and ^{231}Pa during pulsed hydrothermal activity at 20°S East Pacific Rise. Geochim. Cosmochim. Acta 52, 669-677.

Shimmield, G.B., Derrick, S., Mackensen, A., Grobe, H. and Pudsey, C. (1994): The history of barium, biogenic silica and organic carbon accumulation in the Weddell Sea and Antarctic Ocean over the last 150,000 years. In: Carbon Cycling in the Glacial Ocean: Constraints on the Ocean's Role in Global Change. Zahn, R. Pedersen, T.F., Kaminski, M.A. and Labeyrie, L., NATO ASI Ser., Ser. 1, vol. 17, Springer Verlag Berlin Heidelberg, 555-574.

Siegenthaler, U. and Wenk, T. (1984): Rapid atmospheric CO_2 variations and ocean circulation. Nature 308, 624-626.

Smith, W.O.Jr. and Nelson, D.M. (1986): Importance of the ice edge: phytoplankton production in the Southern Ocean. BioScience 36, 251-257.

Spindler, M., Dieckmann, G. and Thomas, D. (1993): The Expedition Antarktis X/3 of RV "Polarstern" 1992. Reports on Polar Research 121, 1-204.

Steger, H.F. and Bowman, W.S. (1980): DL-1a: A certified uranium-thorium reference ore, 15pp. Canmet report 80-10E, Canmet, Energy, Mines and Resources Canada.

Stuiver, M., Quay, P.D., Ostlund, H.G. (1984): Abyssal water carbon-14 distributions and the age of the world oceans. Science 219, 849-851.

Suman, D.O. and Bacon, M.P. (1989): Variations in Holocene sedimentation in the North American Basin determined by Th ^{230} measurements. Deep-Sea Res. 36, 869-878.

Taguchi, K., Harada, K. and Tsunogai, S. (1989): Particulate removal of ^{230}Th and ^{231}Pa in the biological productive northern North Pacific. Earth Planet. Sci. Lett. 93, 223-232.

Van-Bennekom, A.J., Berger, G.W., van der Gaast, S.J. and De Vries, R.T.P.(1988): Primary productivity and the silica cycle in the Southern Ocean (Atlantic Sector). Paleogeogr. Paleoclimatol. Paleocol. 67, 19-30.

Vogler, S., Scholten, J., Rutgers van der Loeff, M.M., Mangini, A.: ^{230}Th in the eastern North Atlantic: the importance of water mass ventilation in the balance of ^{230}Th (submitted to Earth Planet. Sci. Lett.).

Walter, H.J., Rutgers van der Loeff, M.M. and Höltzen, H. (1997): Enhanced scavenging of ^{231}Pa relative to ^{230}Th in the South Atlantic south of the Polar Front. Implications for the use of the ^{231}Pa/^{230}Th ratio as a paleoproductivity proxy. Earth Planet. Sci. Lett.

Walter, H.J. Rutgers van der Loeff, M.M. and Francois, R. Reliability of the ^{231}Pa/^{230}Th activity ratio as a tracer for bioproductivity of the ocean. in: Proxies in paleoceanography, examples from the South Atlantic. editors: Fischer G. and Wefer G., University of Bremen, Germany, accepted.

Wefer, G., Fischer, G, Fütterer D. and Gersonde, R. (1988): Seasonal particle flux in the Bransfield Strait, Antarctica. Deep-Sea Res. 35, 891-898.

Wefer, G. (1989): Particle flux in the ocean: effects of episodic production. In: Productivity of the Ocean: past and present, Berger W.H., Smetacek V., Wefer G. (eds), Wiley, New York, pp. 139-154.

Wefer, G., Fischer, G., Fütterer, D., Gersonde, R., Honjo, S. and Ostermann, D. (1990): Particle sedimentation and productivity in Antarctic waters of the Atlantic Sector. In: U. Bleil and J. Thiede (Editors), Geological History of the Polar Oceans: Arctic versus Antarctic. Kluwer Academic, Dordrecht, pp. 363-379.

Wefer, G. and Fischer, G. (1991): Annual primary production and export flux in the Southern Ocean from sediment trap data. Mar. Chem. 35, 597-614.

Wolf-Gladrow, D. (1994): The Ocean as part of the global carbon cycle. Environ. Sci. and Pollut. Res. 1 (2), 99-106.

Yang, H.-S., Nozaki, Y., Sakai, H. and Masuda, A. (1986): The distribution of ^{230}Th and ^{231}Pa in the deep-sea surface sediments of the Pacific Ocean. Geochim. Cosmochim. Acta 50, 81-89.

Yang, Y.-L., Elderfeld, H., Pederson, T.F. (1995): Geochemical record of the Panama basin during the last glacial maximum carbon event shows that the glacial ocean was not suboxic. Geology 23, 1115-1118.

Yu, E.F. (1994): Variations in the particulate flux of ^{230}Th and ^{231}Pa and paleoceanographic applications of the ^{231}Pa/^{230}Th ratio. Ph.D. Thesis, 269pp., WHOI, Woods Hole, Mssachusetts.

Yu, E.F., Francois, R. and Bacon, M.P. (1996): Similar rates of modern and last-glacial ocean thermohaline circulation inferred from radiochemical data. Nature 379, 689-694.

Folgende Hefte der Reihe „Berichte zur Polarforschung" sind bisher erschienen:

* **Sonderheft Nr. 1/1981** – „Die Antarktis und ihr Lebensraum",
Eine Einführung für Besucher – Herausgegeben im Auftrag von SCAR
Heft Nr. 1/1982 – „Die Filchner-Schelfeis-Expedition 1980/81",
zusammengestellt von Heinz Kohnen
* **Heft Nr. 2/1982** – „Deutsche Antarktis-Expedition 1980/81 mit FS 'Meteor'",
First International BIOMASS Experiment (FIBEX) – Liste der Zooplankton- und Mikronektonnetzfänge
zusammengestellt von Norbert Klages
Heft Nr. 3/1982 – „Digitale und analoge Krill-Echolot-Rohdatenerfassung an Bord des Forschungsschiffes 'Meteor'" (im Rahmen von FIBEX 1980/81, Fahrtabschnitt ANT III), von Bodo Morgenstern
Heft Nr. 4/1982 – „Filchner-Schelfeis-Expedition 1980/81",
Liste der Planktonfänge und Lichtstärkemessungen
zusammengestellt von Gerd Hubold und H. Eberhard Drescher
* **Heft Nr. 5/1982** – „Joint Biological Expedition on RRS 'John Biscoe', February 1982",
by G. Hempel and R. B. Heywood
* **Heft Nr. 6/1982** – „Antarktis-Expedition 1981/82 (Unternehmen 'Eiswarte')",
zusammengestellt von Gode Gravenhorst
Heft Nr. 7/1982 – „Marin-Biologisches Begleitprogramm zur Standorterkundung 1979/80 mit MS 'Polarsirkel' (Pre-Site Survey)" – Stationslisten der Mikronekton- und Zooplanktonfänge sowie der Bodenfischerei
zusammengestellt von R. Schneppenheim
Heft Nr. 8/1983 – „The Post-Fibex Data Interpretation Workshop",
by D. L. Cram and J.-C. Freytag with the collaboration of J. W. Schmidt, M. Mall, R. Kresse, T. Schwinghammer
* **Heft Nr. 9/1983** – „Distribution of some groups of zooplankton in the inner Weddell Sea in summer 1979/80",
by I. Hempel, G. Hubold, B. Kaczmaruk, R. Keller, R. Weigmann-Haass
Heft Nr. 10/1983 – „Fluor im antarktischen Ökosystem" – DFG-Symposium November 1982
zusammengestellt von Dieter Adelung
Heft Nr. 11/1983 – „Joint Biological Expedition on RRS 'John Biscoe', February 1982 (II)",
Data of micronecton and zooplankton hauls, by Uwe Piatkowski
Heft Nr. 12/1983 – „Das biologische Programm der ANTARKTIS-I-Expedition 1983 mit FS 'Polarstern'",
Stationslisten der Plankton-, Benthos- und Grundschleppnetzfänge und Liste der Probennahme an Robben und Vögeln, von H. E. Drescher, G. Hubold, U. Piatkowski, J. Plötz und J. Voß
* **Heft Nr. 13/1983** – „Die Antarktis-Expedition von MS 'Polarbjörn' 1982/83" (Sommerkampagne zur Atka-Bucht und zu den Kraul-Bergen), zusammengestellt von Heinz Kohnen
* **Sonderheft Nr. 2/1983** – „Die erste Antarktis-Expedition von FS 'Polarstern' (Kapstadt, 20. Januar 1983 – Rio de Janeiro, 25. März 1983)", Bericht des Fahrtleiters Prof. Dr. Gotthilf Hempel
Sonderheft Nr. 3/1983 – „Sicherheit und Überleben bei Polarexpeditionen",
zusammengestellt von Heinz Kohnen
* **Heft Nr. 14/1983** – „Die erste Antarktis-Expedition (ANTARKTIS I) von FS 'Polarstern' 1982/83",
herausgegeben von Gotthilf Hempel
Sonderheft Nr. 4/1983 – „On the Biology of Krill *Euphausia superba*" – Proceedings of the Seminar and Report of the Krill Ecology Group, Bremerhaven 12.-16. May 1983, edited by S. B. Schnack
Heft Nr. 15/1983 – „German Antarctic Expedition 1980/81 with FRV 'Walther Herwig' and RV 'Meteor'" – First International BIOMASS Experiment (FIBEX) – Data of micronekton and zooplankton hauls
by Uwe Piatkowski and Norbert Klages
Sonderheft Nr. 5/1984 – „The observatories of the Georg von Neumayer Station", by Ernst Augstein
Heft Nr. 16/1984 – „FIBEX cruise zooplankton data",
by U. Piatkowski, I. Hempel and S. Rakusa-Suszczewski
Heft Nr. 17/1984 – „Fahrtbericht (cruise report) der 'Polarstern'-Reise ARKTIS I, 1983",
von E. Augstein, G. Hempel und J. Thiede
Heft Nr. 18/1984 – „Die Expedition ANTARKTIS II mit FS 'Polarstern' 1983/84",
Bericht von den Fahrtabschnitten 1, 2 und 3, herausgegeben von D. Fütterer
Heft Nr. 19/1984 – „Die Expedition ANTARKTIS II mit FS 'Polarstern' 1983/84",
Bericht vom Fahrtabschnitt 4, Punta Arenas-Kapstadt (Ant-II/4), herausgegeben von H. Kohnen
Heft Nr. 20/1984 – „Die Expedition ARKTIS II des FS 'Polarstern' 1984, mit Beiträgen des FS 'Valdivia' und des Forschungsflugzeuges 'Falcon 20' zum Marginal Ice Zone Experiment 1984 (MIZEX)",
von E. Augstein, G. Hempel, J. Schwarz, J. Thiede und W. Weigel
Heft Nr. 21/1985 – „Euphausiid larvae in plankton samples from the vicinity of the Antarctic Peninsula, February 1982", by Sigrid Marschall and Elke Mizdalski

Heft Nr. 22/1985 – „Maps of the geographical distribution of macrozooplankton in the Atlantic sector of the Southern Ocean", by Uwe Piatkowski
Heft Nr. 23/1985 – „Untersuchungen zur Funktionsmorphologie und Nahrungsaufnahme der Larven des Antarktischen Krills *Euphausia superba* Dana", von Hans-Peter Marschall
Heft Nr. 24/1985 – „Untersuchungen zum Periglazial auf der König-Georg-Insel Südshetlandinseln/ Antarktika. Deutsche physiogeographische Forschungen in der Antarktis. – Bericht über die Kampagne 1983/84", von Dietrich Barsch, Wolf-Dieter Blümel, Wolfgang Flügel, Roland Mäusbacher, Gerhard Stäblein, Wolfgang Zick
* **Heft Nr. 25/1985** – „Die Expedition ANTARKTIS III mit FS 'Polarstern' 1984/85", herausgegeben von Gotthilf Hempel
* **Heft Nr. 26/1985** – „The Southern Ocean"; A survey of oceanographic and marine meteorological research work by Hellmer et al.
Heft Nr. 27/1986 – „Spätpleistozäne Sedimentationsprozesse am antarktischen Kontinentalhang vor Kapp Norvegia, östliche Weddell-See", von Hannes Grobe
Heft Nr. 28/1986 – „Die Expedition ARKTIS III mit 'Polarstern' 1985", mit Beiträgen der Fahrtteilnehmer, herausgegeben von Rainer Gersonde
* **Heft Nr. 29/1986** – „5 Jahre Schwerpunktprogramm 'Antarktisforschung' der Deutschen Forschungsgemeinschaft." Rückblick und Ausblick. Zusammengestellt von Gotthilf Hempel, Sprecher des Schwerpunktprogramms
Heft Nr. 30/1986 – „The Meteorological Data of the Georg-von-Neumayer-Station for 1981 and 1982", by Marianne Gube and Friedrich Obleitner
Heft Nr. 31/1986 – „Zur Biologie der Jugendstadien der Notothenioidei (Pisces) an der Antarktischen Halbinsel", von A. Kellermann
Heft Nr. 32/1986 – „Die Expedition ANTARKTIS-IV mit FS 'Polarstern' 1985/86", mit Beiträgen der Fahrtteilnehmer, herausgegeben von Dieter Fütterer
Heft Nr. 33/1987 – „Die Expedition ANTARKTIS-IV mit FS 'Polarstern' 1985/86 – Bericht zu den Fahrtabschnitten ANT-IV/3-4", von Dieter Karl Fütterer
Heft Nr. 34/1987 – „Zoogeographische Untersuchungen und Gemeinschaftsanalysen an antarktischem Makroplankton", von U. Piatkowski
Heft Nr. 35/1987 – „Zur Verbreitung des Meso- und Makrozooplanktons in Oberflächenwasser der Weddell See (Antarktis)", von E. Boysen-Ennen
Heft Nr. 36/1987 – „Zur Nahrungs- und Bewegungsphysiologie von *Salpa thompsoni* und *Salpa fusiformis*", von M. Reinke
Heft Nr. 37/1987 – „The Eastern Weddell Sea Drifting Buoy Data Set of the Winter Weddell Sea Project (WWSP) 1986", by Heinrich Hoeber und Marianne Gube-Lehnhardt
Heft Nr. 38/1987 – „The Meteorological Data of the Georg von Neumayer Station for 1983 and 1984", by M. Gube-Lenhardt
Heft Nr. 39/1987 – „Die Winter-Expedition mit FS 'Polarstern' in die Antarktis (ANT V/1-3)", herausgegeben von Sigrid Schnack-Schiel
Heft Nr. 40/1987 – „Weather and Synoptic Situation during Winter Weddell Sea Project 1986 (ANT V/2) July 16 – September 10, 1986", by Werner Rabe
Heft Nr. 41/1988 – „Zur Verbreitung und Ökologie der Seegurken im Weddellmeer (Antarktis)", von Julian Gutt
Heft Nr. 42/1988 – „The zooplankton community in the deep bathyal and abyssal zones of the eastern North Atlantic", by Werner Beckmann
Heft Nr. 43/1988 – „Scientific cruise report of Arctic Expedition ARK IV/3", Wissenschaftlicher Fahrtbericht der Arktis-Expedition ARK IV/3, compiled by Jörn Thiede
Heft Nr. 44/1988 – „Data Report for FV 'Polarstern' Cruise ARK IV/1, 1987 to the Arctic and Polar Fronts", by Hans-Jürgen Hirche
Heft Nr. 45/1988 – „Zoogeographie und Gemeinschaftsanalyse des Makrozoobenthos des Weddellmeeres (Antarktis)", von Joachim Voß
Heft Nr. 46/1988 – „Meteorological and Oceanographic Data of the Winter-Weddell-Sea Project 1986 (ANT V/3)", by Eberhard Fahrbach
Heft Nr. 47/1988 – „Verteilung und Herkunft glazial-mariner Gerölle am Antarktischen Kontinentalrand des östlichen Weddellmeeres", von Wolfgang Oskierski
Heft Nr. 48/1988 – „Variationen des Erdmagnetfeldes an der GvN-Station", von Arnold Brodscholl
* **Heft Nr. 49/1988** – „Zur Bedeutung der Lipide im antarktischen Zooplankton", von Wilhelm Hagen
Heft Nr. 50/1988 – „Die gezeitenbedingte Dynamik des Ekström-Schelfeises, Antarktis", von Wolfgang Kobarg
Heft Nr. 51/1988 – „Ökomorphologie notothenioider Fische aus dem Weddellmeer, Antarktis", von Werner Ekau
Heft Nr. 52/1988 – „Zusammensetzung der Bodenfauna in der westlichen Fram-Straße", von Dieter Piepenburg
* **Heft Nr. 53/1988** – „Untersuchungen zur Ökologie des Phytoplanktons im südöstlichen Weddellmeer (Antarktis) im Jan./Febr. 1985", von Eva-Maria Nöthig

Heft Nr. 54/1988 – „Die Fischfauna des östlichen und südlichen Weddellmeeres: geographische Verbreitung, Nahrung und trophische Stellung der Fischarten", von Wiebke Schwarzbach
Heft Nr. 55/1988 – „Weight and length data of zooplankton in the Weddell Sea in austral spring 1986 (ANT V/3)", by Elke Mizdalski
Heft Nr. 56/1989 – „Scientific cruise report of Arctic expeditions ARK IV/1, 2 & 3", by G. Krause, J. Meincke und J. Thiede
Heft Nr. 57/1989 – „Die Expedition ANTARKTIS V mit FS 'Polarstern' 1986/87", Bericht von den Fahrtabschnitten ANT V/4-5 von H. Miller und H. Oerter
* **Heft Nr. 58/1989** – „Die Expedition ANTARKTIS VI mit FS 'Polarstern' 1987/88", von D. K. Fütterer
Heft Nr. 59/1989 – „Die Expedition ARKTIS V/1a, 1b und 2 mit FS 'Polarstern' 1988", von M. Spindler
Heft Nr. 60/1989 – „Ein zweidimensionales Modell zur thermohalinen Zirkulation unter dem Schelfeis", von H. H. Hellmer
Heft Nr. 61/1989 – „Die Vulkanite im westlichen und mittleren Neuschwabenland, Vestfjella und Ahlmannryggen, Antarktika", von M. Peters
* **Heft-Nr. 62/1989** – „The Expedition ANTARKTIS VII/1 and 2 (EPOS I) of RV 'Polarstern' in 1988/89", by I. Hempel
Heft Nr. 63/1989 – „Die Eisalgenflora des Weddellmeeres (Antarktis): Artenzusammensetzung und Biomasse, sowie Ökophysiologie ausgewählter Arten", von Annette Bartsch
Heft Nr. 64/1989 – „Meteorological Data of the G.-v.-Neumayer-Station (Antarctica)", by L. Helmes
Heft Nr. 65/1989 – „Expedition Antarktis VII/3 in 1988/89", by I. Hempel, P. H. Schalk, V. Smetacek
Heft Nr. 66/1989 – „Geomorphologisch-glaziologische Detailkartierung des arid-hochpolaren Borgmassivet, Neuschwabenland, Antarktika", von Karsten Brunk
Heft-Nr. 67/1990 – „Identification key and catalogue of larval Antarctic fishes", edited by Adolf Kellermann
Heft-Nr. 68/1990 – „The Expediton Antarktis VII/4 (Epos leg 3) and VII/5 of RV 'Polarstern' in 1989", edited by W. Arntz, W. Ernst, I. Hempel
Heft-Nr. 69/1990 – „Abhängigkeiten elastischer und rheologischer Eigenschaften des Meereises vom Eisgefüge", von Harald Hellmann
Heft-Nr. 70/1990 – „Die beschalten benthischen Mollusken (Gastropoda und Bivalvia) des Weddellmeeres, Antarktis", von Stefan Hain
Heft-Nr. 71/1990 – „Sedimentologie und Paläomagnetik an Sedimenten der Maudkuppe (Nordöstliches Weddellmeer)", von Dieter Cordes
Heft-Nr. 72/1990 – „Distribution and abundance of planktonic copepods (Crustacea) in the Weddell Sea in summer 1980/81", by F. Kurbjeweit and S. Ali-Khan
Heft-Nr. 73/1990 – „Zur Frühdiagenese von organischem Kohlenstoff und Opal in Sedimenten des südlichen und östlichen Weddellmeeres", von M. Schlüter
Heft-Nr. 74/1991 – „Expeditionen ANTARKTIS-VIII/3 und VIII/4 mit FS 'Polarstern' 1989", von Rainer Gersonde und Gotthilf Hempel
Heft-Nr. 75/1991 – „Quartäre Sedimentationsprozesse am Kontinentalhang des Süd-Orkney-Plateaus im nordwestlichen Weddelmeer (Antarktis)", von Sigrun Grünig
Heft-Nr. 76/1991 – „Ergebnisse der faunistischen Arbeiten in Benthal von King George Island (Südshetlandinseln, Antarktis)", Martin Rauschert
Heft-Nr. 77/1991 – „Verteilung von Mikroplankton-Organismen nordwestlich der Antarktischen Halbinsel unter dem Einfluß sich ändernder Umweltbedingungen in Herbst", von Heinz Klöser
Heft-Nr. 78/1991 – „Hochauflösende Magnetostratigraphie spätquartärer Sedimente arktischer Meeresgebiete", von Norbert R. Nowaczyk
Heft-Nr. 79/1991 – „Ökophysiologische Untersuchungen zur Salinitäts- und Temperaturtoleranz antarktischer Grünalgen unter besonderer Berücksichtigung des ß-Dimethylsulfoniumpropionat (DMSP) – Stoffwechsels", von Ulf Karsten
Heft-Nr. 80/1991 – „Die Expedition ARKTIS VII/1 mit FS 'POLARSTERN' 1990", herausgegeben von Jörn Thiede und Gotthilf Hempel
Heft-Nr. 81/1991 – „Paläoglaziologie und Paläozeanographie im Spätquartär am Kontinentalrand des südlichen Weddellmeeres, Antarktis", von Martin Melles
Heft-Nr. 82/1991 – „Quantifizierung von Meereiseigenschaften: Automatische Bildanalyse von Dünnschnitten und Parametrisierung von Chlorophyll- und Salzgehaltsverteilungen", von Hajo Eicken
Heft-Nr. 83/1991 – „Das Fließen von Schelfeisen – numerische Simulationen mit der Methode der finiten Differenzen", von Jürgen Determann
Heft-Nr. 84/1991 – Die Expedition ANTARKTIS VIII/1-2, 1989 mit der Winter Weddell Gyre Study der Forschungsschiffe 'Polarstern' und 'Akademik Fedorov' ", von Ernst Augstein, Nicolai Bagriantsev und Hans Werner Schenke
Heft-Nr. 85/1991 – „Zur Entstehung von Unterwassereis und das Wachstum und die Energiebilanz des Meereises in der Atka Bucht, Antarktis", von Josef Kipfstuhl

Heft-Nr. 86/1991 – „Die Expedition ANTARKTIS-VIII mit FS 'Polarstern' 1989/90. Bericht vom Fahrtabschnitt ANT-VIII/5", herausgegeben von Heinz Miller und Hans Oerter
Heft-Nr. 87/1991 – „Scientific cruise reports of Arctic expeditions ARK-VI/1-4 of RV 'Polarstern' in 1989", edited by G. Krause, J. Meincke & H. J. Schwarz
Heft-Nr. 88/1991 – „Zur Lebensgeschichte dominanter Copepodenarten *(Calanus finmarchicus, C. glacialis, C. hyperboreus, Metridia longa)* in der Framstraße", von Sabine Diel
Heft-Nr. 89/1991 – „Detaillierte seismische Untersuchungen am östlichen Kontinentalrand des Weddell-Meeres vor Kapp Norvegia, Antarktis", von Norbert E. Kaul
Heft-Nr. 90/1991 – „Die Expedition ANTARKTIS VIII mit FS 'Polarstern' 1989/90. Bericht von Fahrtabschnitten ANT VIII/6-7", herausgegeben von Dieter Karl Fütterer und Otto Schrems
Heft-Nr. 91/1991 – „Blood physiology and ecological consequences in Weddell Sea fishes (Antarctica)", by Andreas Kunzmann.
Heft-Nr. 92/1991 – „Zur sommerlichen Verteilung des Mesozooplanktons im Nansen-Becken, Nordpolarmeer", von Nicolai Mumm.
Heft-Nr. 93/1991 – Die Expedition ARKTIS VII mit FS 'Polarstern' 1990. Bericht von Fahrtabschnitten ARK VII/2", herausgegeben vom Gunther Krause.
Heft-Nr. 94/1991 – „Die Entwicklung des Phytoplanktons im östlichen Weddellmeer (Antarktis) beim Übergang vom Spätwinter zum Frühjahr", von Renate Scharek.
Heft-Nr. 95/1991 – „Radioisotopenstratigraphie, Sedimentologie und Geochemie jungquartärer Sedimente des östlichen Arktischen Ozeans", von Horst Bohrmann.
Heft-Nr. 96/1991 – „Holozäne Sedimentationsentwicklung im Scoresby Sund, Ost-Grönland", von Peter Marienfeld
Heft-Nr. 97/1991 – „Strukturelle Entwicklung und Abkühlungsgeschichte der Heimefrontfjella (Westliches Dronning Maud Land / Antarktika)", von Joachim Jacobs
Heft-Nr. 98/1991 – „Zur Besiedlungsgeschichte des antarktischen Schelfes am Beispiel der Isopoda (Crustacea, Malacostraca)", von Angelika Brandt
Heft-Nr. 99/1992 – „The Antarctic ice sheet and environmental change: a three-dimensional modelling study", by Philippe Huybrechts
* **Heft-Nr. 100/1992** – „Die Expeditionen ANTARKTIS IX/1-4 des Forschungsschiffes 'Polarstern' 1990/91", herausgegeben von Ulrich Bathmann, Meinhard Schulz-Baldes, Eberhard Fahrbach, Victor Smetacek und Hans-Wolfgang Hubberten
Heft-Nr. 101/1992 – „Wechselbeziehungen zwischen Spurenmetallkonzentrationen (Cd, Cu, Pb, Zn) im Meerwasser und in Zooplanktonorganismen (Copepoda) der Arktis und des Atlantiks", von Christa Pohl
Heft-Nr. 102/1992 – „Physiologie und Ultrastruktur der antarktischen Grünalge *Prasiola crispa* ssp. *antarctica* unter osmotischem Streß und Austrocknung", von Andreas Jacob
Heft-Nr. 103/1992 – „Zur Ökologie der Fische im Weddellmeer", von Gerd Hubold
Heft-Nr. 104/1992 – „Mehrkanalige adaptive Filter für die Unterdrückung von multiplen Reflexionen in Verbindung mit der freien Oberfläche in marinen Seismogrammen", von Andreas Rosenberger
Heft-Nr. 105/1992 – „Radiation and Eddy Flux Experiment 1991 *(REFLEX I)*", von Jörg Hartmann, Christoph Kottmeier und Christian Wamser
Heft-Nr. 106/1992 – „Ostracoden im Epipelagial vor der Antarktischen Halbinsel - ein Beitrag zur Systematik sowie zur Verbreitung und Populationsstruktur unter Berücksichtigung der Saisonalität", von Rüdiger Kock
Heft-Nr. 107/1992 – „ARCTIC '91: Die Expedition ARK-VIII/3 mit FS 'Polarstern' 1991", herausgegeben von Dieter K. Fütterer
Heft-Nr. 108/1992 – „Dehnungsbeben an einer Störungszone im Ekström-Schelfeis nördlich der Georg-von-Neumayer Station, Antarktis. - Eine Untersuchung mit seismologischen und geodätischen Methoden", von Uwe Nixdorf
Heft-Nr. 109/1992 – „Spätquartäre Sedimentation am Kontinentalrand des südöstlichen Weddellmeeres, Antarktis", von Michael Weber
Heft-Nr. 110/1992 – „Sedimentfazies und Bodenwasserstrom am Kontinentalhang des nordwestlichen Weddellmeeres", von Isa Brehme
Heft-Nr. 111/1992 – „Die Lebensbedingungen in den Solekanälchen des antarktischen Meereises", von Jürgen Weissenberger
Heft-Nr. 112/1992 – „Zur Taxonomie von rezenten benthischen Foraminiferen aus dem Nansen Becken, Arktischer Ozean", von Jutta Wollenburg
Heft-Nr. 113/1992 – „Die Expedition ARKTIS VIII/1 mit FS 'Polarstern' 1991", herausgegeben von Gerhard Kattner
* **Heft-Nr. 114/1992** – „Die Gründungsphase deutscher Polarforschung, 1865-1875", von Reinhard A. Krause
Heft-Nr. 115/1992 – „Scientific Cruise Report of the 1991 Arctic Expedition ARK VIII/2 of RV "Polarstern" (EPOS II)", by Eike Rachor

Heft-Nr. 116/1992 – „The Meteorological Data of the Georg-von-Neumayer-Station (Antarctica) for 1988, 1989, 1990 and 1991", by Gert König-Langlo
Heft-Nr. 117/1992 – „Petrogenese des metamorphen Grundgebirges der zentralen Heimefrontfjella (westliches Dronning Maud Land / Antarktis)", von Peter Schulze
Heft-Nr. 118/1993 – „Die mafischen Gänge der Shackleton Range / Antarktika: Petrographie, Geochemie, Isotopengeochemie und Paläomagnetik", von Rüdiger Hotten
* **Heft-Nr. 119/1993** – „Gefrierschutz bei Fischen der Polarmeere", von Andreas P. A. Wöhrmann
* **Heft-Nr. 120/1993** – „East Siberian Arctic Region Expedition '92: The Laptev Sea – its Significance for Arctic Sea-Ice Formation and Transpolar Sediment Flux", by D. Dethleff, D. Nürnberg, E. Reimnitz, M. Saarso and Y.P. Savchenko. – „Expedition to Novaja Zemlja and Franz Josef Land with RV 'Dalnie Zelentsy' ", by D. Nürnberg and E. Groth
* **Heft-Nr. 121/1993** – „Die Expedition ANTARKTIS X/3 mit FS 'Polarstern' 1992", herausgegeben von Michael Spindler, Gerhard Dieckmann und David Thomas
Heft-Nr. 122/1993 – „Die Beschreibung der Korngestalt mit Hilfe der Fourier-Analyse: Parametrisierung der morphologischen Eigenschaften von Sedimentpartikeln", von Michael Diepenbroek
* **Heft-Nr. 123/1993** – „Zerstörungsfreie hochauflösende Dichteuntersuchungen mariner Sedimente", von Sebastian Gerland
Heft-Nr. 124/1993 – „Umsatz und Verteilung von Lipiden in arktischen marinen Organismen unter besonderer Berücksichtigung unterer trophischer Stufen", von Martin Graeve
Heft-Nr. 125/1993 – „Ökologie und Respiration ausgewählter arktischer Bodenfischarten", von Christian F. von Dorrien
Heft-Nr. 126/1993 – „Quantitative Bestimmung von Paläoumweltparametern des Antarktischen Oberflächenwassers im Spätquartär anhand von Transferfunktionen mit Diatomeen", von Ulrich Zielinski
Heft-Nr. 127/1993 – „Sedimenttransport durch das arktische Meereis: Die rezente lithogene und biogene Materialfracht", von Ingo Wollenburg
Heft-Nr. 128/1993 – „Cruise ANTARKTIS X/3 of RV 'Polarstern': CTD-Report", von Marek Zwierz
Heft-Nr. 129/1993 – „Reproduktion und Lebenszyklen dominanter Copepodenarten aus dem Weddellmeer, Antarktis", von Frank Kurbjeweit
Heft-Nr. 130/1993 – „Untersuchungen zu Temperaturregime und Massenhaushalt des Filchner-Ronne-Schelfeises, Antarktis, unter besonderer Berücksichtigung von Anfrier- und Abschmelzprozessen", von Klaus Grosfeld
Heft-Nr. 131/1993 – „Die Expedition ANTARKTIS X/5 mit FS 'Polarstern' 1992", herausgegeben von Rainer Gersonde
Heft-Nr. 132/1993 – „Bildung und Abgabe kurzkettiger halogenierter Kohlenwasserstoffe durch Makroalgen der Polarregionen", von Frank Laturnus
Heft-Nr. 133/1994 – „Radiation and Eddy Flux Experiment 1993 *(REFLEX II)*", by Christoph Kottmeier, Jörg Hartmann, Christian Wamser, Axel Bochert, Christof Lüpkes, Dietmar Freese and Wolfgang Cohrs
* **Heft-Nr. 134/1994** – „The Expedition ARKTIS-IX/1", edited by Hajo Eicken and Jens Meincke
Heft-Nr. 135/1994 – „Die Expeditionen ANTARKTIS X/6-8", herausgegeben von Ulrich Bathmann, Victor Smetacek, Hein de Baar, Eberhard Fahrbach und Gunter Krause
Heft-Nr. 136/1994 – „Untersuchungen zur Ernährungsökologie von Kaiserpinguinen *(Aptenodytes forsteri)* und Königspinguinen *(Aptenodytes patagonicus)*", von Klemens Pütz
* **Heft-Nr. 137/1994** – „Die känozoische Vereisungsgeschichte der Antarktis", von Werner U. Ehrmann
Heft-Nr. 138/1994 – „Untersuchungen stratosphärischer Aerosole vulkanischen Ursprungs und polarer stratosphärischer Wolken mit einem Mehrwellenlängen-Lidar auf Spitzbergen (79°N, 12°E)", von Georg Beyerle
Heft-Nr. 139/1994 – „Charakterisierung der Isopodenfauna (Crustacea, Malacostraca) des Scotia-Bogens aus biogeographischer Sicht: Ein multivariater Ansatz", von Holger Winkler
Heft-Nr. 140/1994 – „Die Expedition ANTARKTIS X/4 mit FS 'Polarstern' 1992", herausgegeben von Peter Lemke
Heft-Nr. 141/1994 – „Satellitenaltimetrie über Eis – Anwendung des GEOSAT-Altimeters über dem Ekströmisen, Antarktis", von Klemens Heidland
Heft-Nr. 142/1994 – „The 1993 Northeast Water Expedition. Scientific cruise report of RV 'Polarstern' Arctic cruises ARK IX/2 and 3, USCG 'Polar Bear' cruise NEWP and the NEWLand expedition", edited by Hans-Jürgen Hirche and Gerhard Kattner
Heft-Nr. 143/1994 – „Detaillierte refraktionsseismische Untersuchungen im inneren Scoresby Sund/ Ost Grönland", von Notker Fechner
Heft-Nr. 144/1994 – „Russian-German Cooperation in the Siberian Shelf Seas: Geo-System Laptev Sea", edited by Heidemarie Kassens, Hans-Wolfgang Hubberten, Sergey M. Pryamikov and Rüdiger Stein
* **Heft-Nr. 145/1994** – „The 1993 Northeast Water Expedition. Data Report of RV ‚Polarstern' Arctic Cruises IX/2 and 3", edited by Gerhard Kattner and Hans-Jürgen Hirche
Heft-Nr. 146/1994 – „Radiation Measurements at the German Antarctic Station Neumeyer 1982 – 1992", by Torsten Schmidt and Gert König-Langlo

Heft-Nr. 147/1994 – „Krustenstrukturen und Verlauf des Kontinentalrandes im Weddell Meer/Antarktis", von Christian Hübscher
Heft-Nr. 148/1994 – „The expeditions NORILSK/TAYMYR 1993 and BUNGER OASIS 1993/94 of the AWI Research Unit Potsdam", edited by Martin Melles
****Heft-Nr. 149/1994** – „Die Expedition ARCTIC '93. Der Fahrtabschnitt ARK-IX/4 mit FS ‚Polarstern' 1993", herausgegeben von Dieter K. Fütterer
Heft-Nr. 150/1994 – „Der Energiebedarf der Pygoscelis-Pinguine: eine Synopse", von Boris M. Culik
Heft-Nr. 151/1994 – „Russian-German Cooperation: The Transdrift I Expedition to the Laptev Sea", edited by Heidemarie Kassens and Valeriy Y. Karpiy
Heft-Nr. 152/1994 – „Die Expedition ANTARKTIS-X mit FS 'Polarstern' 1992. Bericht von den Fahrtabschnitten ANT X/1a und 2", herausgegeben von Heinz Miller
Heft-Nr. 153/1994 – „Aminosäuren und Huminstoffe im Stickstoffkreislauf polarer Meere", von Ulrike Hubberten
Heft-Nr. 154/1994 – „Regional and seasonal variability in the vertical distribution of mesozooplankton in the Greenland Sea", by Claudio Richter
Heft-Nr. 155/1995 – „Benthos in polaren Gewässern", herausgegeben von Christian Wiencke und Wolf Arntz
Heft-Nr. 156/1995 – „An adjoint model for the determination of the mean oceanic circulation, air-sea fluxes and mixing coefficients", by Reiner Schlitzer
Heft-Nr. 157/1995 – „Biochemische Untersuchungen zum Lipidstoffwechsel antarktischer Copepoden", von Kirsten Fahl
****Heft-Nr. 158/1995** – „Die deutsche Polarforschung seit der Jahrhundertwende und der Einfluß Erich von Drygalskis", von Cornelia Lüdecke
Heft-Nr. 159/1995 – „The distribution of $\delta^{18}O$ in the Arctic Ocean: Implications for the freshwater balance of the halocline and the sources of deep and bottom waters", by Dorothea Bauch
*** Heft-Nr. 160/1995** – „Rekonstruktion der spätquartären Tiefenwasserzirkulation und Produktivität im östlichen Südatlantik anhand von benthischen Foraminiferenvergesellschaftungen", von Gerhard Schmiedl
Heft-Nr. 161/1995 – „Der Einfluß von Salinität und Lichtintensität auf die Osmolytkonzentrationen, die Zellvolumina und die Wachstumsraten der antarktischen Eisdiatomeen *Chaetoceros* sp. und *Navicula* sp. unter besonderer Berücksichtigung der Aminosäure Prolin", von Jürgen Nothnagel
Heft-Nr. 162/1995 – „Meereistransportiertes lithogenes Feinmaterial in spätquartären Tiefseesedimenten des zentralen östlichen Arktischen Ozeans und der Framstraße", von Thomas Letzig
Heft-Nr. 163/1995 – „Die Expedition ANTARKTIS-XI/2 mit FS 'Polarstern' 1993/94", herausgegeben von Rainer Gersonde
Heft-Nr. 164/1995 – „Regionale und altersabhängige Variation gesteinsmagnetischer Parameter in marinen Sedimenten der Arktis", von Thomas Frederichs
Heft-Nr. 165/1995 – „Vorkommen, Verteilung und Umsatz biogener organischer Spurenstoffe: Sterole in antarktischen Gewässern", von Georg Hanke
Heft-Nr. 166/1995 – „Vergleichende Untersuchungen eines optimierten dynamisch-thermodynamischen Meereismodells mit Beobachtungen im Weddellmeer", von Holger Fischer
Heft-Nr. 167/1995 – „Rekonstruktionen von Paläo-Umweltparametern anhand von stabilen Isotopen und Faunen-Vergesellschaftungen planktischer Foraminiferen im Südatlantik", von Hans-Stefan Niebler
Heft-Nr. 168/1995 – „Die Expedition ANTARKTIS XII mit FS 'Polarstern' 1994/95. Bericht von den Fahrtabschnitten ANT XII/1 und 2", herausgegeben von Gerhard Kattner und Dieter Karl Fütterer
Heft-Nr. 169/1995 – „Medizinische Untersuchung zur Circadianrhythmik und zum Verhalten bei Überwinterern auf einer antarktischen Forschungsstation", von Hans Wortmann
Heft-Nr. 170/1995 – DFG-Kolloquium: Terrestrische Geowissenschaften – Geologie und Geophysik der Antarktis
Heft-Nr. 171/1995 – „Strukturentwicklung und Petrogenese des metamorphen Grundgebirges der nördlichen Heimefrontfjella (westliches Dronning Maud Land/Antarktika)", von Wilfried Bauer
Heft-Nr. 172/1995 – „Die Struktur der Erdkruste im Bereich des Scoresby Sund, Ostgrönland: Ergebnisse refraktionsseismischer und gravimetrischer Untersuchungen", von Holger Mandler
Heft-Nr. 173/1995 – „Paläozoische Akkretion am paläopazifischen Kontinentalrand der Antarktis in Nordvictorialand – P-T-D-Geschichte und Deformationsmechanismen im Bowers Terrane", von Stefan Matzer
Heft-Nr. 174/1995 – „The Expediton ARKTIS-X/2 of RV 'Polarstern' in 1994", edited by Hans-W. Hubberten
Heft-Nr. 175/1995 – „Russian-German Cooperation: The Expedition TAYMYR 1994", edited by Christine Siegert and Dmitry Bolshiyanov
Heft-Nr. 176/1995 – „Russian-German Cooperation: Laptev Sea System", edited by Heidemarie Kassens, Dieter Piepenburg, Jörn Thiede, Leonid Timokhov, Hans-Wolfgang Hubberten and Sergey M. Priamikov
Heft-Nr. 177/1995 – „Organischer Kohlenstoff in spätquartären Sedimenten des Arktischen Ozeans: Terrigener Eintrag und marine Produktivität", von Carsten J. Schubert
Heft-Nr. 178/1995 – „Cruise ANTARKTIS XII/4 of RV 'Polarstern' in 1995: CTD-Report", by Jüri Sildam
Heft-Nr. 179/1995 – „Benthische Foraminiferenfaunen als Wassermassen-, Produktions- und Eisdriftanzeiger im Arktischen Ozean", von Jutta Wollenburg

Heft-Nr. 180/1995 – „Biogenopal und biogenes Barium als Indikatoren für spätquartäre Produktivitäts-änderungen am antarktischen Kontinentalhang, atlantischer Sektor", von Wolfgang J. Bonn
Heft-Nr. 181/1995 – „Die Expedition ARKTIS X/1 des Forschungsschiffes 'Polarstern' 1994", herausgegeben von Eberhard Fahrbach
Heft-Nr. 182/1995 – „Laptev Sea System: Expeditions in 1994", edited by Heidemarie Kassens
Heft-Nr. 183/1996 – „Interpretation digitaler Parasound Echolotaufzeichnungen im östlichen Arktischen Ozean auf der Grundlage physikalischer Sedimenteigenschaften", von Uwe Bergmann
Heft-Nr. 184/1996 – „Distribution and dynamics of inorganic nitrogen compounds in the troposphere of continental, coastal, marine and Arctic areas", by María Dolores Andrés Hernández
Heft-Nr. 185/1996 – „Verbreitung und Lebensweise der Aphroditiden und Polynoiden (Polychaeta) im östlichen Weddellmeer und im Lazarevmeer (Antarktis)", von Michael Stiller
Heft-Nr. 186/1996 – „Reconstruction of Late Quaternary environmental conditions applying the natural radionuclides ^{230}Th, ^{10}Be, ^{231}Pa and ^{238}U: A study of deep-sea sediments from the eastern sector of the Antarctic Circumpolar Current System", by Martin Frank
Heft-Nr. 187/1996 – „The Meteorological Data of the Neumayer Station (Antarctica) for 1992, 1993 and 1994", by Gert König-Langlo and Andreas Herber
Heft-Nr. 188/1996 – „Die Expedition ANTARKTIS-XI/3 mit FS 'Polarstern' 1994", herausgegeben von Heinz Miller und Hannes Grobe
Heft-Nr. 189/1996 – „Die Expedition ARKTIS-VII/3 mit FS 'Polarstern' 1990", herausgegeben von Heinz Miller und Hannes Grobe
Heft-Nr. 190/1996 – „Cruise report of the Joint Chilean-German-Italian Magellan 'Victor Hensen' Campaign in 1994", edited by Wolf Arntz and Matthias Gorny
Heft-Nr. 191/1996 – „Leitfähigkeits- und Dichtemessung an Eisbohrkernen", von Frank Wilhelms
Heft-Nr. 192/1996 – „Photosynthese-Charakteristika und Lebensstrategien antarktischer Makroalgen", von Gabriele Weykam
Heft-Nr. 193/1996 – Heterogene Reaktionen von N_2O_5 und HBr und ihr Einfluß auf den Ozonabbau in der polaren Stratosphäre", von Sabine Seisel
Heft-Nr. 194/1996 – „Ökologie und Populationsdynamik antarktischer Ophiuroiden (Echinodermata)", von Corinna Dahm
Heft-Nr. 195/1996 – „Die planktische Foraminifere *Neogloboquadrina pachyderma* (Ehrenberg) im Weddellmeer, Antarktis", von Doris Berberich
Heft-Nr. 196/1996 – „Untersuchungen zum Beitrag chemischer und dynamischer Prozesse zur Variabilität des stratosphärischen Ozons über der Arktis", von Birgit Heese
Heft-Nr. 197/1996 – „The Expedition ARKTIS-XI/2 of RV 'Polarstern' in 1995", edited by Gunther Krause
Heft-Nr. 198/1996 – „Geodynamik des Westantarktischen Riftsystems basierend auf Apatit-Spaltspuranalysen", von Frank Lisker
Heft-Nr. 199/1996 – „The 1993 Northeast Water Expedition. Data Report on CTD Measurements of RV 'Polarstern' Cruises ARKTIS IX/2 and 3", by Gereon Budéus and Wolfgang Schneider
Heft-Nr. 200/1996 – „Stability of the Thermohaline Circulation in analytical and numerical models", by Gerrit Lohmann
Heft-Nr. 201/1996 – „Trophische Beziehungen zwischen Makroalgen und Herbivoren in der Potter Cove (King George-Insel, Antarktis)", von Katrin Iken
Heft-Nr. 202/1996 – „Zur Verbreitung und Respiration ökologisch wichtiger Bodentiere in den Gewässern um Svalbard (Arktis)", von Michael K. Schmid
Heft-Nr. 203/1996 – „Dynamik, Rauhigkeit und Alter des Meereises in der Arktis – Numerische Untersuchungen mit einem großskaligen Modell", von Markus Harder
Heft-Nr. 204/1996 – „Zur Parametrisierung der stabilen atmosphärischen Grenzschicht über einem antarktischen Schelfeis", von Dörthe Handorf
Heft-Nr. 205/1996 – „Textures and fabrics in the GRIP ice core, in relation to climate history and ice deformation", by Thorsteinn Thorsteinsson
Heft-Nr. 206/1996 – „Der Ozean als Teil des gekoppelten Klimasystems: Versuch der Rekonstruktion der glazialen Zirkulation mit verschieden komplexen Atmosphärenkomponenten", von Kerstin Fieg
Heft-Nr. 207/1996 – „Lebensstrategien dominanter antarktischer Oithonidae (Cyclopoida, Copepoda) und Oncaeidae (Poecilostomatoida, Copepoda) im Bellingshausenmeer", von Cornelia Metz
Heft-Nr. 208/1996 – „Atmosphäreneinfluß bei der Fernerkundung von Meereis mit passiven Mikrowellen-radiometern", von Christoph Oelke
Heft-Nr. 209/1996 – „Klassifikation von Radarsatellitendaten zur Meereiserkennung mit Hilfe von Line-Scanner-Messungen", von Axel Bochert
Heft-Nr. 210/1996 – „Die mit ausgewählten Schwämmen (Hexactinellida und Demospongiae) aus dem Weddellmeer, Antarktis, vergesellschaftete Fauna", von Kathrin Kunzmann
Heft-Nr. 211/1996 – „Russian-German Cooperation: The Expedition TAYMYR 1995 and the Expedition KOLYMA 1995", by Dima Yu. Bolshiyanov and Hans-W. Hubberten

Heft-Nr. 212/1996 – „Surface-sediment composition and sedimentary processes in the central Arctic Ocean and along the Eurasian Continental Margin", by Ruediger Stein, Gennadij I. Ivanov, Michael A. Levitan, and Kirsten Fahl
Heft-Nr. 213/1996 – „Gonadenentwicklung und Eiproduktion dreier *Calanus*-Arten (Copepoda): Freilandbeobachtungen, Histologie und Experimente", von Barbara Niehoff
Heft-Nr. 214/1996 – „Numerische Modellierung der Übergangszone zwischen Eisschild und Eisschelf", von Christoph Mayer
Heft-Nr. 215/1996 – „Arbeiten der AWI-Forschungsstelle Potsdam in Antarktika, 1994/95", herausgegeben von Ulrich Wand
Heft-Nr. 216/1996 – „Rekonstruktion quartärer Klimaänderungen im atlantischen Sektor des Südpolarmeeres anhand von Radiolarien", von Uta Brathauer
Heft-Nr. 217/1996 – „Adaptive Semi-Lagrange-Finite-Elemente-Methode zur Lösung der Flachwassergleichungen: Implementierung und Parallelisierung", von Jörn Behrens
Heft-Nr. 218/1997 – „Radiation and Eddy Flux Experiment 1995 *(REFLEX III)*", by Jörg Hartmann, Axel Bochert, Dietmar Freese, Christoph Kottmeier, Dagmar Nagel, and Andreas Reuter
Heft-Nr. 219/1997 – „Die Expedition ANTARKTIS-XII mit FS 'Polarstern' 1995. Bericht vom Fahrtabschnitt ANT-XII/3", herausgegeben von Wilfried Jokat und Hans Oerter
Heft-Nr. 220/1997 – „Ein Beitrag zum Schwerefeld im Bereich des Weddellmeeres, Antarktis. Nutzung von Altimetermessungen des GEOSAT und ERS-1", von Tilo Schöne
Heft-Nr. 221/1997 – „Die Expedition ANTARKTIS-XIII/1-2 des Forschungsschiffes 'Polarstern' 1995/96", herausgegeben von Ulrich Bathmann, Mike Lucas und Victor Smetacek
Heft-Nr. 222/1997 – „Tectonic Structures and Glaciomarine Sedimentation in the South-Eastern Weddell Sea from Seismic Reflection Data", by László Oszkó
Heft-Nr. 223/1997 – „Bestimmung der Meereisdicke mit seismischen und elektromagnetisch-induktiven Verfahren", von Christian Haas
Heft-Nr. 224/1997 – „Troposphärische Ozonvariationen in Polarregionen", von Silke Wessel
Heft-Nr. 225/1997 – „Biologische und ökologische Untersuchungen zur kryopelagischen Amphipodenfauna des arktischen Meereises", von Michael Poltermann
Heft-Nr. 226/1997 – „Scientific Cruise Report of the Arctic Expedition ARK-XI/1 of RV 'Polarstern' in 1995", edited by Eike Rachor
Heft-Nr. 227/1997 – „Der Einfluß kompatibler Substanzen und Kryoprotektoren auf die Enzyme Malatdehydrogenase (MDH) und Glucose-6-phosphat-Dehydrogenase (G6P-DH) aus *Acrosiphonia arcta* (Chlorophyta) der Arktis und Antarktis", von Katharina Kück
Heft-Nr. 228/1997 – „Die Verbreitung epibenthischer Mollusken im chilenischen Beagle-Kanal", von Katrin Linse
Heft-Nr. 229/1997 – „Das Mesozooplankton im Laptevmeer und östlichen Nansen-Becken – Verteilung und Gemeinschaftsstrukturen im Spätsommer", von Hinrich Hanssen
Heft-Nr. 230/1997 – „Modell eines adaptierbaren, rechnergestützten, wissenschaftlichen Arbeitsplatzes am Alfred-Wegener-Institut für Polar- und Meeresforschung", von Lutz-Peter Kurdelski
Heft-Nr. 231/1997 – „Zur Ökologie arktischer und antarktischer Fische: Aktivität, Sinnesleistungen und Verhalten", von Christopher Zimmermann
Heft-Nr. 232/1997 – „Persistente chlororganische Verbindungen in hochantarktischen Fischen", von Stephan Zimmermann
Heft-Nr. 233/1997 – „Zur Ökologie des Dimethylsulfoniumpropionat (DMSP)-Gehaltes temperierter und polarer Phytoplanktongemeinschaften im Vergleich mit Laborkulturen der Coccolithophoride *Emiliania huxleyi* und der antarktischen Diatomee *Nitzschia lecointei*", von Doris Meyerdierks
Heft-Nr. 234/1997 – „Die Expedition ARCTIC '96 des FS 'Polarstern' (ARK XIII) mit der Arctic Climate System Study (ACSYS)", von Ernst Augstein und den Fahrtteilnehmern
Heft-Nr. 235/1997 – „Polonium-210 und Blei-210 im Südpolarmeer: Natürliche Tracer für biologische und hydrographische Prozesse im Oberflächenwasser des Antarktischen Zirkumpolarstroms und des Weddellmeeres", von Jana Friedrich
Heft-Nr. 236/1997 – „Determination of atmospheric trace gas amounts and corresponding natural isotopic ratios by means of ground-based FTIR spectroscopy in the high Arctic", by Arndt Meier
Heft-Nr. 237/1997 – „Russian-German Cooperation: The Expedition TAYMYR / SEVERNAYA ZEMLYA 1996", edited by Martin Melles, Birgit Hagedorn and Dmitri Yu. Bolshiyanov.
Heft-Nr. 238/1997 – „Life strategy and ecophysiology of Antarctic macroalgae", by Iván M. Gómez.
Heft-Nr. 239/1997 – „Die Expedition ANTARKTIS XIII/4-5 des Forschungsschiffes ‚Polarstern' 1996", herausgegeben von Eberhard Fahrbach und Dieter Gerdes.
Heft-Nr. 240/1997 – „Untersuchungen zur Chrom-Speziation in Meerwasser, Meereis und Schnee aus ausgewählten Gebieten der Arktis", von Heide Giese.
Heft-Nr. 241/1997 – „Late Quaternary glacial history and paleoceanographic reconstructions along the East Greenland continental margin: Evidence from high-resolution records of stable isotopes and ice-rafted debris", by Seung-Il Nam.

Heft-Nr. 242/1997 – „Thermal, hydrological and geochemical dynamics of the active layer at a continuous permafrost site, Taymyr Peninsula, Siberia", by Julia Boike.
Heft-Nr. 243/1997 – „Zur Paläoozeanographie hoher Breiten: Stellvertreterdaten aus Foraminiferen", von Andreas Mackensen.
Heft-Nr. 244/1997 – „The Geophysical Observatory at Neumayer Station, Antarctica. Geomagnetic and seismological observations in 1995 and 1996", by Alfons Eckstaller, Thomas Schmidt, Viola Gaw, Christian Müller and Johannes Rogenhagen.
Heft-Nr. 245/1997 – „Temperaturbedarf und Biogeographie mariner Makroalgen – Anpassung mariner Makroalgen an tiefe Temperaturen", von Bettina Bischoff-Bäsmann.
Heft-Nr. 246/1997 – „Ökologische Untersuchungen zur Fauna des arktischen Meereises", von Christine Friedrich.
Heft-Nr. 247/1997 – „Entstehung und modifizierung von marinen gelösten organischen Substanzen", von Berit Kirchhoff.
Heft-Nr. 248/1997 – „Laptev Sea System: Expeditions in 1995", edited by Heidemarie Kassens.
Heft-Nr. 249/1997 – „The Expedition ANTARKTIS XIII/3 (EASIZ I) of RV ‚Polarstern' to the eastern Weddell Sea in 1996", edited by Wolf Arntz and Julian Gutt.
Heft-Nr. 250/1997 – „Vergleichende Untersuchungen zur Ökologie und Biodiversität des Mega-Epibenthos der Arktis und Antarktis", von Andreas Starmans.
Heft-Nr. 251/1997 – „Zeitliche und räumliche Verteilung von Mineralvergesellschaftungen in spätquartären Sedimenten des Arktischen Ozeans und ihre Nützlichkeit als Klimaindikatoren während der Glazial/Interglazial-Wechsel", von Christoph Vogt.
Heft-Nr. 252/1997 – „Solitäre Ascidien in der Potter Cove (King George Island, Antarktis). Ihre ökologische Bedeutung und Populationsdynamik", von Stephan Kühne.
Heft-Nr. 253/1997 – „Distribution and role of microprotozoa in the Southern Ocean", by Christine Klaas.
Heft-Nr. 254/1997 – „Die spätquartäre Klima- und Umweltgeschichte der Bunger-Oase, Ostantarktis", von Thomas Kulbe.
Heft-Nr. 255/1997 – „Scientific Cruise Report of the Arctic Expedition ARK-XIII/2 of RV ‚Polarstern' in 1997", edited by Ruediger Stein and Kirsten Fahl.
Heft-Nr. 256/1998 – „Das Radionuklid Tritium im Ozean: Meßverfahren und Verteilung von Tritium im Südatlantik und im Weddellmeer", von Jürgen Sültenfuß.
Heft-Nr. 257/1998 – „Untersuchungen der Saisonalität von atmosphärischem Dimethylsulfid in der Arktis und Antarktis", von Christoph Kleefeld.
Heft-Nr. 258/1998 – „Bellingshausen- und Amundsenmeer: Entwicklung eines Sedimentationsmodells", von Frank-Oliver Nitsche.
Heft-Nr. 259/1998 – „The Expedition ANTARKTIS-XIV/4 of RV ‚Polarstern' in 1997", by Dieter K. Fütterer.
Heft-Nr. 260/1998 – „Die Diatomeen der Laptevsee (Arktischer Ozean): Taxonomie und biogeographische Verbreitung", von Holger Cremer
Heft-Nr. 261/98 – „Die Krustenstruktur und Sedimentdecke des Eurasischen Beckens, Arktischer Ozean: Resultate aus seismischen und gravimetrischen Untersuchungen", von Estella Weigelt.
Heft-Nr. 262/98 – „The Expedition ARKTIS-XIII/3 of RV 'Polarstern' in 1997", by Gunther Krause.
Heft-Nr. 263/98 – „Thermo-tektonische Entwicklung von Oates Land und der Shackleton Range (Antarktis) basierend auf Spaltspuranalysen", von Thorsten Schäfer.
Heft-Nr. 264/98 – „Messungen der stratosphärischen Spurengase ClO, HCl, O_3, N_2O, H_2O und OH mittels flugzeuggetragener Submillimeterwellen-Radiometrie", von Joachim Urban.
Heft-Nr. 265/98 – „Untersuchungen zu Massenhaushalt und Dynamik des Ronne Ice Shelfs, Antarktis", von Astrid Lambrecht.
Heft-Nr. 266/98 – „Scientific Cruise Report of the Kara Sea Expedition of RV 'Akademik Boris Petrov' in 1997", edited by Jens Matthiessen and Oleg Stepanets.
Heft-Nr. 267/98 – „Die Expedition ANTARKTIS-XIV mit FS 'Polarstern' 1997. Bericht vom Fahrtabschnitt ANT-XIV/3", herausgegeben von Wilfried Jokat und Hans Oerter.
Heft-Nr. 268/98 – „Numerische Modellierung der Wechselwirkung zwischen Atmosphäre und Meereis in der arktischen Eisrandzone", von Gerit Birnbaum.
Heft-Nr. 269/98 – „ Katabatic wind and Boundary Layer Front Experiment around Greenland (KABEG '97)", by Günther Heinemann.
Heft-Nr. 270/98 – „Architecture and evolution of the continental crust of East Greenland from integrated geophysical studies", by Vera Schlindwein.
Heft-Nr. 271/98 – „Winter Expedition to the Southwestern Kara Sea - Investigations on Formation and Transport of Turbid Sea-Ice", by Dirk Dethleff, Per Loewe, Dominik Weiel, Hartmut Nies, Gesa Kuhlmann, Christian Bahe and Gennady Tarasov.
Heft-Nr. 272/98 – „FTIR-Emissionsspektroskopische Untersuchungen der arktischen Atmosphäre", von Edo Becker.
Heft-Nr. 273/98 – „Sedimentation und Tektonik im Gebiet des Agulhas-Rückens und des Agulhas-Plateaus (‚SETARAP')", von Gabriele Uenzelmann-Neben.

Heft-Nr. 274/98 – „The Expedition ANTARKTIS XIV/2", by Gerhard Kattner.
Heft-Nr. 275/98 – „Die Auswirkungen der ‚NorthEastWater'-Polynya auf die Sedimentation vor NO-Grönland und Untersuchungen zur Paläo-Ozeanographie seit dem Mittelweichsel"., von Hanne Notholt.
Heft-Nr. 276/98 – „Interpretation und Analyse von Potentialfelddaten im Weddellmeer, Antarktis: der Zerfall des Superkontinents Gondwana"., von Michael Studinger.
Heft-Nr. 277/98 – „Koordiniertes Programm Antarktisforschung". Berichtskolloquium im Rahmen des Koordinierten Programms „Antarktisforschung mit vergleichenden Untersuchungen in arktischen Eisgebieten", herausgegeben von Hubert Miller.
Heft-Nr. 278/98 – „Messung stratosphärischer Spurengase über Ny-Ålesund, Spitzbergen, mit Hilfe eines bodengebundenen Mikrowellen-Radiometers", von Uwe Raffalski.
Heft-Nr. 279/98 – „Arctic Paleo-River Discharge (APARD). A new Research Programme of the Arctic Ocean Science Board (AOSB)", edited by Ruediger Stein.
Heft-Nr. 280/98 – „Fernerkundungs- und GIS-Studien in Nordostgrönland", von Friedrich Jung-Rothenhäusler.
Heft-Nr. 281/98 – „Rekonstruktion der Oberflächenwassermassen der östlichen Laptevsee im Holozän anhand von aquatischen Palynomorphen", von Martina Kunz-Pirrung.
Heft-Nr. 282/98 – „Scavenging of ^{231}Pa and ^{230}Th in the South Atlantic: Implications for the use of the ^{231}Pa/^{230}Th ratio as a paläoproductivity proxy", by Hans-Jürgen Walter.

* vergriffen/out of print
** nur noch beim Autor/only from the author